박사 학위논문

Ph. D. Dissertation

다당류 바이오폴리머 처리된 모래:
특성 및 거동

Polysaccharide Biopolymers in Sands:
Properties and Behaviors
2020

임주영 (任主榮 Jooyoung Im)

한국과학기술원
Korea Advanced Institute of Science and Technology

Ph. D. Dissertation

다당류 바이오폴리머 처리된 모래: 특성 및 거동

Polysaccharide Biopolymers in Sands: Properties and Behaviors

2020

임주영 (任主榮 Jooyoung Im)

Korea Advanced Institute of Science and Technology
Department of Civil and Environmental Engineering

Polysaccharide Biopolymers in Sands: Properties and Behaviors

임주영 任主榮 (Jooyoung Im)

The present dissertation has been approved by the dissertation committee as a Ph.D. thesis at KAIST

June. 15. 2020

Committee head	조 계 춘
Committee member	이 승 래
Committee member	권 태 혁
Committee member	김 동 수
Committee member	장 일 한
Committee member	정 문 경

Polysaccharide Biopolymers in Sands: Properties and Behaviors

Advisor : Professor Cho, Gye Chun

by

임주영 任主榮 (Jooyoung Im)

Department of Civil and Environmental Engineering

KAIST

A thesis submitted to the faculty of KAIST in partial fulfillment of the requirements for the degree of Doctor of Philosophy in Engineering in the Department of Civil and Environmental Engineering. The study was conducted in accordance with Code of Research Ethics[1]

06. 15. 2020

Approved by

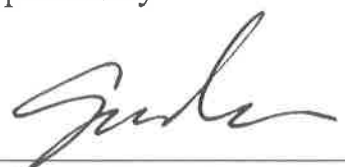

Professor Gye-Chun Cho

[1]Declaration of Ethical Conduct in Research: I, as a graduate student of KAIST, hereby declare that I have not committed any acts that may damage the credibility of my research. These include, but are not limited to: falsification, thesis written by someone else, distortion of research findings or plagiarism. I affirm that my thesis contains honest conclusions based on my own careful research under the guidance of my thesis advisor.

CCE 임 주 영. 다당류 바이오폴리머 처리된 모래: 특성 및 거동. 건설 및 환경공학과. 2020. 92p. 지도교수: 조계춘 교수님. Text in English

Im, Jooyoung. Polysaccharide Biopolymers in Sands: Properties and Behaviors. Department Civil and Environmental Engineering. 2020. 92p. Advisor: Prof. Cho, Gye-Chun. Text in English

ABSTRACT

Humanity's impact on the environment has been one of growing concern in the recent years. As industries grow and globalization becomes ever present, so too has the impact on the environment. From environmental pollution to the depletion of natural resources, there are many direct and secondary effects of human activities seen in our world today. Studies have shown that there is a direct correlation between the increasing CO_2 present in our atmosphere and the increase in the occurrence of geotechnical hazards in our world. As a result, ecofriendly sustainable methods of soil improvement have been studied by various researchers around the world, one of such methods is the use of biopolymers.

Several studies have shown the strengthening effects of biopolymers in soils, however, an in-depth study on how the properties of these biopolymers effect the properties of soils has not been thoroughly studied. It is the objective of this study to observe the behaviors and properties of these biopolymers and see how these properties affect the properties of sands. This study focuses on polysaccharide biopolymers, specifically xanthan and gellan gum. The strength and loading behaviors of biopolymer treated sands are correlated with the physical properties of the biopolymers themselves. Additionally, two methods of enhancing the biopolymers strength in water are discussed.

Results showed that xanthan and gellan biopolymers had a critical concentration at which the behaviors shifted from a hydrogel to a biopolymer film. The biopolymer's strengthening mechanisms in sands were shown to be mostly dependent on the tensile strength provided by the biopolymer, and higher concentrations of biopolymers the strengthening efficiency was shown to be a factor of the degree of biopolymer saturation. Loading behaviors with biopolymers showed that viscosity in sands showed highly expansive behaviors and gels in sands had slight cementation effects in which the cohesion of the sands was enhanced. It was also seen that crosslinking biopolymers and the use of hydrophobic biopolymers had capabilities of enhancing the saturated strength of biopolymer treated sands.

Keywords: Biopolymer, Sands, Polysaccharides, Strength, Critical State, Modelling

초록

최근 몇 년간 인류가 환경에 미치는 영향에 대한 우려는 증가되고 있는 실정이다. 산업의 성장과 세계화의 진행은 환경에도 영향을 미친다. 환경 오염에서 천연 자원 고갈에 이르기까지, 인간의 활동으로 인한 직간접적 영향은 오늘날 세계에서 폭넓게 관찰되고 있다. 선행연구에 따르면 대기 중에 존재하는 CO2 증가와 지구에서 지반공학적 위험 발생 사이에는 직접적인 상관 관계가 존재한다. 그 결과, 전 세계 여러 연구자들이 친환경적으로 지속 가능한 토양 개선 방법을 연구해 왔으며, 이러한 방법 중 하나는 바이오 폴리머를 사용하는 것이다.

몇몇 연구를 통해 토양에서 바이오 폴리머 처리에 의한 강도 증진 효과를 확인했지만, 바이오폴리머의 특성이 토양에 어떤 영향을 미치는지에 대한 심층적인 연구는 미비한 실정이다. 본 연구의 목적은 다당류 바이오폴리머(잔탄 및 젤란검)의 거동과 특성을 관찰하고 관찰된 특성이 모래의 특성에 끼치는 영향을 확인하는 것이다. 바이오폴리머가 처리된 모래의 강도 및 재하시 거동은 바이오폴리머 자체의 물리적 특성과 관련이 있음을 밝혔다. 또한, 습윤상태에서 바이오폴리머 강도를 향상시키는 2 가지 방법을 제안한다.

연구 결과를 통해 잔탄 및 젤란검 바이오폴리머의 형상이 하이드로겔에서 바이오폴리머 필름으로 이동하는 임계농도를 가짐을 확인했다. 모래에서 바이오폴리머의 강도증진 기작은 대부분 바이오폴리머가 제공하는 인장 강도에 의존하는 것으로 나타났으며, 고농도에서 바이오폴리머의 강도증진효율은 바이오폴리머 포화도에 영향을 받는 것으로 나타났다. 바이오폴리머를 사용했을 때 재하시의 거동은 모래의 점도에 의해 팽창하는 거동을 보였으며, 모래에 함유된 바이오폴리머겔은 약간의 고결효과를 보여 모래의 점착력을 증진하는 것으로 확인했다. 또한, 가교 바이오폴리머 및 소수성 바이오폴리머의 사용을 통해 바이오폴리머 처리 된 모래의 포화강도를 향상시킬 수 있음을 확인했다.

핵심낱말: 바이오 폴리머, 모래, 다당류, 강도, 모델링

Table of Contents

List of Tables

List of Figures

Chapter 1. Introduction

1.1 Research Background

Humanity's impact on the environment has been one of growing concern in the recent years. As industries grow and globalization becomes ever present, so too has the impact on the environment. From environmental pollution to the depletion of natural resources, there are many direct and secondary effects of human activities seen in our world today. One of the most widely known and accepted byproducts of human activity is the excess generation of greenhouse gases, in particular the emission of carbon dioxide (CO_2) [2-4]. The large buildup of greenhouse gases in our atmosphere has been closely related to the progression of climate change and its secondary effects on our world [2].

Two of the major global impacts associated with climate change are: 1) Extreme precipitation and 2) Melting of the ice caps [5-7]. Extreme precipitation occurs when warmer global temperatures, a result of global warming, enables a larger volume of water to stay suspended in the atmosphere as water vapor [8-10]. The increase in water vapor present in our atmosphere can in turn lead to heavier downpours and localized droughts, which disrupts the water circulation processes leading to more extreme precipitation events and longer intervals between the dry and wet periods [11]. These secondary effects can then in turn result in the development of geotechnical hazards such as landslides, ground subsidence, and soil degradation.

The melting of the ice caps is another effect of global warming. As the freshwater from the ice caps move into the ocean, there is a definitive rise in the sea level [12, 13], along with the disruption of the ocean circulation [14, 15]. As the ocean circulation acts as a heat transport mechanism for our world, its disruption could lead to larger extremes of hot and cold areas. These effects along with a higher average ocean temperature would result in an increase in ascending air currents, which in turn would result in the formation of stronger, longer-lasting, and more frequent storm systems [5]. The result of such changes in our weather would increase the erosion and flooding events that lead to levee failures, coastal decomposition, and ground subsidence [16].

Such changes in our climate would inevitably result in the increased occurrence of geotechnical hazards. A previous study by Chang (2019) directly correlates the increase in CO_2 in our atmosphere with the number of occurrences of geotechnical hazards shown in Fig. 1.1 [5]. As the CO_2 concentration has increased throughout the years, the number of geotechnical hazards has also been proportionally increasing. This indicates that without taking the proper precautions against the excessive emission of greenhouse gases, the natural occurrence of geotechnical hazards will only increase, implicating millions of additional lives.

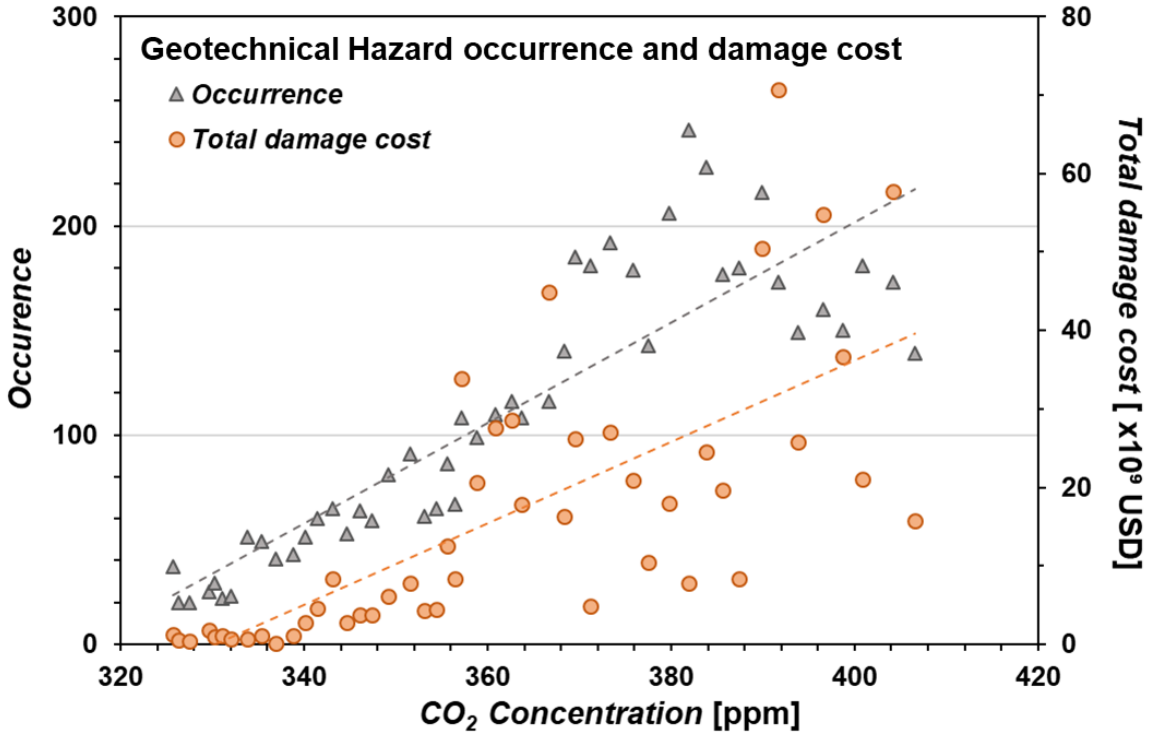

Fig. 1.1 Correlation between the increase in CO_2 and geotechnical hazards (source: Chang 2019) [5]

1.2 Related Research Trends

In order to combat the increase in geotechnical hazards without contributing to the emission of greenhouse gases, sustainable development for alternative materials for ground improvement has been largely studied. Several methods include: synthetic polymers, geopolymers, and bio-based materials.

1.2.1 Synthetic Polymers and Geopolymers

Synthetic Polymers

Synthetic polymers are man-made polymers that are generally made up of carbon-carbon bonds [17]. They are found in a variety of consumer products such as textiles and plastics. Examples of synthetic polymers used for ground improvement include: Polyacrylamide (PAM), sodium silicate, acrylics, lignosulfonates, and phenolasts.

PAM is synthesized from acrylamide ($CH_2CHCONH_2$) into a simple linear or cross-linked form. It has a negative charge density that allows for it to electrostatically bond with clay particles [18, 19]. When mixed with soils it has been shown to reduce soil erosion and runoff [20]. However, although PAM is nontoxic to humans, animals, and plants, its acrylamide monomer is a known neurotoxin and potential carcinogen [21].

Other chemical polymers such as sodium silicate and lignosulfonates have been used in soil grouting practices, however, much like other synthetic polymers, its concerns over toxicity has restricted its use [22].

Geopolymers

Geopolymers make use of pozzolan materials to create a rigid polymer within the soil to help strengthen the soil [23-26]. The geopolymerization process involves the use of an alkaline solution to dissolve the silicon and aluminum ions on either the soil or pozzolan materials (*e.g.* fly ash, blast furnace slag) [27]. After which, the hydroxyl ions in the alkaline solution react, forming one free water molecule and oxide ion [27]. The oxide ions react with the silicon and aluminum ions, and with the addition of heat, the silicon/aluminum hydroxide molecules polymerize into a rigid structure providing high strength in the soil [23, 28].

Geopolymers have been used to replace the usage of cement, a known source of greenhouse gas emissions. Moreover, as geopolymers make use of industrial wastes (*e.g.* fly ash, blast furnace slag) it can be said to be sustainable in both low greenhouse emissions and waste reuse [29]. However, proper polymerization of geopolymers require heating above 60°C [30, 31], which greatly limits the on-site applicability. Moreover, studies have shown that geopolymers are highly susceptible to water, particularly acid solutions further limiting is widespread use [32].

1.2.2 Bio-Based Materials

Biological approaches to ground improvement have also been a focus of study for sustainable development. Biological approaches can be further subcategorized as follows: 1) Bio-gas, 2) Bio-mineralization, and 3) Biopolymers.

Bio-Gas

Bio-gas makes use of gas generation from organisms to alter specific properties of the soil. As the formation of gas within the soil can keep the soil from densifying, and the presence of biological materials providing sustenance, bio-gas has mostly been used in the fields of agriculture. Studies have shown that the use of bio-gas can help improve the fertility of soils for crop production [33, 34].

Bio-Mineralization

Bio-mineralization makes use of mineral precipitation within the soil pores through the use of biological organisms for strengthening purposes [35]. Among such methods, the most widely used and studied method is microbial induced calcite precipitation (MICP).

MICP makes use of microorganisms, such as *Sporosarcina pasteurii* and *Bacillus pasteurii*, that precipitate calcium carbonate crystals to provide inter-particle cementation [36, 37]. In MICP urea hydrolysis is used for calcium carbonate precipitation [38]. The microorganisms used convert urea to ammonium and carbonate, at which point the carbonate reacts with the calcium ions to form calcium carbonate precipitates [39]. The calcium carbonate precipitates acts as a cementing material between soil particles thereby increasing its strength and stiffness [40]. MICP has also been found to be applicable for heavy metal remediation [41], CO_2 sequestration [42], and the repair of concrete [43, 44]. However, the use of MICP results in the byproduct of ammonia, which is difficult to remove in the field. Additionally, as MICP makes use of microorganisms directly in the soil, it is most applicable to coarse soils with some difficulties when applied to fine grained soils.

Biopolymers

Biopolymers are organic precipitates of biological organisms. There are three main types of biopolymers: 1) polynucleotides (RNA, DNA), 2) polypeptides (amino acids, proteins), and 3) polysaccharides, which are the most commonly applied biopolymers in various fields [45, 46].

Various biopolymers have been studied by researchers around the world, showing large strengthening efficiencies [1, 47, 48], increases in erosion resistance [49, 50], reduction of hydraulic conductivity [51, 52], and even vegetation growth [49, 53]. The use of biopolymers has shown great promise for various geotechnical applications. However, most of these biopolymers are highly susceptible to the presence of water and soil composition, and its strengthening efficiency and behavior may vary greatly dependent on the water content and soil used [47, 54, 55].

Through previously conducted studies on biopolymers, it has been learned that the general strengthening mechanism of these biopolymers in sands is by encompassing the sand particles in stiff biopolymer films, shown in Fig. 1.2. However, other parameters that have been shown to be affected by biopolymers, are not easily explained by traditional soil behaviors.

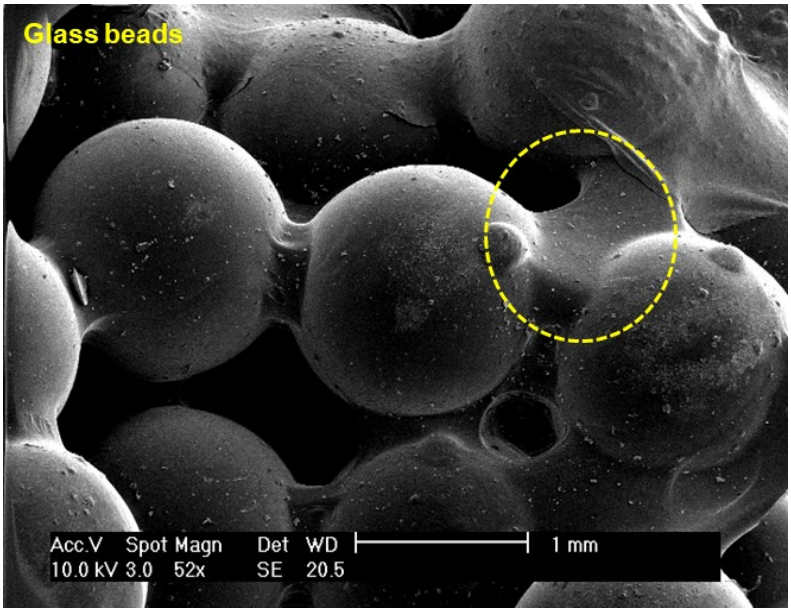

Fig. 1.2 Formation of biopolymer films on glass beads (source: Chang 2012) [1]

One such example is shown in Fig. 1.3, in which xanthan gum was seen to greatly decrease the erodability of silica sand (Fig. 1.3a) [56]. According to Shields equation (1.1), the threshold Shields parameter (θ_{cr}), used to calculate the initiation of sediment motion, is dependent on the soil parameters and the threshold shear stress (τ_{cr}) [57].

$$\theta_{cr} = \tau_{cr} / [\rho g(G_s-1)d_{50}] \quad (1.1)$$

However, direct shear experiments (Fig. 1.3b) show that when saturated, xanthan gum treatment shows little to no increase in the shear strength of sands. As the soil composition remains constant between the xanthan treated and untreated samples, and there is no large difference in the threshold shear stress, the reduction in erodability of xanthan treated silica sand must be accounted for by other parameters, such as the increase in pore fluid viscosity. Therefore, a deeper understanding on how the properties of the biopolymers effect different geotechnical parameters is necessary.

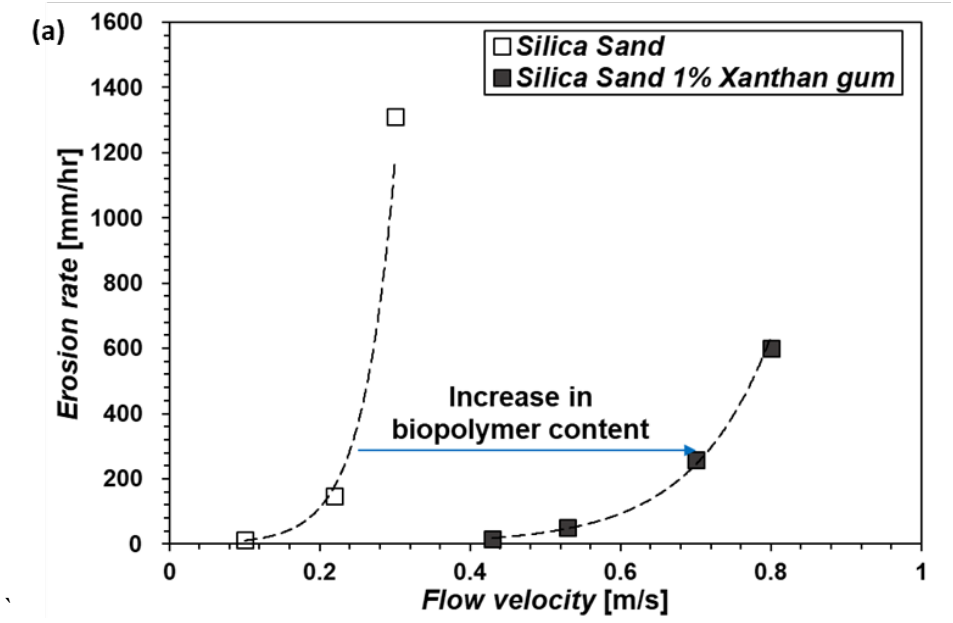

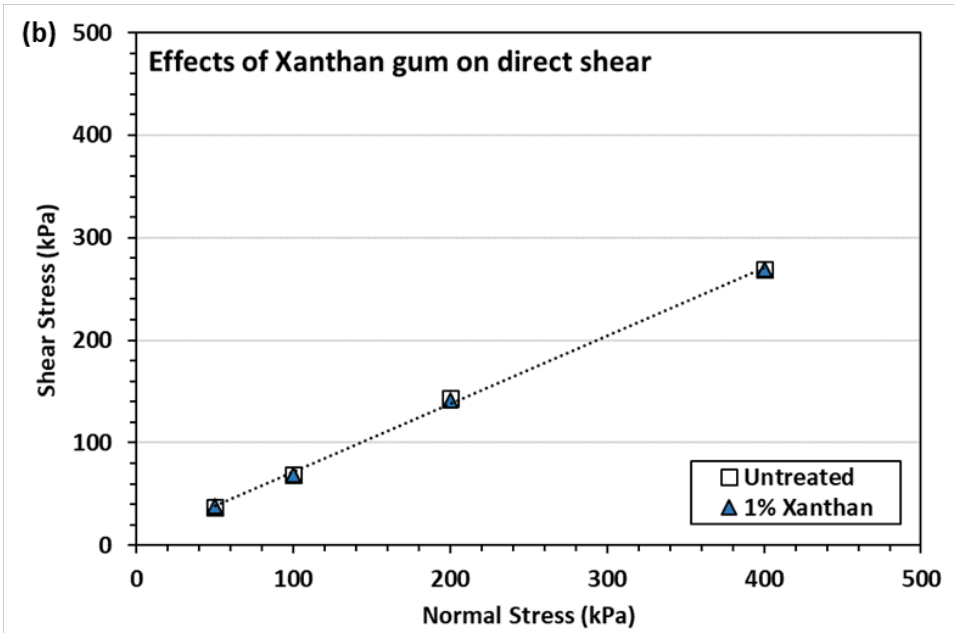

Fig. 1.3 (a) Decrease in erodability with xanthan gum treated silica sand (source: Kwon 2020) [56] (b) Saturated direct shear of xanthan gum treated jumunjin sand

1.3 Research Objective

It is the objective of this study to deepen the understanding of how the properties of the biopolymers, specifically the viscosity and tensile strength, effect the properties of sands. This was done by using a viscous and gelling biopolymer to:

i. Investigating the parameters in which biopolymers provide viscosity and tensile strength.
ii. Correlating the tensile strength of the biopolymers with its strengthening efficiency in sands.
iii. Observing the behavioral changes that occur with loading when a viscous or gelling biopolymer are present in the pore spaces of the sands.

In addition, two methods of increasing the saturated strength of biopolymer treated soils is suggested.

1.4 Scope

In Ch. 2 background information on polysaccharide biopolymers is investigated. This covers information regarding its structure and properties, behaviors in water, and an experimental program to investigate its viscosity and tensile strength dependent on the biopolymer concentration.

Ch. 3 investigates the strengthening mechanisms of biopolymers in sands through it uniaxial compressive strengths. The tensile strengths of the biopolymers obtained from Ch. 2 are then be used to estimate the strengths obtained from the experiment to better understand what parameters control the biopolymer strengthening mechanisms in sands.

Ch. 4 investigates the loading behavior of biopolymer treated sands through the use of triaxial tests. This chapter focuses mainly on the effects of viscosity and gelling on the loading behavior.

As previous studies have shown biopolymers to be highly susceptible to water, in Ch. 5 two possible methods of overcoming this limitation are shown through the use of crosslinking and the use of hydrophobic biopolymers.

Ch. 6 presents the closing discussion.

Chapter 2. Polysaccharide Biopolymers

2.1 Polysaccharides

Polysaccharides are biopolymers that are commonly composed of reoccurring glucose chains, and are readily found in nature [58]. Depending on the linkage type, position, and physical structure (i.e. length/size of polymers) the characteristics of the polysaccharide may vary greatly. There are two main linkage types: 1) α-linkage and 2) β-linkage, while typical linkage positions connect any of the 6 points on the glucose molecule, shown in Fig. 2.1. Polysaccharides are used in a variety of fields such as food production, agriculture, medicine, and cosmetics as stabilizers, thickeners, and gel forming agents [59-61]. Several commonly used polysaccharides and their properties are shown in Table 2.1.

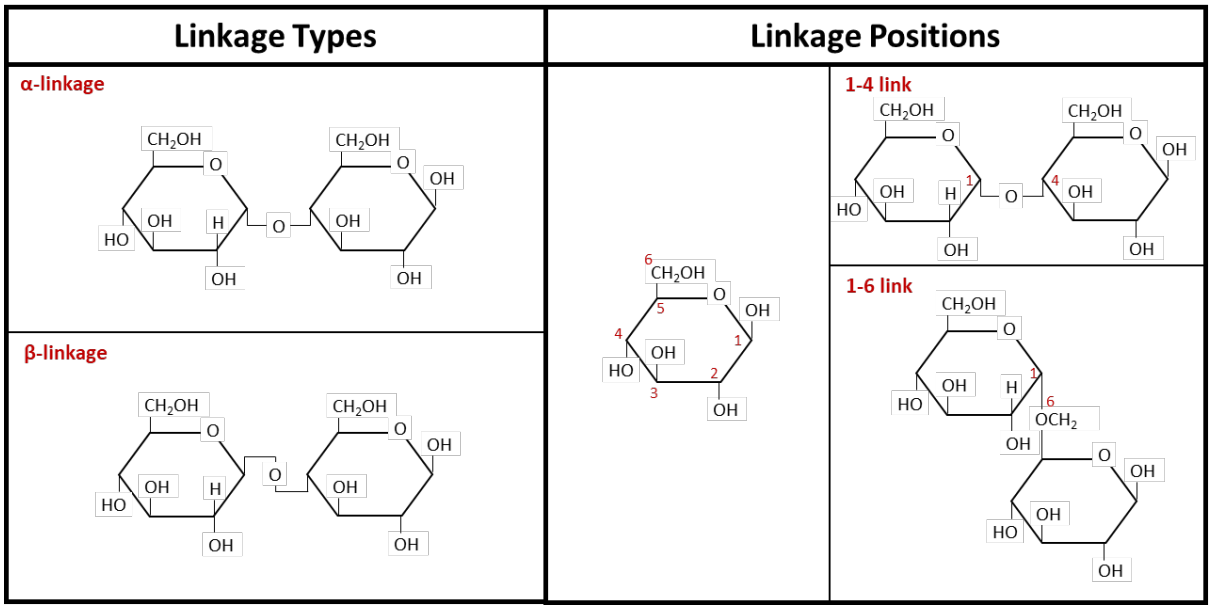

Fig. 2.1 Glucose link type and positions

There are many different polysaccharides with varying properties, however, they can be generally categorized into 1) insoluble and 2) soluble polysaccharides [62]. Insoluble polysaccharides are biopolymers that do not naturally dissolve in water without external help while soluble polysaccharides are commonly hydrophilic polymers that readily react with

water. This study focuses on two soluble polysaccharides: 1) viscous and 2) gelling biopolymers.

Table 2.1 Characteristics of commonly found polysaccharides [63-69]

Biopolymer	Composition	Characteristics
Cellulose	*β-(1-4)-D-glucose* linkages	- Hydrophilic - Properties depend on the chain length
Starch	*α-(1-4) D-glucose linkages*	- Soluble in heated water - Viscous, gelatinization
Chitosan	*β -(1-4)-2--D-glucosamine linkages*	- Soluble in acidic solvents - Bioadhesive for (-) charged surfaces - Biodegradable
Xanthan	*β-(1-4)(1-2)(1-3)-D-glucose* linkages	- Highly viscous - Negatively charged
Curdlan	*B-(1-3)-D-glucose* linkages	- Gel formation via heating in aqueous solutions
Beta-Glucan	*B-(1-3)-D-glucose* glycosidic bonds	- Capable of immune activation in humans - Cholesterol absorption capabilities

2.1.1 Viscous Biopolymers

Viscous biopolymers are polymers when reacted with water swell and create a viscous fluid [70]. The exact mechanism in which these viscous biopolymers increase the viscosity of the fluid is shown in Fig. 2.2. These biopolymers commonly have a branching polymer chain connected to the main polymer chain. These branches make it so that the polymers take on a ‘Y’ shaped structure or that resembling the diverging branches on a tree. It is in this structure that the biopolymers absorb the surrounding water, swelling in size and limiting the free water available in the fluid [70]. Several examples of viscous biopolymers and their chemical structure are shown in Table 2.2.

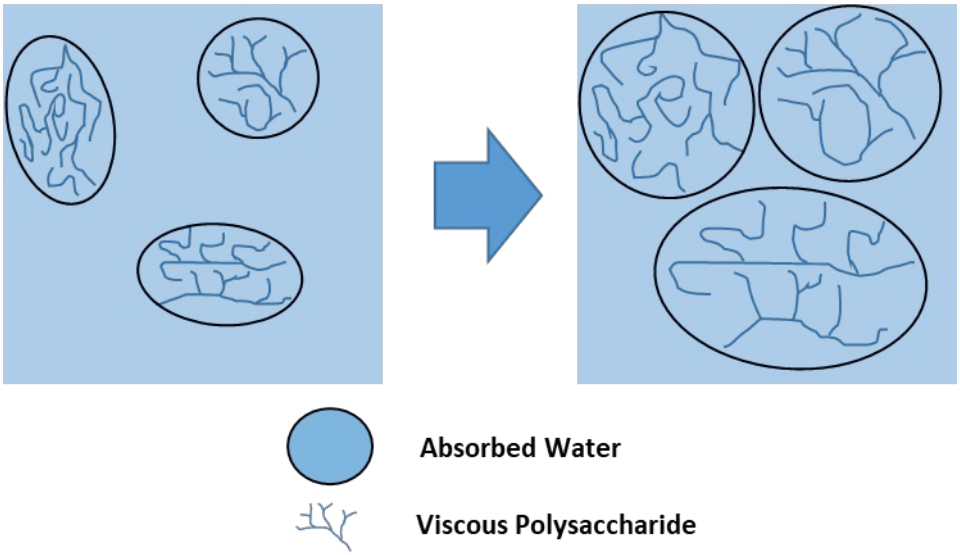

Fig. 2.2 Swelling of Viscous Polysaccharides

2.1.2 Gelling Biopolymers

On the other hand, gelling biopolymers are commonly linear in nature with no branching polymer chains. These linear polymer chains allow for the restructuring of the polymer chains into double helix formations [71]. This physical structure allows for the formation of rigid gels and is often initiated with the presence of heat, shown in Fig. 2.3 [72]. Commonly used gelling biopolymers are shown in Table 2.3

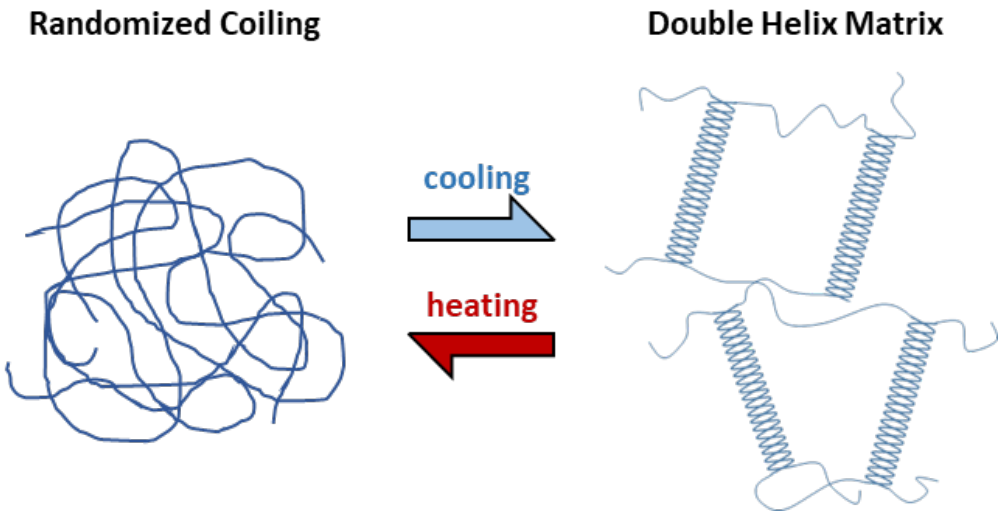

Fig. 2.3 Gelling of Polysaccharides

Table 2.2 Common viscous biopolymers and their chemical structures

Biopolymer	Composition
Xanthan gum	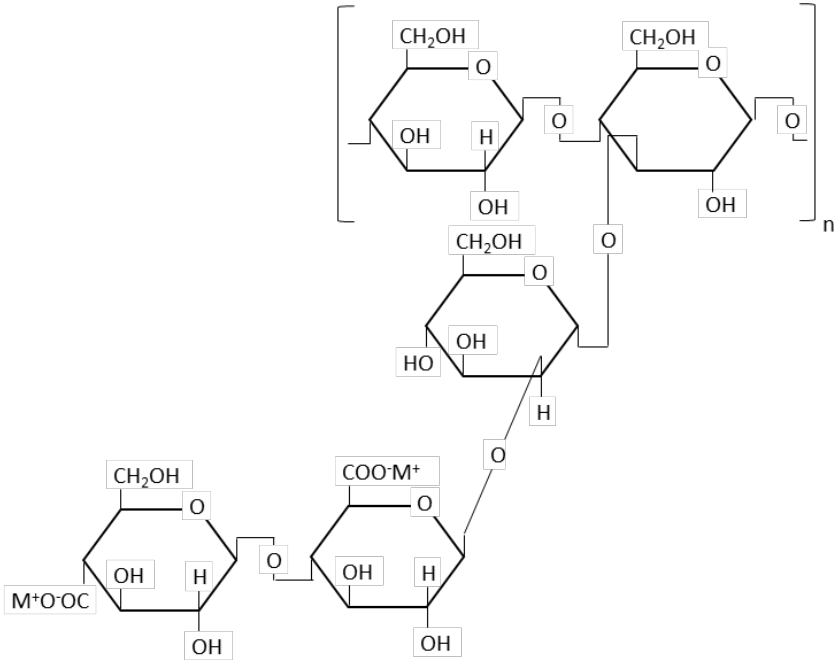

Guar gum	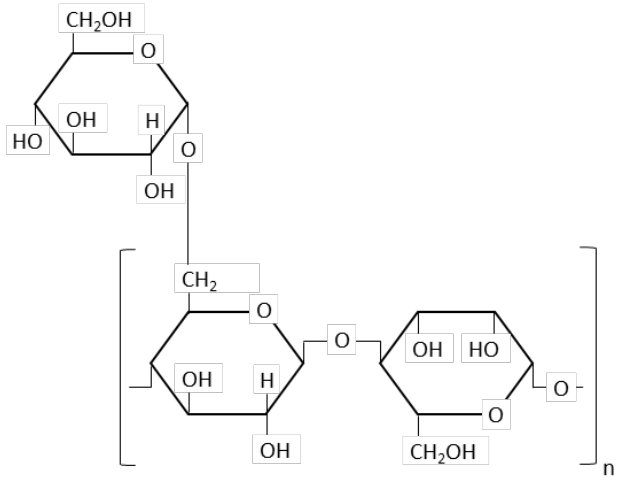
Amylopectin	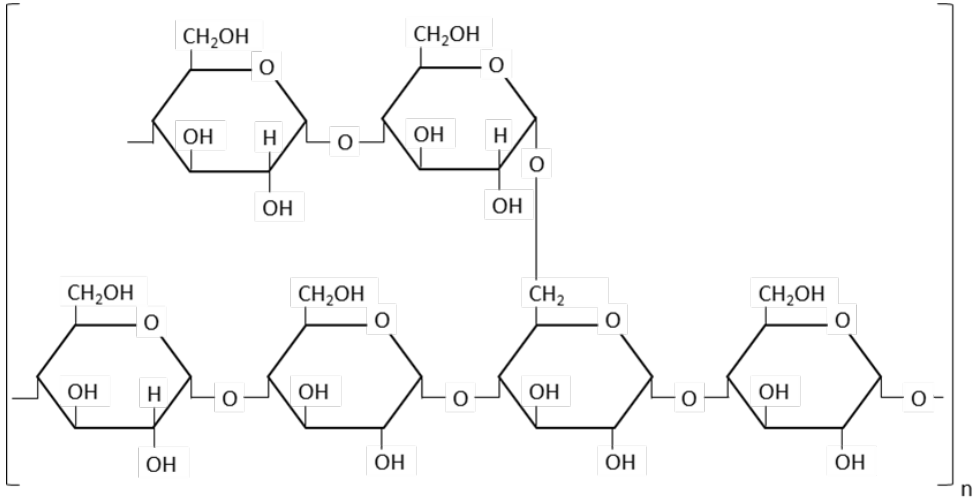

Table 2.3 Common gelling biopolymers and their chemical structures

Biopolymer	Composition
Gellan gum	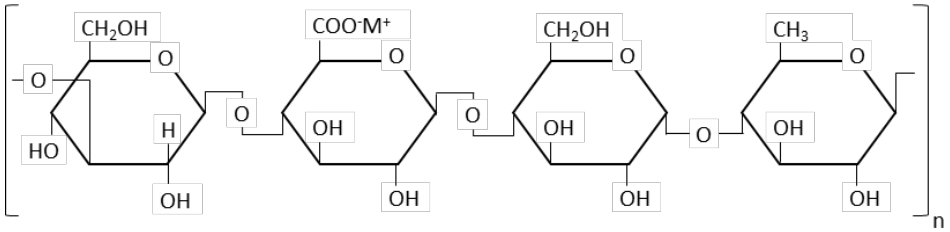
Agar gum	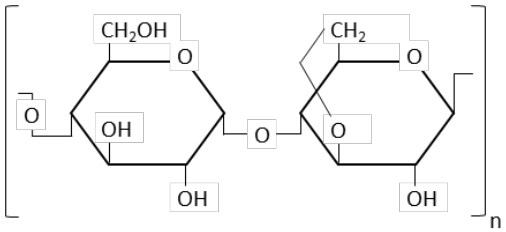
Amylose	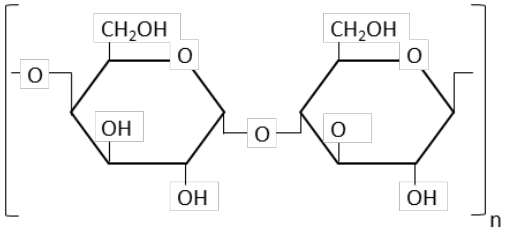

2.2 Experimental Setup

In order to better understand the properties of both viscous and gelling biopolymers, viscosity tests and tensile tests were performed. As previous studies have shown, the physical characteristics of the biopolymers are highly dependent on the presence of water, and as the biopolymers dehydrate they go from hydrogels to stiff biopolymer films and its overall strengthening efficiency increases drastically [54, 55]. Therefore, the tests were performed with the biopolymer to water concentration (m_b/m_w), by mass, in consideration. Two important concentrations to note are the initial mixing concentrations (m_b/m_{wi}) and the overall concentrations (in respects to the mass of water) as the samples dehydrate (m_b/m_w).

2.2.1 Materials

Two polysaccharide biopolymers were taken as the focus of this study. Xanthan gum was used in order to analyze the behavior of viscous biopolymers, and gellan gum was used for gelling biopolymers.

Xanthan Gum

Xanthan gum is an organic precipitate from the *Xanthomonas campestris* bacterium. As a result of its hydrocolloid rheology, it is commonly used as a viscosity thickener [64]. For geotechnical approaches, xanthan gum has been used to increase the strength of soils [47, 73] as well as reducing the hydraulic conductivity of soils through pore clogging [52, 74]. Its chemical structure and composition can be seen in Table 2.2.

Gellan Gum

Gellan gum is an organic precipitate formed from the microbe *Spingomonas elodea*. It has a high molecular weight as is commonly used as a substitute for agar gum [75, 76]. Gellan gum hydrates in water, but requires temperatures above 90°C in order to fully dissolve and form the double helix structure shown in Fig. 2.3. Similarly to xanthan gum, gellan gum has been used in the field of geotechnical engineering for soil improvement [77] and hydraulic conductivity reduction [51].

2.2.2 Experimental Apparatus

Viscosity

Viscosity measurement were taken using the DV2T Brookfield viscometer. The xanthan gum biopolymer was mixed at varying m_b/m_w ratios and testing was performed. The LV-4 spindle was used at 0.1 rpm in this study. It should be noted that shear thinning properties of xanthan gum (i.e. reduction in viscosity with higher strain rates) have been documented, however, they were not considered in this study due to the low loading rates in which the tests were performed. The viscosity measurements of gellan gum were not performed as the preparation of gellan gum resulted in a rigid gel.

Tensile Strength

For the measurements of tensile strength, a cantilever beam was used, as shown in Fig. 2.4. The sample was placed between two surfaces with a gap of approximately 2.5 mm. Samples were then dehydrated to varying m_b/m_w concentrations before testing. During testing the horizontal deflection of the cantilever was measured at failure, and the total deflection was kept within 5 mm in order to reduce the effects of moment on the samples.

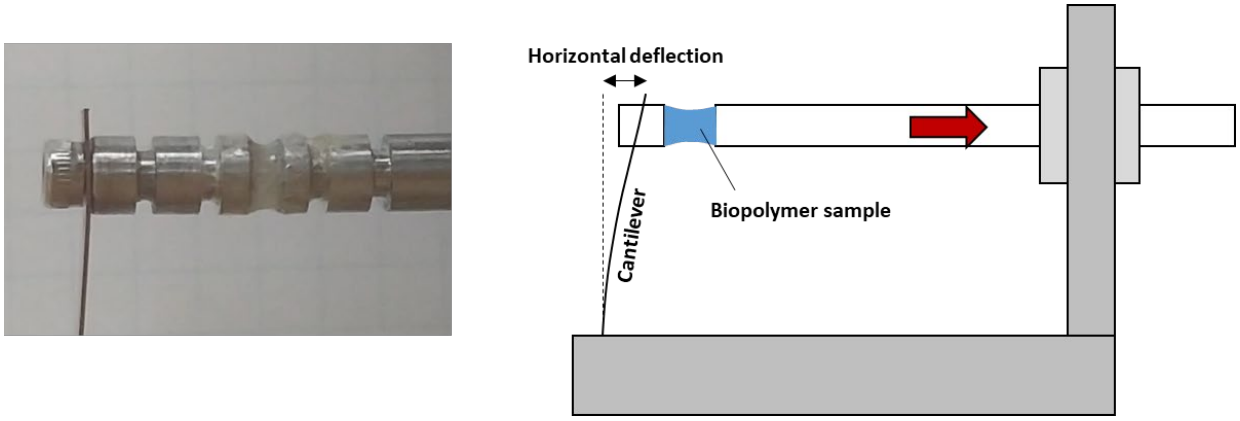

Fig. 2.4 Tensile Strength Apparatus

2.2.3 Testing Procedure

Xanthan Gum Sample Preparation

A xanthan gum solution was first prepared by dissolving powdered xanthan gum, purchased from SigmaAldrich (CAS #: 11138-66-2), into deionized water. The powder was

slowly poured into the beaker with the deionized water while a magnetic stirrer was used to mix the solution. The xanthan gum was added incrementally as to avoid the formation of powdered clumps forming in the solution. Once the solution was fully mixed, it was applied onto the testing apparatus. The initial mixing concentrations of xanthan gum to water are summarized in Table 2.4.

Gellan Gum Sample Preparation

Gellan gum solutions were prepared by dissolving the powder form of gellan gum, purchased from SigmaAldrich (CAS #: 71010-52-1), into deionized water heated to 90°C. The mixture was continually stirred using a magnetic stirrer and heat was constantly applied through a hot plate to maintain the temperature at approximately 90°C. The mixture was then allowed to fully dissolve and mix for approximately 15 min at which point a homogeneous mixture was formed. As gellan gum hardens into a hydrogel when cooled back down to room temperature, the mixture was applied to the testing apparatus at high temperatures before allowing the hydrogel to cool back down to room temperature. The initial mixing concentrations of gellan gum to water are summarized in Table 2.4.

Table 2.4 Initial biopolymer mixing concentrations

Biopolymer	Initial Preparation Concentrations m_b/m_{wi} (%)
Xanthan gum	2.5, 5.0, 7.5
Gellan gum	2.5, 5.0, 10.0

Viscosity Testing Procedure

Viscosity measurements were performed by preparing a xanthan gum solution at the desired biopolymer concentration and submerging the spindle to the target depth. Afterwards testing was performed at a strain rate of 0.1 rpm until the viscosity measurement were stabilized (approximately 5 min). The final measured value was taken as the viscosity of the xanthan gum solution at the given concentration.

Tensile Strength Testing Procedure

For the tensile measurements, the biopolymer solution was set between the two surfaces in Fig. 2.4 with a gap of approximately 2.5 mm. The solution was allowed to wrap over and into the grooves placed on either side to act as anchors for the biopolymers. These

anchors help ensure that the failure occurred through tensile strength and not adhesion between the biopolymer solution and the testing surface. With gellan gum, the biopolymer solution was applied onto the testing apparatus at 90°C before allowing the sample to cool down to room temperature. Weight measurements were taken before and after the samples were set, and before the testing was performed in order to accurately gauge the water loss in the sample through dehydration.

The samples were then dehydrated at room temperature up to various target water contents. Once the samples were dehydrated to the desired degree, loading was applied at a rate of approximately 1 mm/s until failure. Video recordings were taken to analyze the point of failure, deflection of the cantilever, and the cross sectional area of the biopolymer at failure. The cross-sectional areas of the samples were approximated using a combination of physical measurements, empirical estimations, and image analysis. All testing was performed at room temperature.

The concentration of biopolymers to water (m_b/m_w) was calculated using the known initial mixing concentrations (m_b/m_{wi}) and the measured water loss through dehydration. As the biopolymer amount in the sample is unchanging, but the amount of water is decreasing with dehydration, the m_b/m_w concentrations increase with dehydration. The tensile strength measurements were then plotted against the m_b/m_w concentrations at various degrees of dehydration. Calibration of the cantilever along with several images of the tests can be found in Appendix A.

2.3 Results and Analysis

2.3.1 Xanthan Gum

The viscosity measurement for xanthan gum can be seen in Fig. 2.5. As shown at low m_b/m_w concentrations the viscosity increases linearly to the xanthan gum concentration.

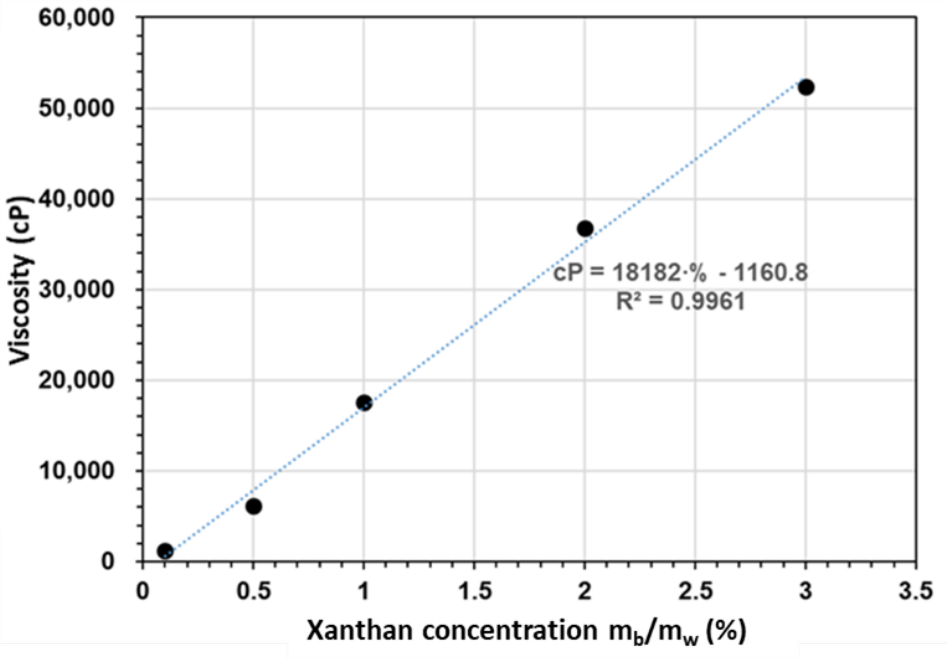

Fig. 2.5 Xanthan Viscosity

The tensile behavior of xanthan gum with dehydration can be seen in Fig. 2.6. From the data it was observed that regardless of the initial biopolymer mixing concentrations (m_b/m_{wi}), the tensile behavior was closely related to the overall m_b/m_w concentrations, showing that the initial mixing concentrations do not have a large variance on the tensile strength of xanthan gum. It was also seen that a maximum tensile strength of approximately 5.88 MPa was observed at m_b/m_w above 100%. Moreover, at approximately 20% m_b/m_w the tensile behavior was observed to drastically increase with dehydration.

These results indicate that there is a critical concentration at around 20% m_b/m_w at which there is a phase change in the xanthan gum solution from a hydrogel to a biopolymer film. It is from this point that the tensile strength increases with the hardening of the xanthan gum biopolymer films caused by dehydration. It can also be assumed that below the 20% m_b/m_w concentrations, the xanthan gum solution exhibits negligible tensile strength and the overall behavior is dictated by the viscosity measurement shown in Fig. 2.5.

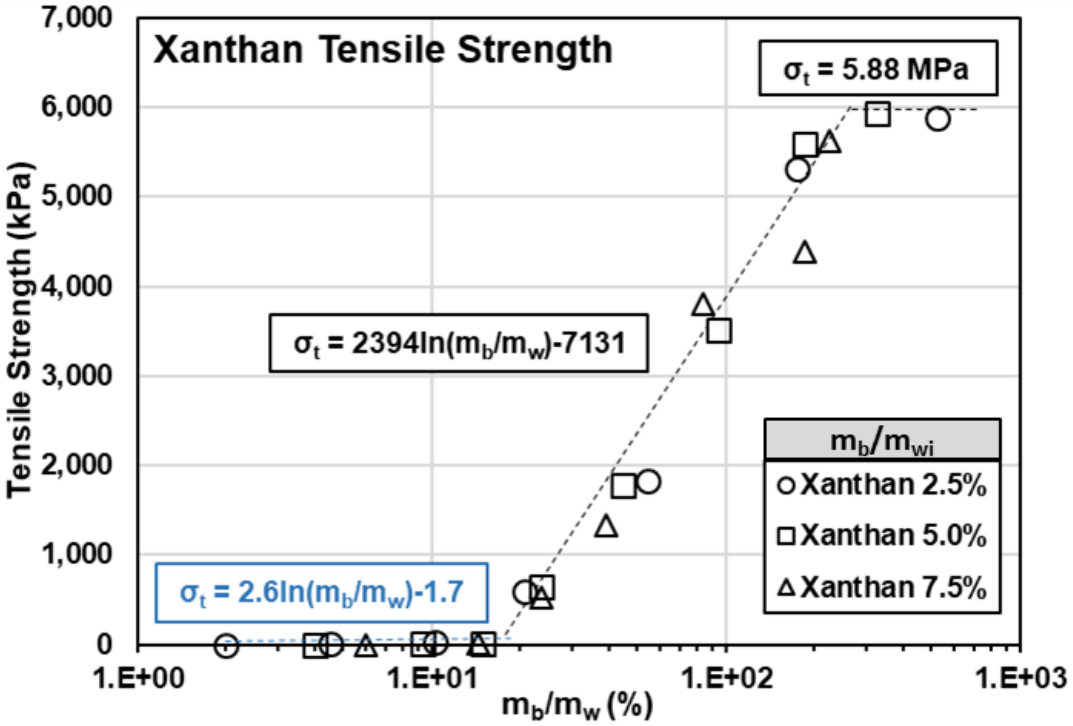

Fig. 2.6 Tensile Strength of Xanthan Gum

2.3.2 Gellan Gum

The tensile behavior of gellan gum can be seen in Fig. 2.7. Unlike xanthan gum the gelation effect of gellan gum exhibits a small amount of tensile strength even at lower m_b/m_w concentrations. As a result, at lower m_b/m_w concentrations, the differences in the initial biopolymer mixing concentration (m_b/m_{wi}) exhibit different tensile strengths (76, 149, and 232 kPa for 2.5, 5.0, and 10.0 m_b/m_{wi} respectively). One interesting thing to note was that similarly to xanthan gum, at approximately 15-20% m_b/m_w concentrations there is a spike in tensile strength, and at concentrations above this critical concentration, all the gellan gum tensile strengths seem to converge into a similar trend regardless of the m_b/m_{wi} concentrations. The maximum tensile strength of approximately 2.08 MPa is achieved at around 100% m_b/m_w concentrations.

Much like the behavior seen in the xanthan gum tensile strengths, these results indicate that above the critical concentration of approximately 20% m_b/m_w, there is a phase shift from a hydrogel to a biopolymer film. However, unlike xanthan gum, gellan gum exhibits a small degree of tensile strength at lower concentrations, due to its gelation properties, and the tensile strength at these points are highly dependent on the initial biopolymer mixing concentration (m_b/m_{wi}).

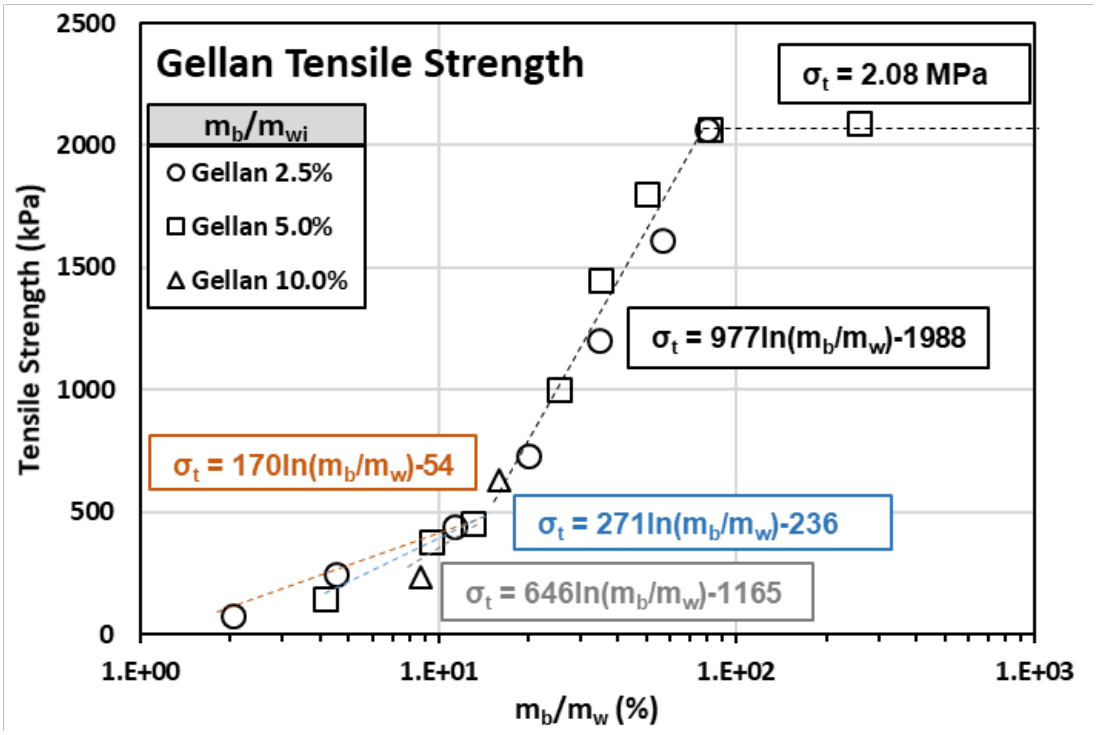

Fig. 2.7 Tensile Strength of Gellan Gum

2.4 Discussion

In regards to the chemical structure of the polysaccharides, viscous polysaccharide biopolymers did not allow for the restructuring of its molecules into a double helix formation while gelling polysaccharide biopolymers did. The different behaviors are due to the fact that the branching behavior of the viscous polysaccharide biopolymers did not easily allow for the restructuring of the polymers, resulting simply in a swelling behavior when subjected to water. On the other hand, gelling polysaccharide biopolymers were generally in the form of a linear polymer chain that is easily restructured into a double helix formation.

When observing the tensile behaviors of these polysaccharides, above a certain critical m_b/m_w concentration, approximately 20% m_b/m_w, there is a phase shift for both xanthan gum and gellan gum in which it goes from a hydrogel to a biopolymer film. Thus it can be said that at concentrations lower than the critical concentration the behavior of these polysaccharides are dictated by the chemical composition (i.e. viscosity and gelling strength), however, above the critical concentration, the behavior is largely dictated by the strength and stiffness of the biopolymer films.

Chapter 3. Uniaxial Compressive Behavior of Polysaccharide Biopolymers

In this chapter the uniaxial compressive strength (UCS) of xanthan gum and gellan gum treated sands are observed at varying water contents. Additionally, the UCS strengths are estimated using the tensile strengths found in Ch. 2.

3.1 Materials

For this study the xanthan gum and gellan gum biopolymers mentioned in Ch. 2 are used to treat jumunjin sand.

Jumunjin Sand

Jumunjin sand is the standard sand use in S. Korea. With a D_{50} of 1.0 mm, it is classified as a poorly graded sand (SP). Some common characteristics of jumunjin sand is as follows: coefficient of uniformity (C_u) of 1.94, coefficient of gradation (C_c) of 1.09, min and max void ratios (e_{min}, e_{max}) of 0.64 and 0.89 respectively, and a specific gravity (G_s) of 2.65. The particle size distribution curve of jumunjin sand is shown in Fig. 3.1.

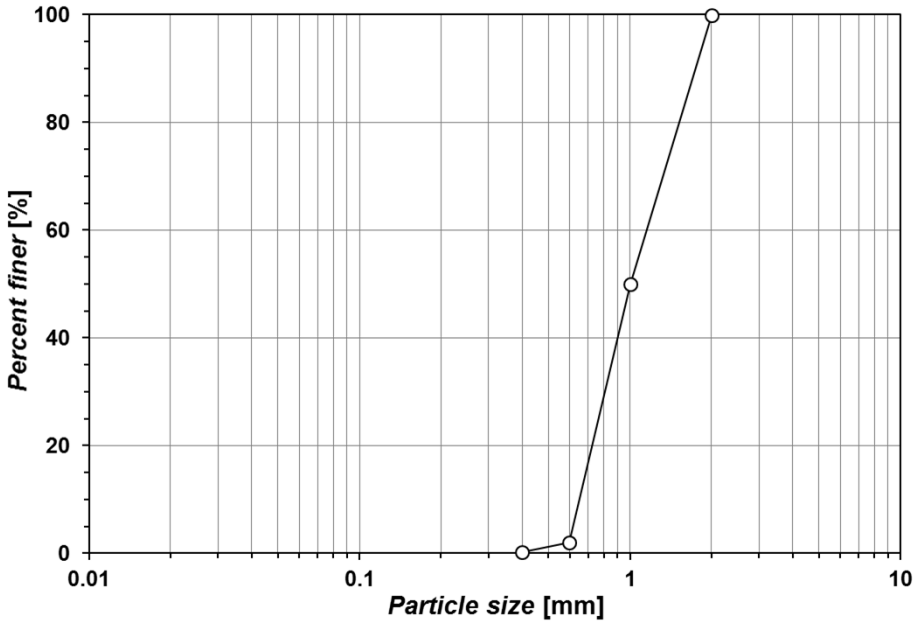

Fig. 3.1 Particle size distribution of jumunjin sand

3.2 Experimental Procedure

3.2.1 Sample Preparation

Xanthan Gum Treated Sand

For biopolymer treated sands, the concentrations were determined by the biopolymer mass to soil mass (m_b/m_s) along with the biopolymer to water mass (m_b/m_w). The preparation of a xanthan gum solution was identical to that explained in Ch. 2. Samples were prepared with an initial mixing water content at 20%, and the xanthan gum concentrations were set at 0.5, 1.0, and 1.5% m_b/m_s or 2.5, 5.0, and 7.5% m_b/m_{wi}. Once the xanthan gum solution was fully prepared, it was directly mixed with jumunjin sand and molded into 40 mm cubic molds and left to dry at room temperature. The samples were then tested at varying points in the dehydration process.

Gellan Gum Treated Sand

The preparation of a gellan gum solution was identical to that explained in Ch. 2. Samples were prepared at an initial mixing water content of 20%. The gellan gum concentrations were set at 0.5, 1.0, and 2.0% m_b/m_s or 2.5, 5.0, and 10.0% m_b/m_{wi}. When the gellan gum was fully dissolved, it was directly mixed with jumunjin sand at 90°C and molded into 40 mm cubic molds. The samples were then left to cool down to room temperature. Once the samples were cooled to room temperature, there were left to dry at room temperature. The samples were tested at varying points in the dehydration process.

3.2.2 Testing Procedure

Once the target water content was achieved, the UCS tests were performed using the Humboldt master loader (HM-5030.3F). Loading of the samples were performed at 0.4 mm/min (1%/min) up to a maximum strain of 15%. An average of 3 samples were taken for each data point. The samples were also tested right after the samples were made and molded (wet condition), after 2 weeks of drying at room temperature (dry condition), and resubmerged in water for 24 hrs after drying (resubmerged condition) for comparison.

3.3 Results and Analysis

3.3.1 Xanthan Gum Treated Sand

UCS results for xanthan gum treated sands can be seen in Fig. 3.2. Results showed that higher xanthan gum concentrations (m_b/m_s) resulted in a nearly linear increase in overall dry strength. It is also noted that the strength of the xanthan gum treated sands increase exponentially at the lower water contents.

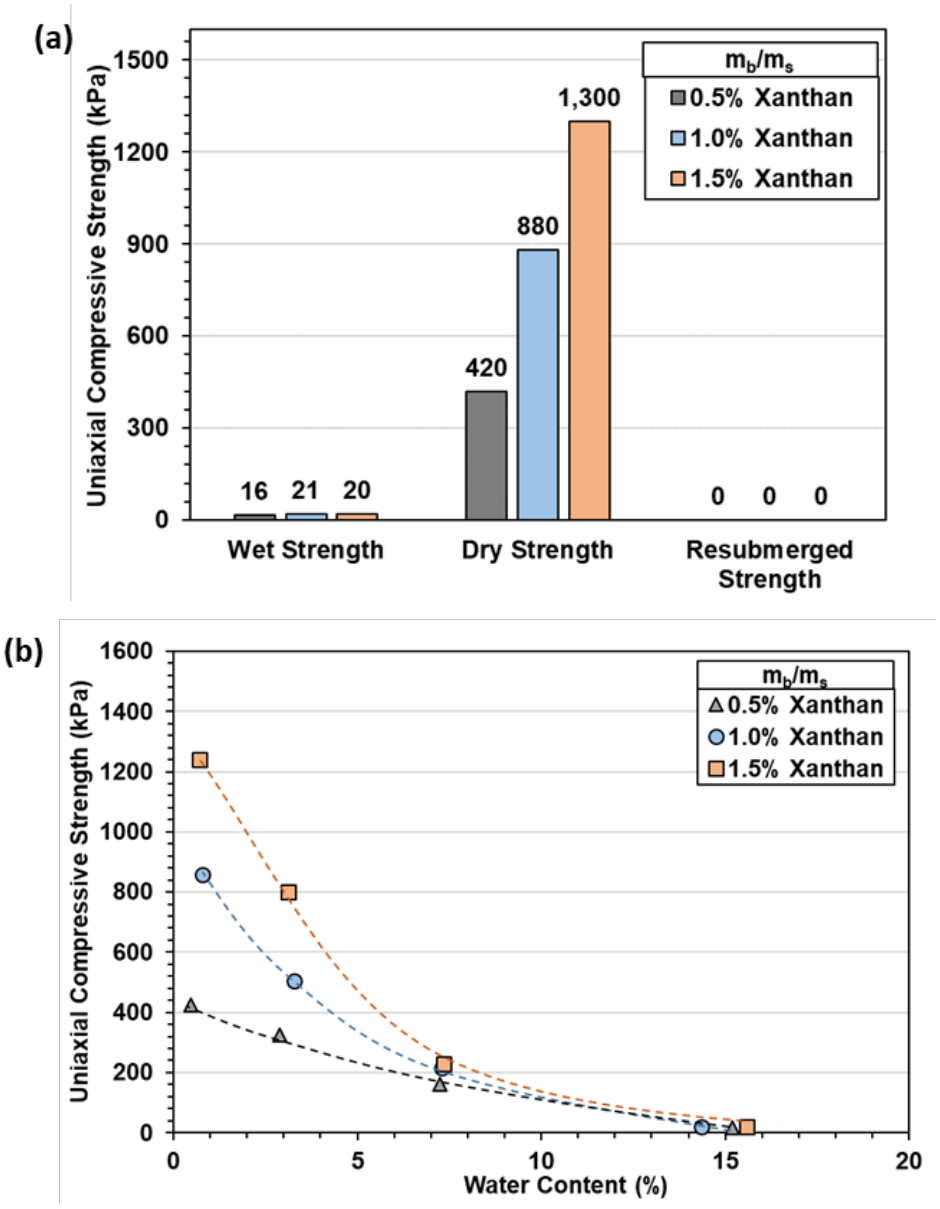

Fig. 3.2 UCS of xanthan gum at (a) dry, wet and resubmerged conditions and (b) with water content

3.3.2 Gellan Gum Treated Sand

UCS results of gellan gum treated sands are shown in Fig. 3.3. The dry strength is shown to be proportional to the gellan gum concentration. It is also noted that due to the formation of a rigid gel, gellan gum treated sands have a significantly higher strength at higher water contents in comparison to xanthan gum treated sands. However, the resubmerged condition shows a significant decrease in strength from the wet condition. This indicates that through the process of drying, the double helix structure that makes up the gellan gel is partially disrupted.

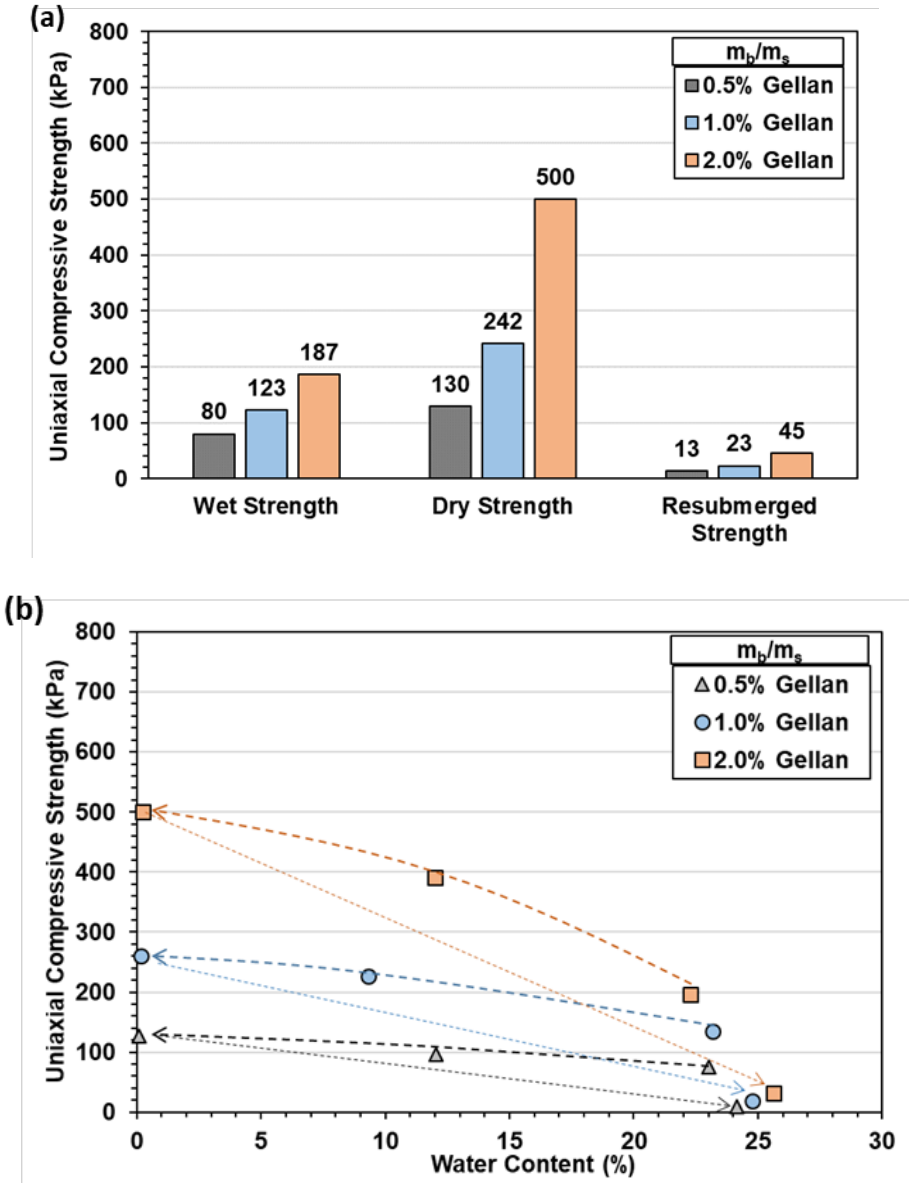

Fig. 3.3 UCS of gellan gum at (a) dry, wet and resubmerged conditions and (b) with water content

3.4 Strengthening Modelling

3.4.1 Theoretical Modelling

A strengthening modelling of biopolymers on sand particles was used to estimate the UCS from the biopolymer tensile strengths. It is assumed that the strengthening behavior closely follows that shown in Fig. 3.4, where F_T is the maximum tensile force applied by the biopolymer, A_{BP} is the cross sectional area of the bonded area, A_S is the total cross sectional area of the sand, and R is the radius of the sand particle. In the book *physicae experimentales et geometricae* by Musschenbroek (1729) it is mentioned that for construction materials, the tensile strength is approximately equal to the shear strength (cohesion) of the material, which was also confirmed in Coulomb's (1773) paper [78, 79]. By acting as a bonding material at the particle contact, it can be assumed that the biopolymer provides cohesion to the sand particles in the form of tensile strength (σ_T) acting over the bonding area (A_{BP}), and that the maximum strength at failure is the cohesive force provided by the biopolymer bond. With these considerations equations (3.1) and (3.2) can be derived.

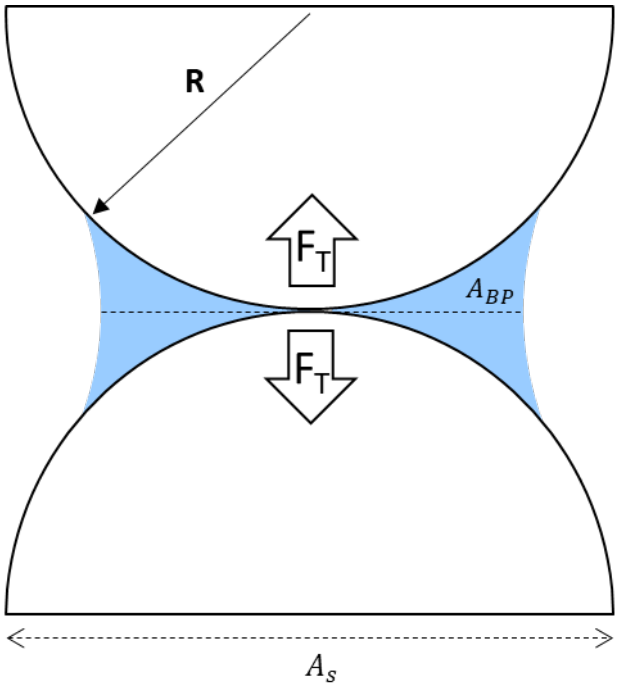

Fig. 3.4 Strengthening model of polysaccharide biopolymers on sand particles

$$UCS = F_T/A_S \quad (3.1)$$

$$F_T = \sigma_T * A_{BP} \quad (3.2)$$

Equations (3.1) and (3.2) can be simplified as:

$$UCS = \sigma_T * A_{BP}/A_S \quad (3.3)$$

As the tensile strength of the biopolymers (σ_T) were measured in Ch. 2, the cross sectional area of the biopolymers (A_{BP}) at various water contents is necessary in order to estimate the F_T provided by the biopolymers.

3.4.2 Micro-Fluid Chip Experiments

In order to understand the drying mechanisms of these biopolymers, micro-fluid chip (MFC) experiments were carried out by Sojeong Lee at the University of New South Wales (UNSW) Canberra.

Experimental Setup

The MFC experiment was conducted as shown in Fig. 3.5. A thin chip with circular columns simulating sand particles were used, and a biopolymer fluid was injected into the voids between the columns. The samples were allowed to dry and a DSLR camera was used to observe the drying process from a top down viewpoint. As the internal thickness within the chips are only 100 μm, the top down images obtained can be considered to be a reasonable approximation of the cross sectional saturation levels of biopolymers in sands. Various chips were used with varying spacing between the columns in order to simulate different porosity conditions.

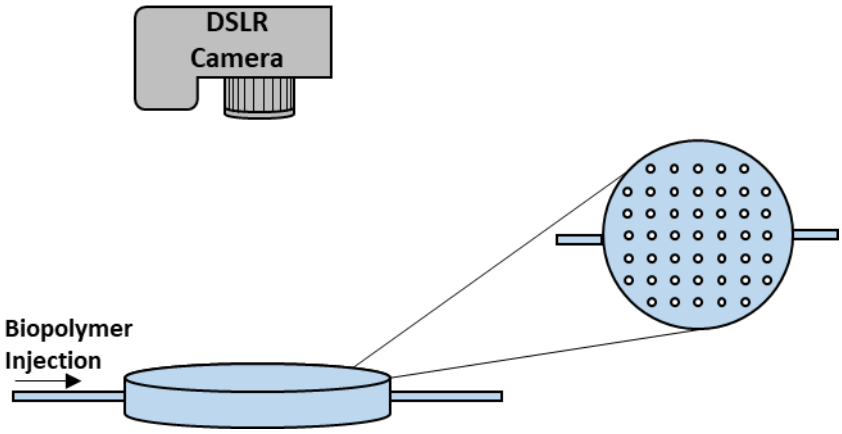

Fig. 3.5 Micro-fluid chip experimental setup

Results and Analysis

Typical results of the MFC experiment can be seen in Appendix B. These images were analyzed to approximate the biopolymer cross sectional saturation (S_{BP}) at various points in the drying process. As the samples dehydrated, the m_b/m_w concentrations increased, and the S_{BP} was plotted against the m_b/m_w concentrations, shown in Fig. 3.6. The S_{BP} in comparison with the normalized mb/mw are shown in Fig. 3.7.

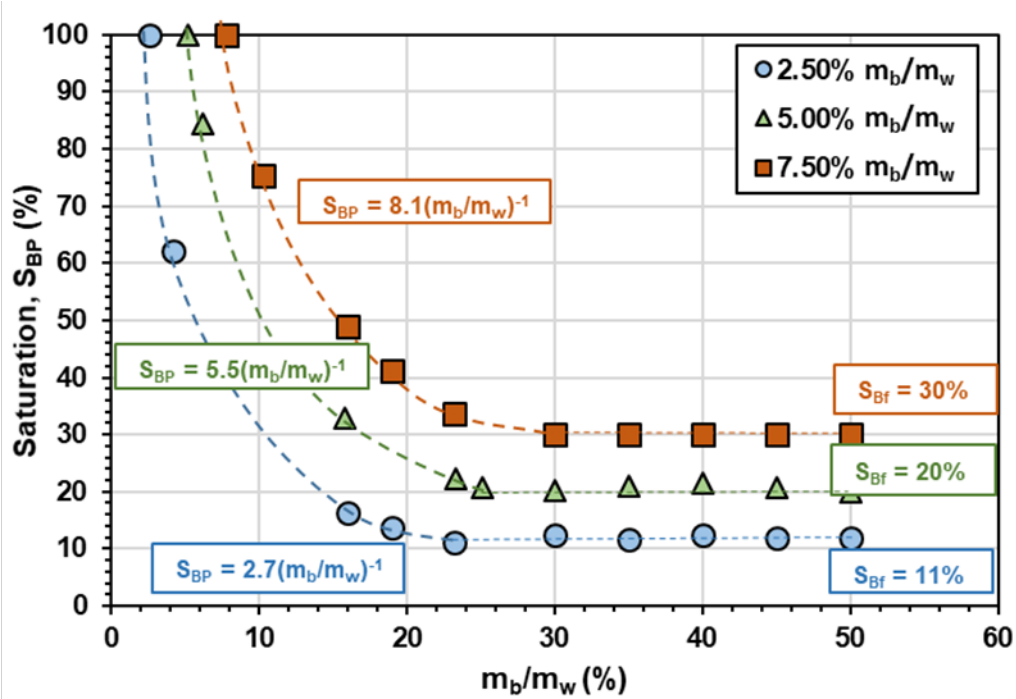

Fig. 3.6 Biopolymer cross sectional saturation (S_{BP}) with drying

In Fig. 3.7 we can see that at higher water contents, regardless of the initial biopolymer mixing concentration (m_b/m_{wi}), the dehydration of the samples results in the same saturation path, however at a certain point further dehydration of the samples does not result in a decrease in the S_{BP}. It can be seen that as the samples dehydrate (m_b/m_w concentrations increase) a final cross sectional biopolymer saturation level (S_{Bf}) is achieved. Moreover, the S_{Bf} increases almost linearly with the m_b/m_{wi} biopolymer concentrations. It was also noted that the point at which the S_{Bf} was achieved fell around the 20 - 25% m_b/m_w concentrations (Fig. 3.6), which is within the range of the critical concentration found in Ch. 2. Therefore, it can be assumed that the critical concentration (approximately 20% m_b/m_w) is the point at which the final biopolymer volume is achieved as the biopolymer shifts from a hydrogel to a biopolymer film.

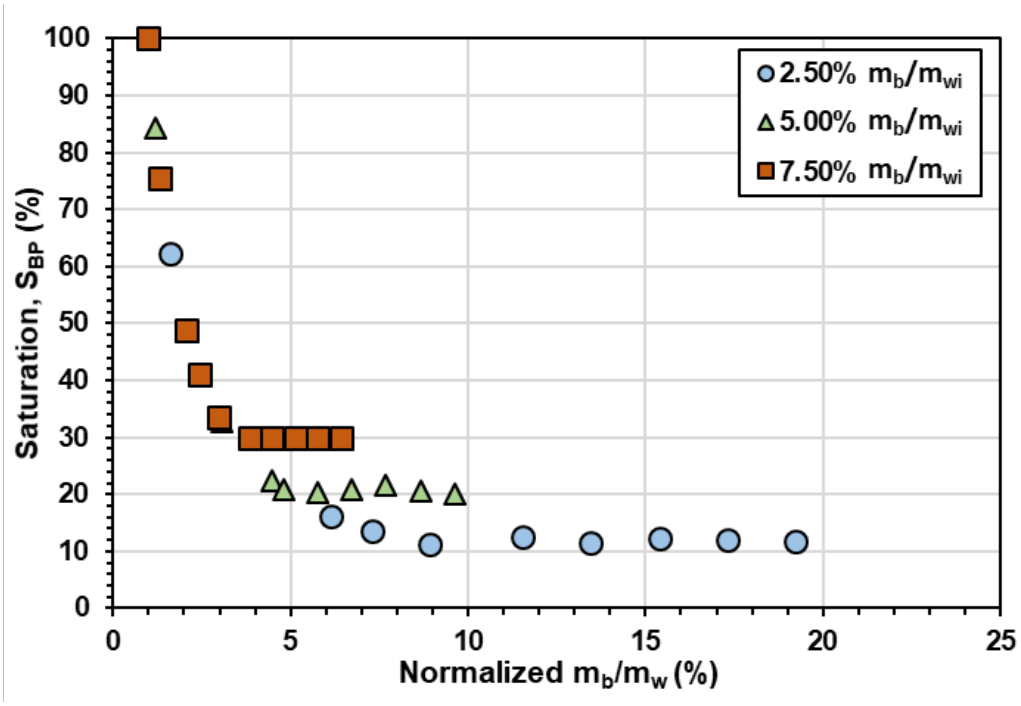

Fig. 3.7 Normalized biopolymer cross sectional saturation (S_{BP}) with drying

As the S_{Bf} was shown to be directly proportional to the m_b/m_{wi} biopolymer concentration, the S_{Bf} with regards to the soil porosity normalized by the m_b/m_s biopolymer concentrations is shown in Fig. 3.8. The results show that at lower porosity values, the S_{Bf} increases, while at higher porosity values the S_{Bf} decreases. This behavior falls in line with the expected results as when the soil particles are further apart, the biopolymers are stretched thin and the resulting cross sectional areas are smaller.

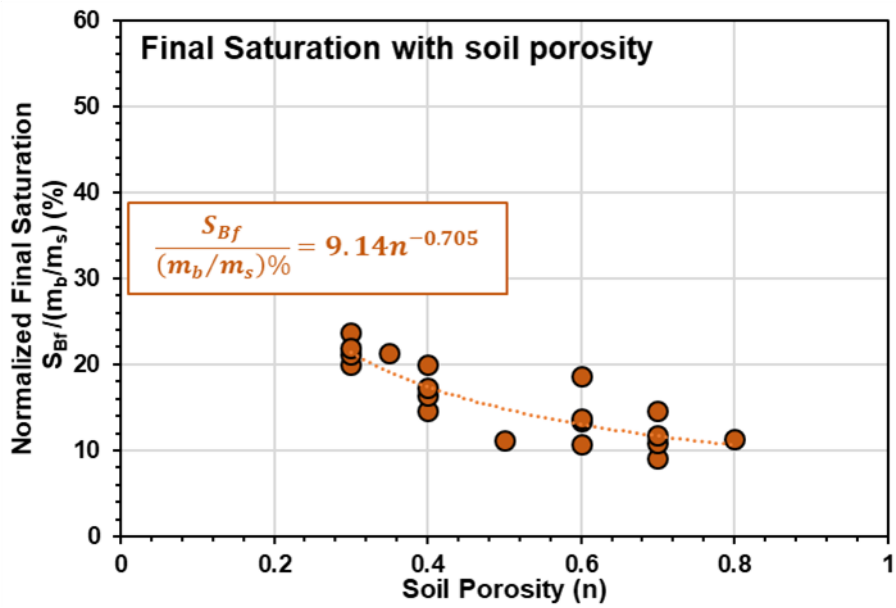

Fig. 3.8 Final biopolymer cross sectional saturation (S_{Bf}) normalized with the m_b/m_s biopolymer concentration

3.4.3 Model Comparison

As $A_{BP}/A_S = S_{BP}$, equation (3.3) can be further simplified as follows:

$$UCS = \sigma_T * S_{BP} \tag{3.4}$$

From the model presented in Fig. 3.4 it was assumed that all the biopolymers coagulated around the contact points to provide cohesion, however, from Fig. 3.9 it can be seen that that is not the case, and a portion of the biopolymers coagulate along the surface of the particles not the contact points. Therefore, images of MFC results were used to approximate the ratio of biopolymers that coagulated onto the contact points (R_C), shown in Fig. 3.10.

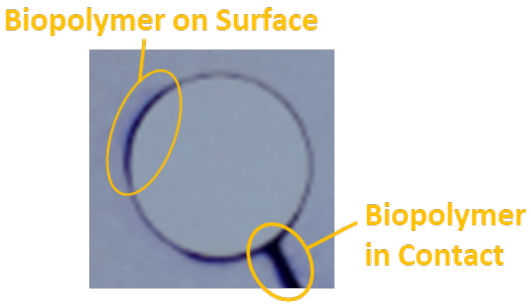

Fig. 3.9 Biopolymer coagulation around particle to particle contact and particle surface

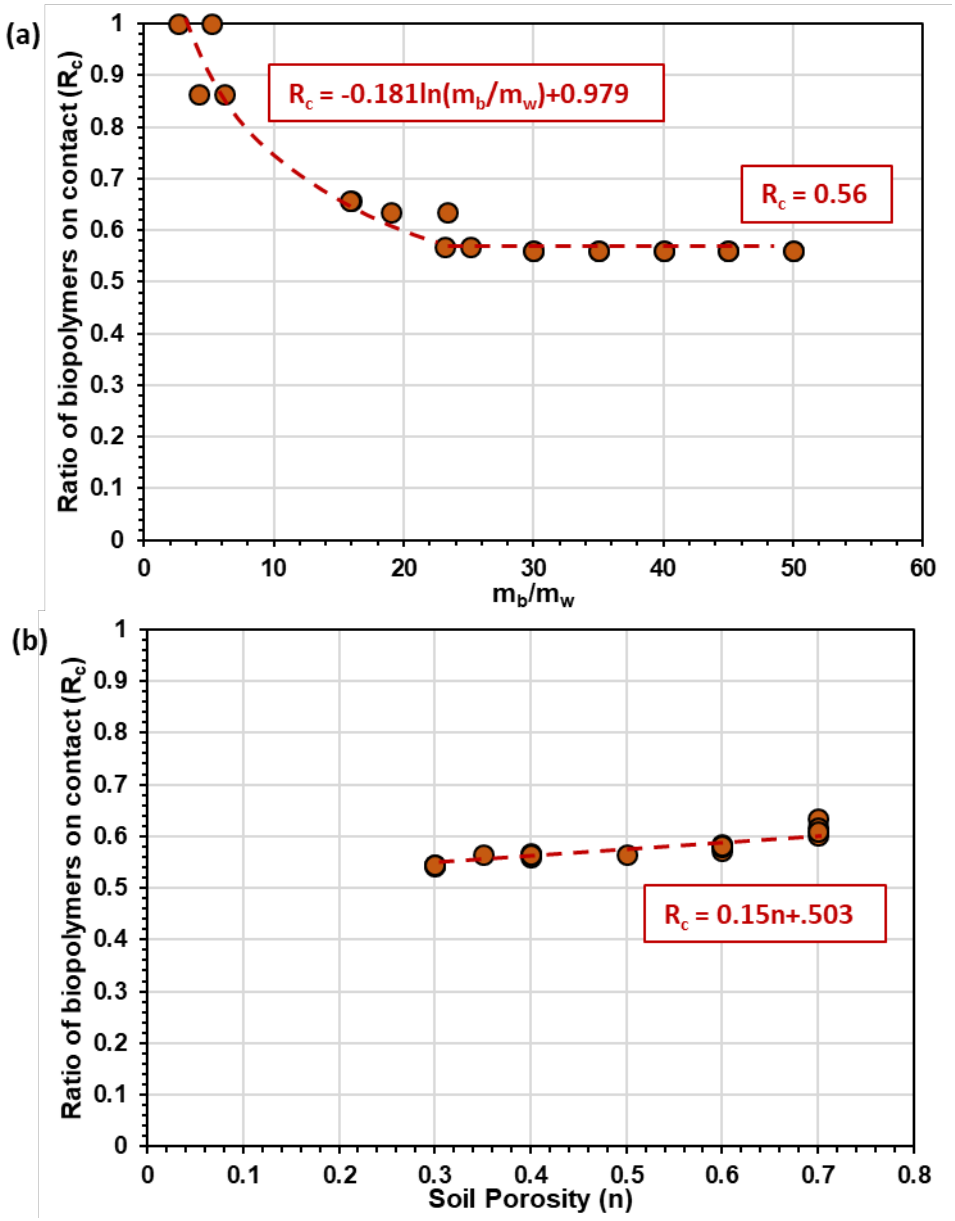

Fig. 3.10 Ratio of biopolymers coagulated onto the sand contact points (a) with dehydration and (b) by porosity

Results show that the R_C averaged at around 0.56 throughout the various porosity conditions regardless of the m_b/m_{wi} biopolymer concentrations. With dehydration, the R_C went from 1 and converged to approximately 0.56. From this, equation (3.4) can be rewritten as follows:

$$UCS = R_c * \sigma_T * S_{BP} \quad (3.5)$$

Using the R_C values obtained in Fig. 3.10, the σ_T values obtained in Ch. 2, and the S_{BP} values obtained in Fig. 3.6, the theorized UCS can be compared with the experimental results obtained in section 3.3. By using a porosity value of 0.48 and 0.22 to estimate the behavior at a simple cubic packing and tetrahedral packing conditions respectively, the lower bound and upper bound of the biopolymer treated sands was theorized. The results are shown in Fig. 3.11 for xanthan gum treated sands and Fig. 3.12 for gellan gum treated sands.

In both cases, the fully dehydrated experimental results showed that they fell within range of the upper and lower bounds of the model. However, at higher water contents, the model underestimates the experimental data. This difference is due to the heterogeneity of drying in the samples, shown in Fig. 3.13.

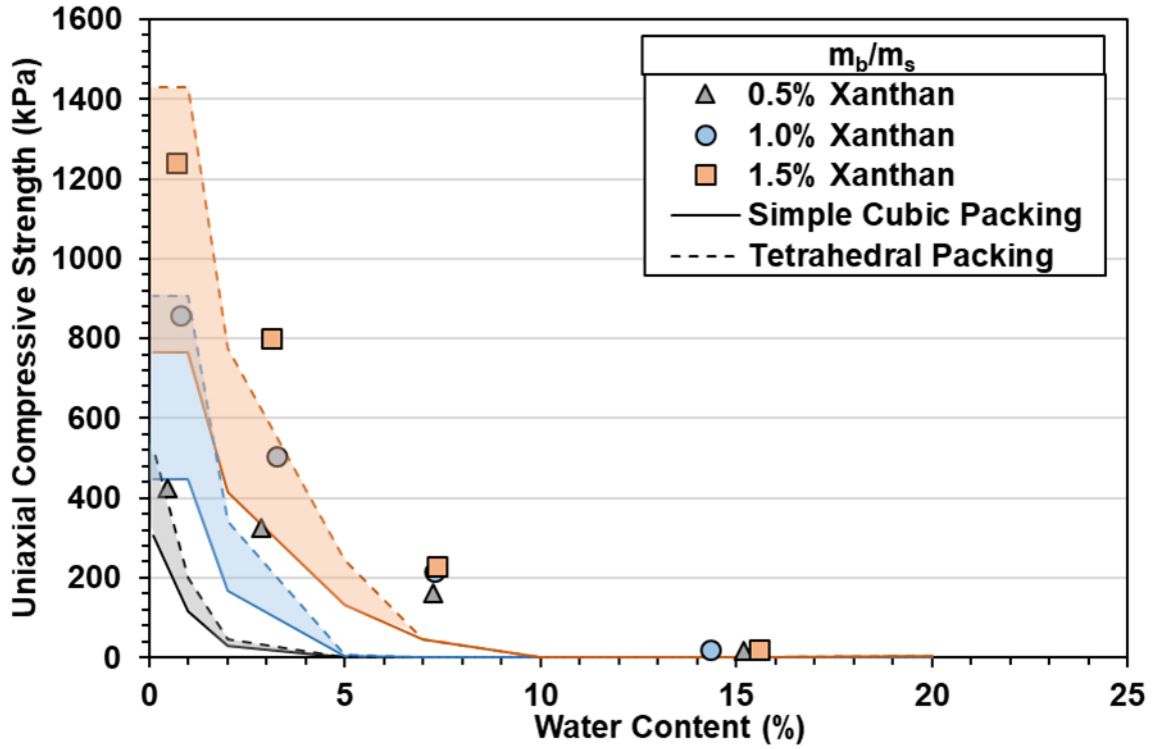

Fig. 3.11 Theoretical modeling of xanthan gum treated sands

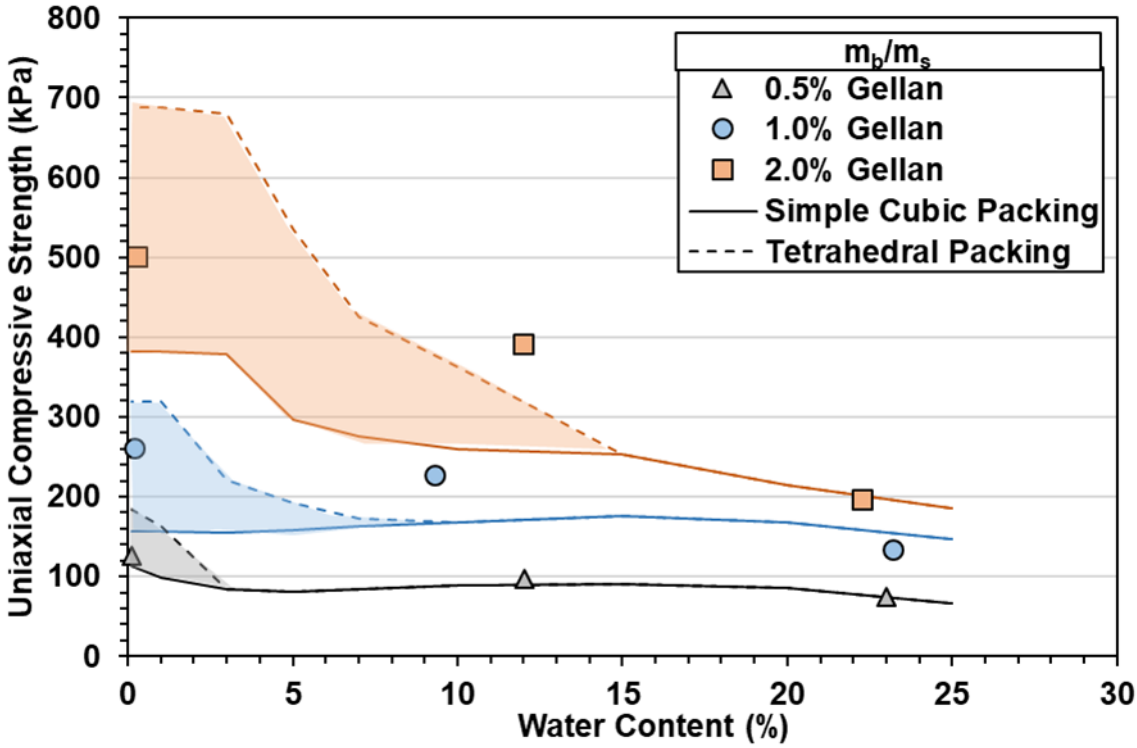

Fig. 3.12 Theoretical modeling of gellan gum treated sands

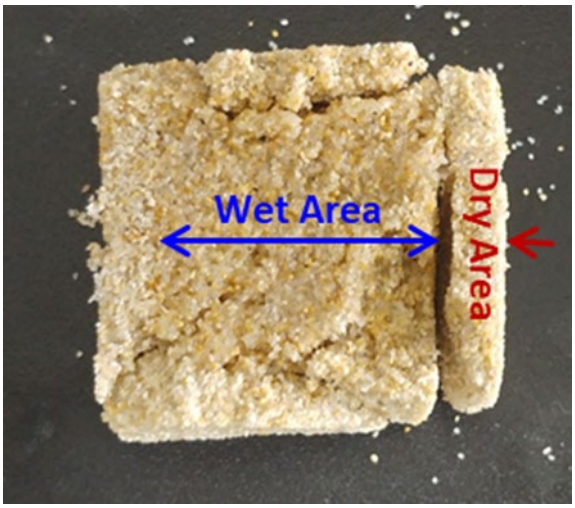

Fig. 3.13 Heterogeneity of sample dehydration

3.5 Discussion

The strengthening model presented in Fig. 3.11 and 3.12 show a decently well fit at low water contents. This shows that the tensile strengths of the biopolymers obtained in Ch. 2 can be used to estimate the overall strengthening capabilities of biopolymer treated sands. Moreover, differences between the xanthan gum and gellan gum treated sands shows that the viscosity of the biopolymer does not have a large impact on the strength of the soil, which seems to be mostly dictated by the tensile strength of the biopolymers.

It was also noted that the differences in strength between the different m_b/m_s biopolymer concentrations was plainly due to the increased volume of the biopolymer bonded areas, and it can be estimated that higher m_b/m_s biopolymer concentrations may not show a linear increase in strength due to the physical limitations of the pore volume.

Additionally, the MFC experiments also showed that the critical concentration (approximately 20% m_b/m_w) shown in Ch. 2 was the point at which the biopolymer solution reached its final saturation level as it went from a hydrogel to a biopolymer film.

Chapter 4. Triaxial Behavior of Polysaccharide Biopolymers

In the previous chapter the behaviors of biopolymer tensile strength on the strengthening of sand was observed. Results showed that the strengthening mechanisms were mostly dictated by the tensile strength of the biopolymers with viscosity having little to no effect on the strength of the sands. However, in order to fully understand the effects of these biopolymers in sands, the effects of viscosity and gelation on the behavior of sands during loading are investigated in this chapter through the use of triaxial tests.

4.1 Experimental Procedure

4.1.1 Testing Apparatus

The experimental apparatus for the triaxial test is shown in Fig. 4.1. Loading of the samples were performed by the Humboldt master loader (HM-5030.3F). The measurement data included the maximum load, cell pressure, pore pressure, and volume change.

One thing to note was that the use of xanthan gum and gellan gum have been found to greatly reduce the hydraulic conductivity of jumunjin sand, as seen in Fig. 4.2. As a result, fluid flow into and out of the sample is expected to be greatly limited. Therefore, the volume change was measured through both the sample pipette and cell pipette for accurate measurements. In Fig. 4.3 the volume change measured by both the cell and sample pipette are shown for untreated sands. The results show that they are nearly identical making this method a viable method for measuring the volume change of these biopolymer treated sands.

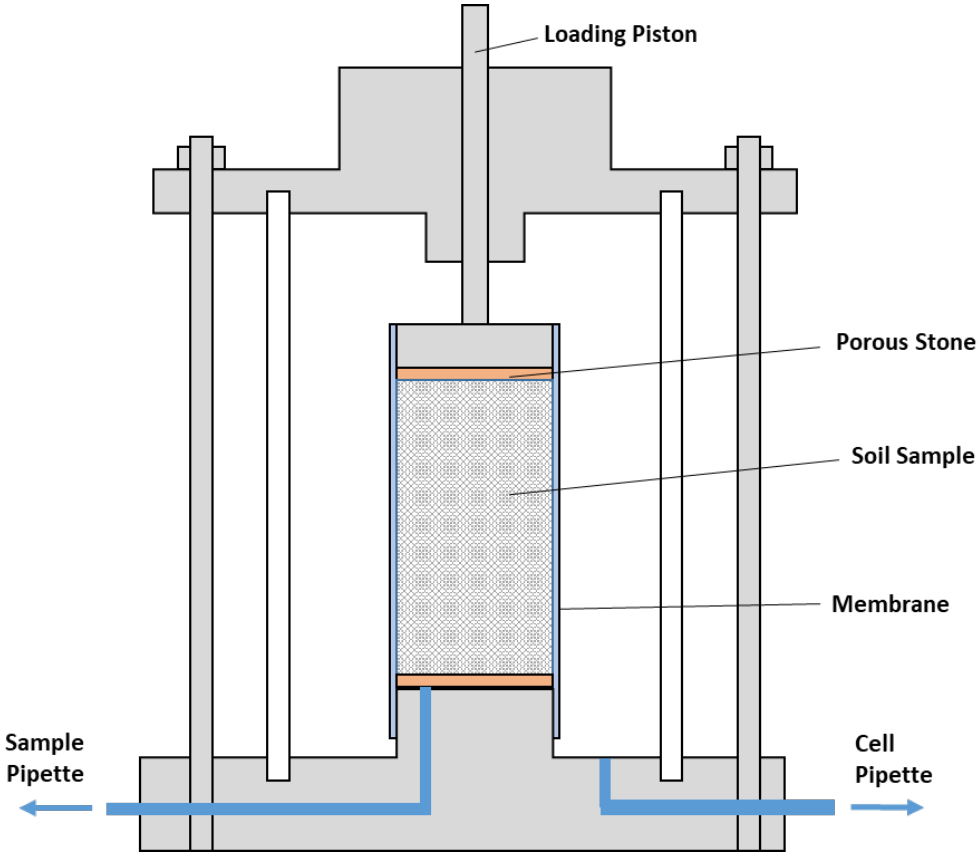

Fig. 4.1 Triaxial testing apparatus

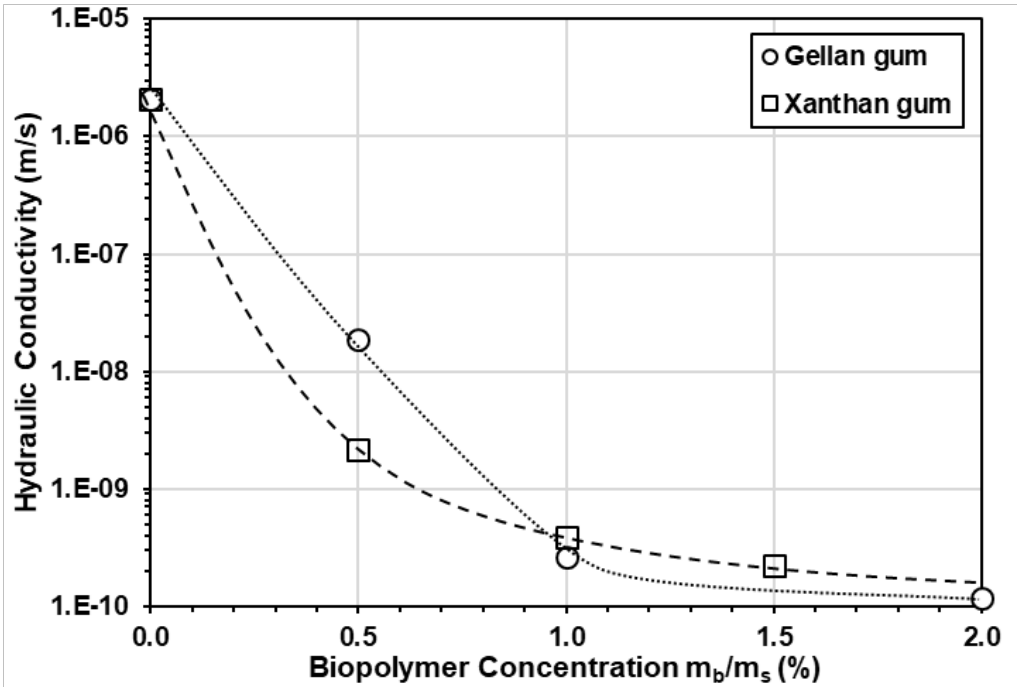

Fig. 4.2 Hydraulic conductivity of xanthan gum and gellan gum treated sands

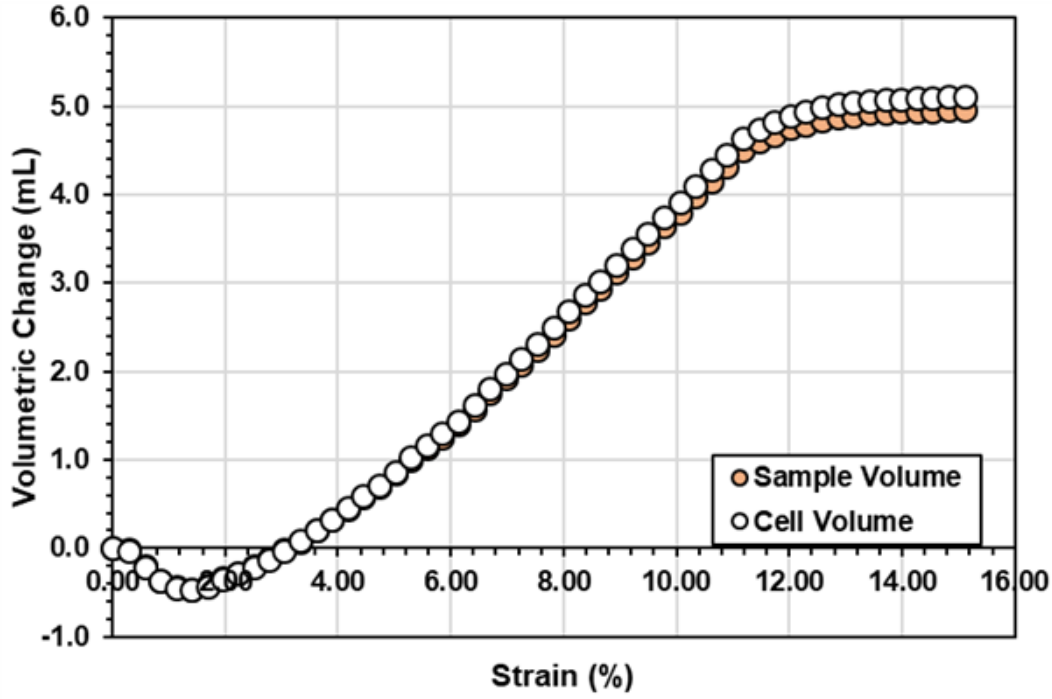

Fig. 4.3 Volume change measurement via sample and cell pipettes of untreated sand

4.1.2 Sample Preparation

Triaxial tests were performed for both biopolymer treated and untreated sands. The sands were testing in both the dense and loose conditions with a target relative density of 0.58 and 0.25 respectively after consolidation. The triaxial molds used in this study were cylindrical molds with a diameter of 50 mm and a height of 100 mm.

Untreated Sands

For dense conditions, a vacuum pressure of 10 kPa was used to hold a membrane against the mold and dry untreated sand was directly poured into the mold from a height of approximately 12 cm. The sand was compacted mostly through settlement with porous stones placed on the top and bottom of the sample. Using o-rings on the top and bottom caps of the sample the samples were sealed within the membrane and a vacuum pressure of 10 kPa was applied onto the soil and the sample's volume measurements were taken at this point. The triaxial test apparatus was then fit around the sample and the triaxial cell was filled with de-aired water. Once the cell was filled with de-aired water, the vacuum applied on the sand was

slowly released while a cell pressure of 10 kPa was applied to hold the specimen during saturation.

CO_2 flushing was utilized during the saturation process. CO_2 was applied into the soil at 5 kPa for a period of 30 min. Afterwards the sample was vacuumed at 5 kPa before CO_2 was reapplied onto the soil. This process was repeated 3 times before the samples were saturated. The samples were saturated using a back pressure of 5 kPa and until approximately 2 volumes worth of the sample size in water (≈ 200 mL) had flowed through the system. Tests were conducted at a B value of 98% or higher. Any volume change that may have occurred in the sample with saturation was monitored using the cell pipette.

For the loose condition, the wet tamping method was used to prepare the samples. A water content of 5% was first mixed into the sand before the sand was placed into the triaxial mold. The samples were lightly compacted at 2 cm intervals at achieve the target dry density conditions. The sample preparation and saturation process was identical to that of the dense conditions.

Xanthan gum Treated Sands

For xanthan gum treated sands, a biopolymer solution was first made and mixed with sand before being placed in the triaxial mold. The biopolymer solution was prepared as mentioned in Ch. 2 and mixed directly into the dry sand. The biopolymer to soil concentrations (m_b/m_s) of 0.5, 1.0, and 1.5% (≈ 2.5, 5.0, and 7.5 m_b/m_{wi}) were used. Due to the high viscosity of the biopolymer solution, the dry density of the biopolymer treated sands could be easily controlled by adjusting the initial mixing water content. For dense conditions (relative density ≈ 0.58 after consolidation) an initial mixing water content of approximately 20% was used, while for loose conditions (relative density ≈ 0.25 after consolidation) an initial mixing water content of 24% was used. As previous analysis on jumunjin sand indicated that at the target density a water content of 19.7% was required for full saturation, the biopolymer solution was assumed to have fully saturated the pore spaces in the sands. The same processes were used to fix and saturate the biopolymer treated sands in the triaxial apparatus as in the untreated sands. One thing to note was that due to the low hydraulic conductivity of the biopolymer treated sands, accurate measurements of the B value were difficult, but the exact same saturation processes were used as the untreated sands.

Gellan gum Treated Sands

Similarly to xanthan gum, gellan gum treated sands were first made before it was placed into the triaxial mold. The gellan gum solution was prepared as mentioned in Ch. 2 and mixed into the sand at 90°C. Gellan gum concentrations were set at 0.5, 1.0 and 2.0% m_b/m_s. (≈ 2.5, 5.0, and 10.0 m_b/m_{wi}) The hot mixture was then placed in a paper mold of 50 mm diameter and 100 mm height before cooling down to room temperature. After the gellan treated sands had reached room temperature, the sample was removed from the mold and fixed to the triaxial testing apparatus. The dry density of the gellan gum treated sands were controlled by the initial mixing water content (20% water content for dense condition, 24% water content for loose condition). The same processes were used to fix and saturate the biopolymer treated sands in the triaxial apparatus as in the untreated sands. As the gellan treated sands exhibited low hydraulic conductivity conditions, the accurate measurements of the B value were difficult, but the exact same saturation processes were used as the untreated sands.

4.1.3 Testing Procedure

Consolidated Drained (CD) Tests

Consolidated drained tests were performed by applying a pore pressure of 10 kPa onto the sample with a cell pressure of 60, 110, 210, and 310 kPa for an effective confining pressure of 50, 100, 200, and 300 kPa respectively. Samples were consolidated and the volume change was measured through both the cell and sample pipettes. Consolidation was applied onto the samples for 24 hrs, or until no further volume change was observed over a 3 hr span. The drained tests were performed at a strain rate of 1% (1 mm/min) up to a maximum strain of 15% or until the critical state of the soil was achieved. Volume change measurements were taken by both the cell and sample pipettes. At least 3 tests were conducted for the same conditions to check for reliability.

Consolidated Undrained (CU) Tests

Consolidated undrained tests were performed by applying a pore pressure of 200 kPa on the sample with a cell pressure of 250, 300, 400, and 500 kPa for an effective confining pressure of 50, 100, 200, and 300 kPa respectively. Consolidation was applied onto the samples for 24 hrs, or until no further volume change was observed over a 3 hr span. During

loading, the valves into the sample were closed to prevent fluid flow and testing was performed at a strain rate of 1% (1 mm/min) up to a maximum strain of 15% or until the critical state of the soil was achieved. The cell pipette was observed for any changes that may have occurred in the volume. At least 3 tests were conducted for the same conditions to check for reliability.

Liquefaction (Loose Consolidated Undrained) Tests

In order to test the liquefaction capabilities of biopolymer treated sands, consolidated undrained tests were performed in loose sands. For this condition, a pore pressure of 20 kPa was applied onto the samples and a cell pressure of 50 kPa was applied for an effective confining pressure of 30 kPa. Samples were consolidated for 24 hrs and loading was applied at a strain rate of 1% (1 mm/min) up to a maximum strain of 15% or until liquefaction of the samples were observed. Loading was conducted in the undrained conditions. The cell pipette was observed for any changes that may have occurred in the volume. At least 3 tests were conducted for the same conditions to check for reliability.

4.2 Results and Analysis

4.2.1 Untreated Sand

The consolidated drained tests for dense untreated sands are shown in Fig. 4.4 and Fig. 4.5. As shown, the sands exhibited expansive behavior with a cohesion of 17.3 kPa and a friction angle of 28.0°. The critical state line of untreated jumunjin sand can be seen in Fig. 4.5b.

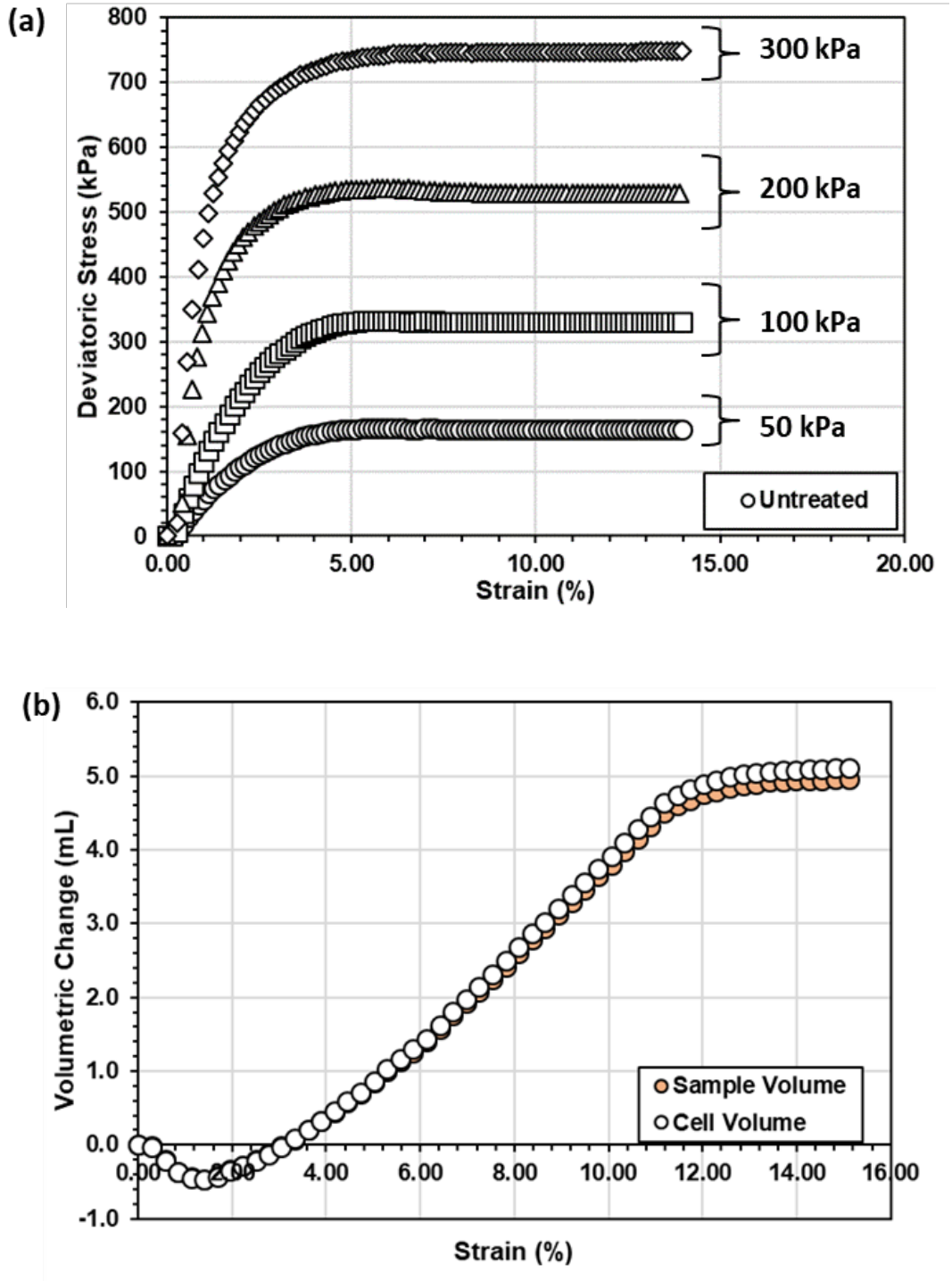

Fig. 4.4 (a) Stress strain curve and (b) typical volume change of CD dense untreated sand

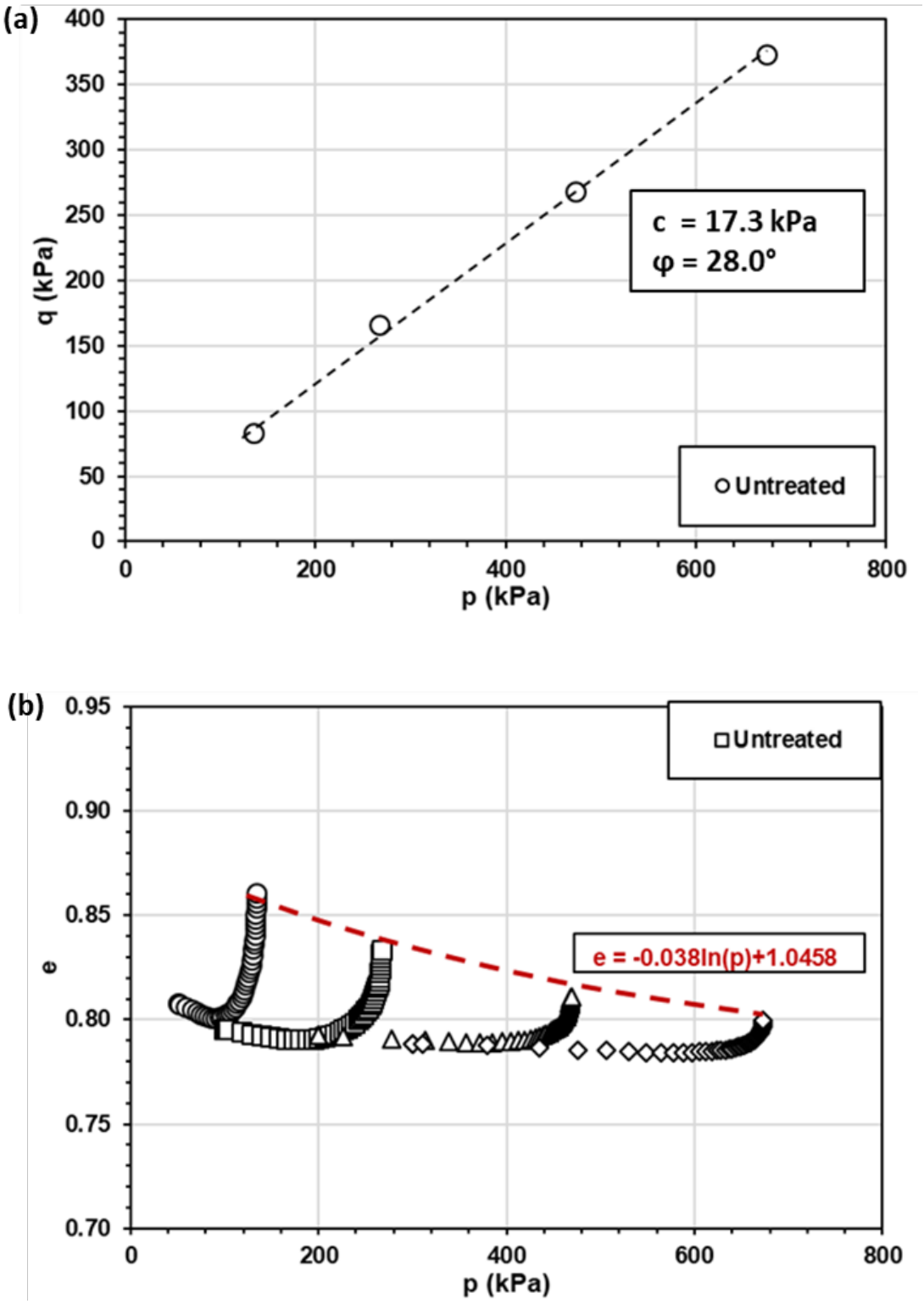

Fig. 4.5 (a) Mohr Coulomb failure curve and (b) critical state line of CD dense untreated sand

4.2.2 Xanthan Gum Treated Sand

Dense Consolidated Drained (CD) Tests

The effects of xanthan gum on CD dense conditions of sand are shown in Fig. 4.6 and Fig. 4.7. Results showed that the use of xanthan gum did not have any significant strengthening effect on the sands. As the m_b/m_w used in this chapter were all below the critical concentration (≈ 20% m_b/m_w) the xanthan gum present in the sand can be considered to have negligible tensile strength (Fig. 2.6), and therefore no strengthening effect.

One thing to note was that, as the hydraulic conductivity of biopolymer treated sands were extremely low, there was a discrepancy between the measured volume change from the cell pipette and the sample pipette. As the cell pipette was not limited by a low hydraulic conductivity, measurement taken from the cell pipette were considered the true volume change of the samples. Measurement results taken from the sample pipette underestimated the true volume change (water flow into the system did not reflect the measured volume change) and as water is considered incompressible, it can be postulated that CD tests of xanthan treated sands resulted in the formation of cavities within the sample. Additionally, as cavitation is generally linked with negative pore pressures it is expected that the effective stress conditions of the sand may change, however, stress strain curves shown in Fig. 4.6a and the stress paths shown in Fig. 4.7b both confirm that there is no change in the effective stress conditions of the sand.

These results indicate that xanthan treatment in sands may limit certain aspects of pore pressure decrease, and that it may result in the easier formation of cavities through expansive behaviors.

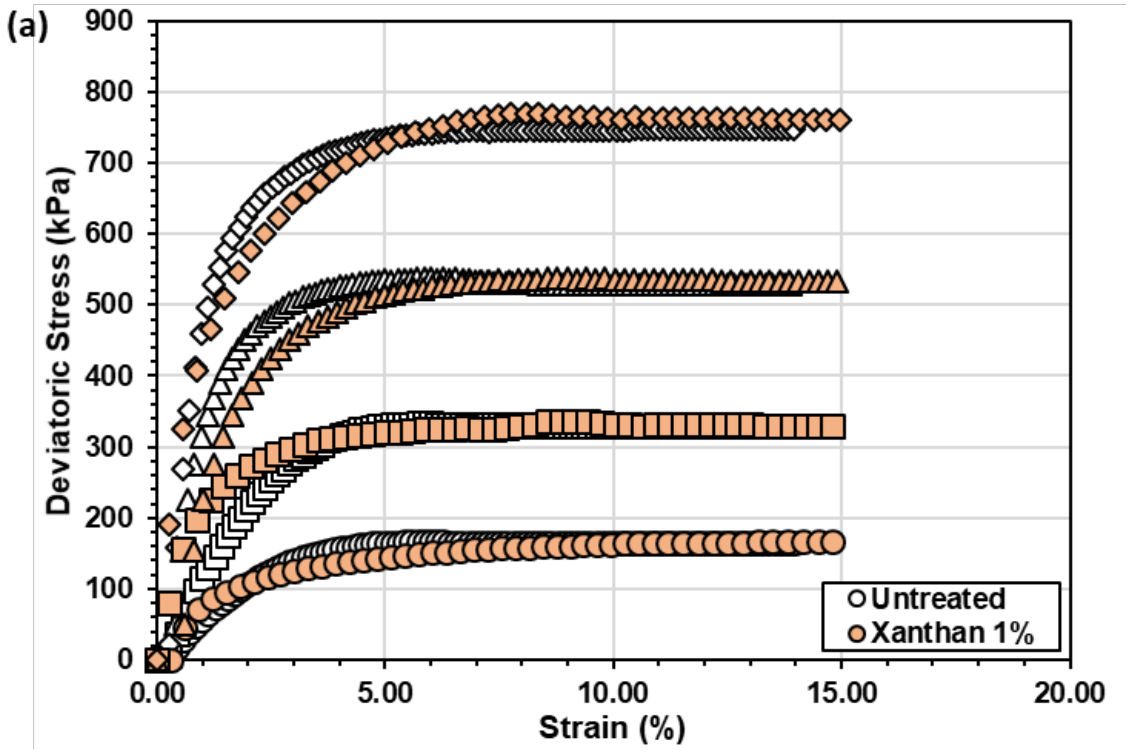

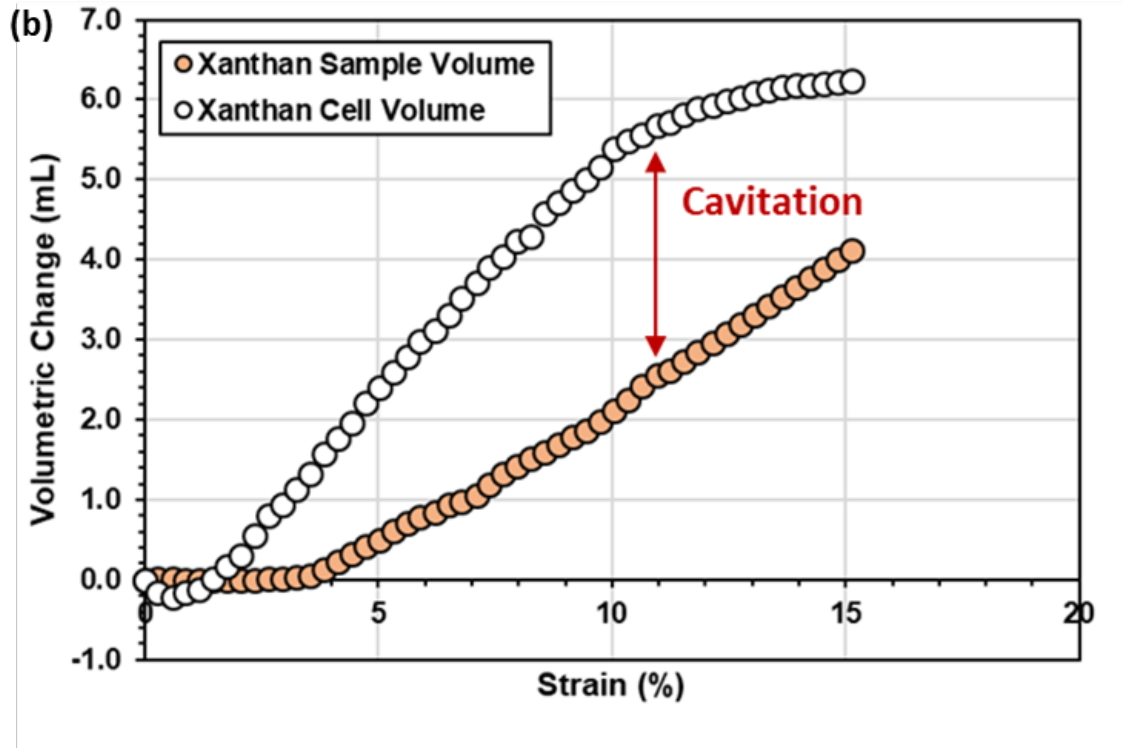

Fig. 4.6 (a) Stress strain curve and (b) typical volume change of 1% xanthan gum treated sand

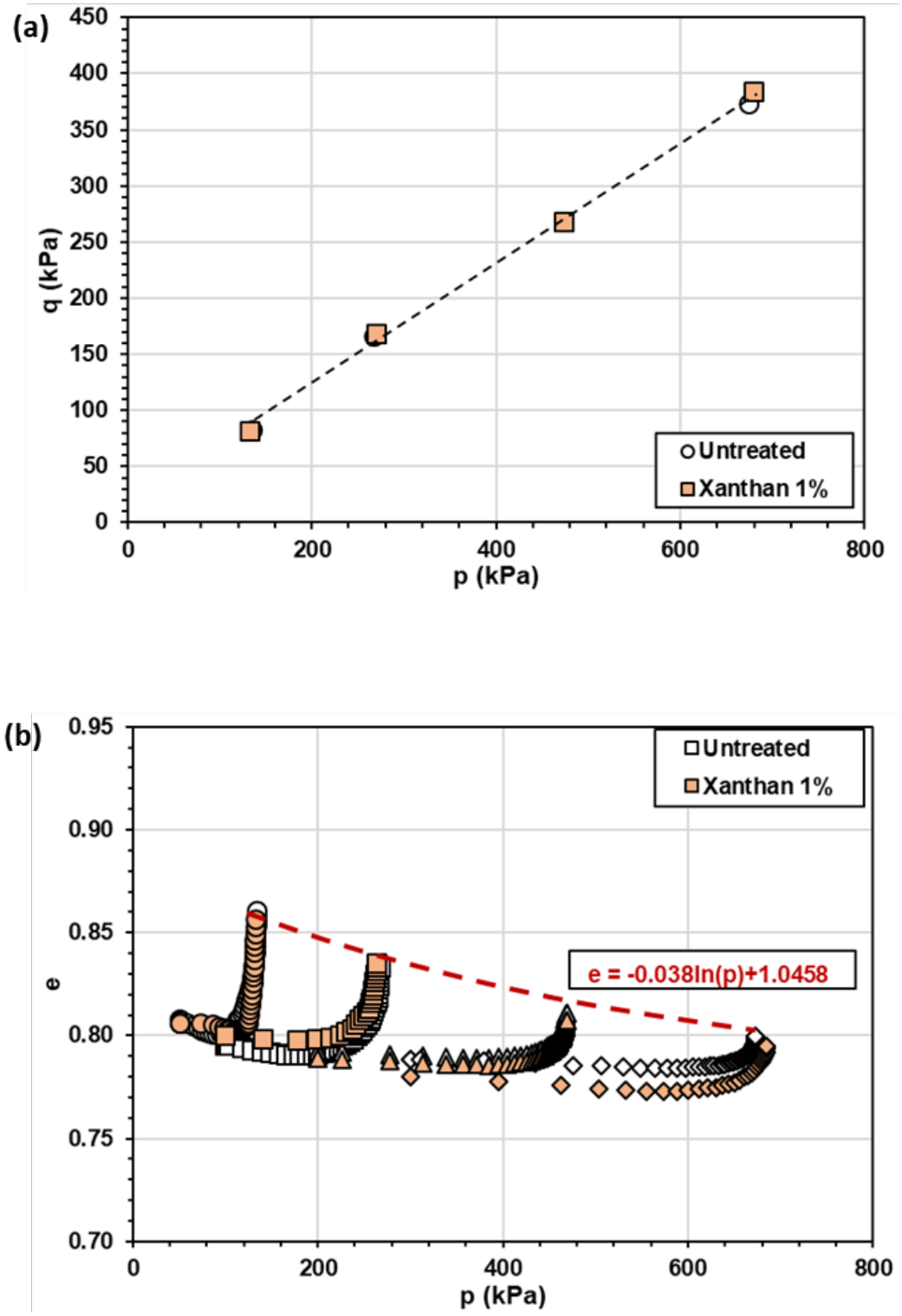

Fig. 4.7 (a) Mohr Coulomb failure curve and (b) critical state line of 1% xanthan gum treated sand

Dense Consolidated Undrained (CU) Tests

For comparison, 1% (m_b/m_s) xanthan treated sands at an effective confining pressure of 100 kPa for dense CD and CU tests are shown in Fig. 4.8 and 4.9. The results were also plotted with untreated sand at the same effective confining pressure in the dense CU condition. Additional tests on other effective confining pressures can be seen in Appendix C.

Dense CU results on untreated sand shows that as the pore pressure decreases with loading, the effective stress increases in the sand and it deviatoric stress is increased. However, xanthan gum treated sands did not exhibit this behavior and although pore pressure measurements indicate a decrease in pore pressure, there did not seem to be any noticeable increase in the effective stress applied on the sample. This once again indicates that xanthan gum treatment in sands seems to limit the increase in effective stress due to the decrease in pore pressure. It should however be noted that the pore pressure measurements of the biopolymer treated samples may not well represent the internal pore pressure conditions of the sample due to its low hydraulic conductivity.

It was also noted that volume change measurement during the dense CU tests for xanthan treated sands (Fig. 4.9a) showed expansive behavior within the soil. As no water flow was permitted into the sample, it can be said that the use of xanthan gum in sands allows for an easier formation of cavities.

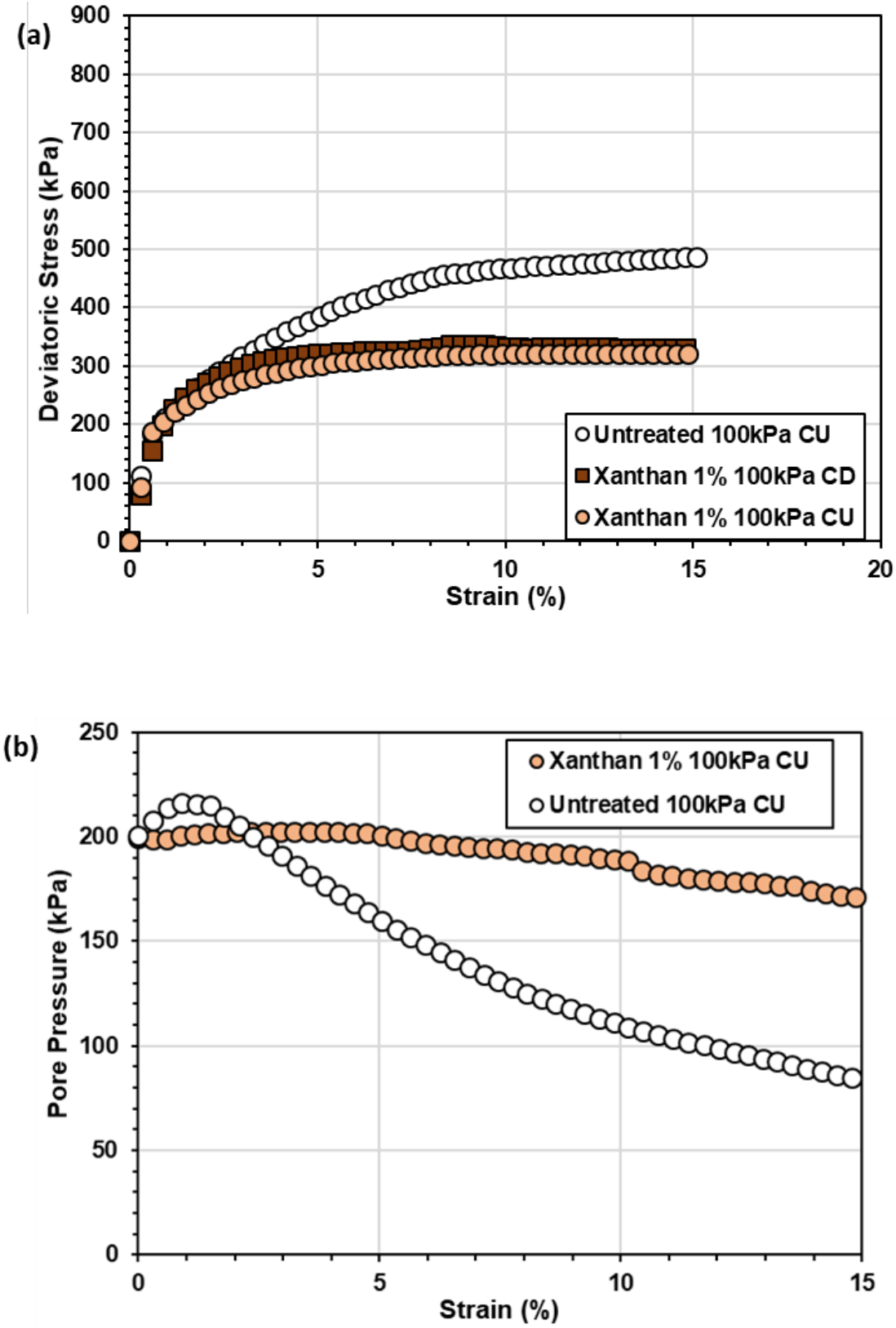

Fig. 4.8 (a) Stress strain curve and (b) pore pressure of 1% xanthan gum treated sand at 100kPa effective confining pressure

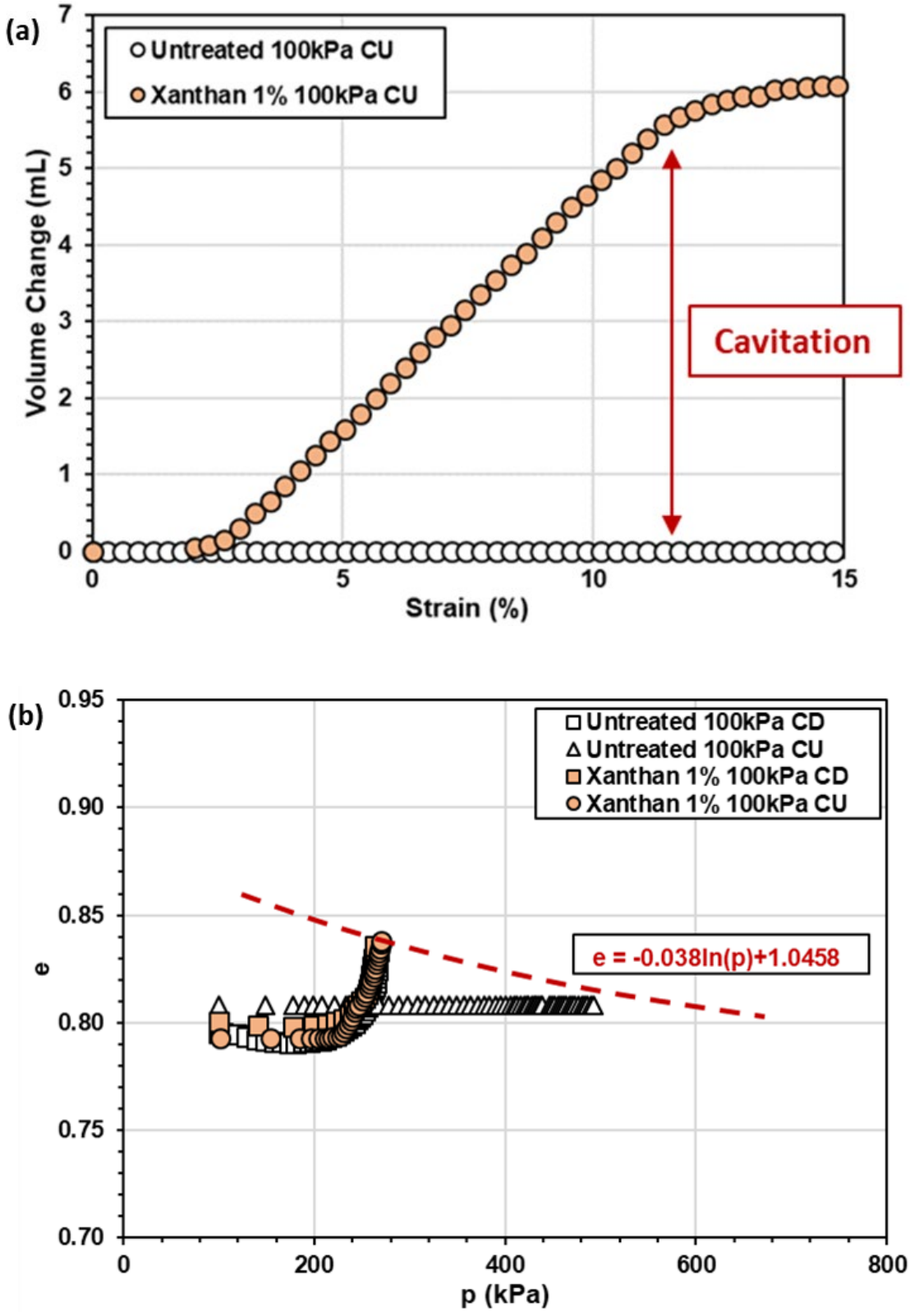

Fig. 4.9 (a) Volume change and (b) stress path of 1% xanthan gum treated sand at 100kPa effective confining pressure

Loose Consolidated Drained (CD) Tests

1% (m_b/m_s) xanthan treated sands at an effective confining pressure of 100 kPa for loose CD tests are shown in Fig. 4.10. Additional tests on xanthan gum treated sands at relative densities below 0.25 can be seen in Appendix C.

In the case of loose CD untreated sand, we see that the sample contracted with loading and converged to the critical state line (Fig. 4.10c). However, xanthan gum treatment showed an overall dilative behavior at the loose condition. With the expansion of the sample, the stress path diverged away from the critical state line. This indicates that the use of xanthan gum in sands exhibits extreme expansive behaviors even in the loose conditions, and as a result the critical state parameters are shifted in the loose condition.

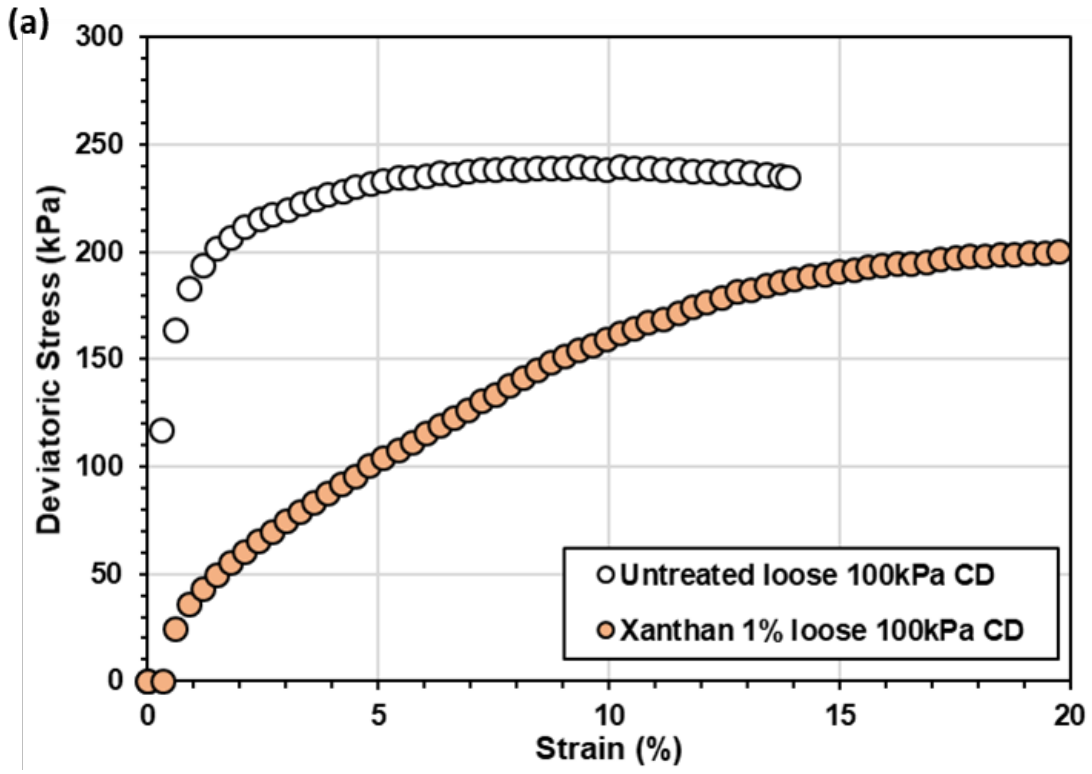

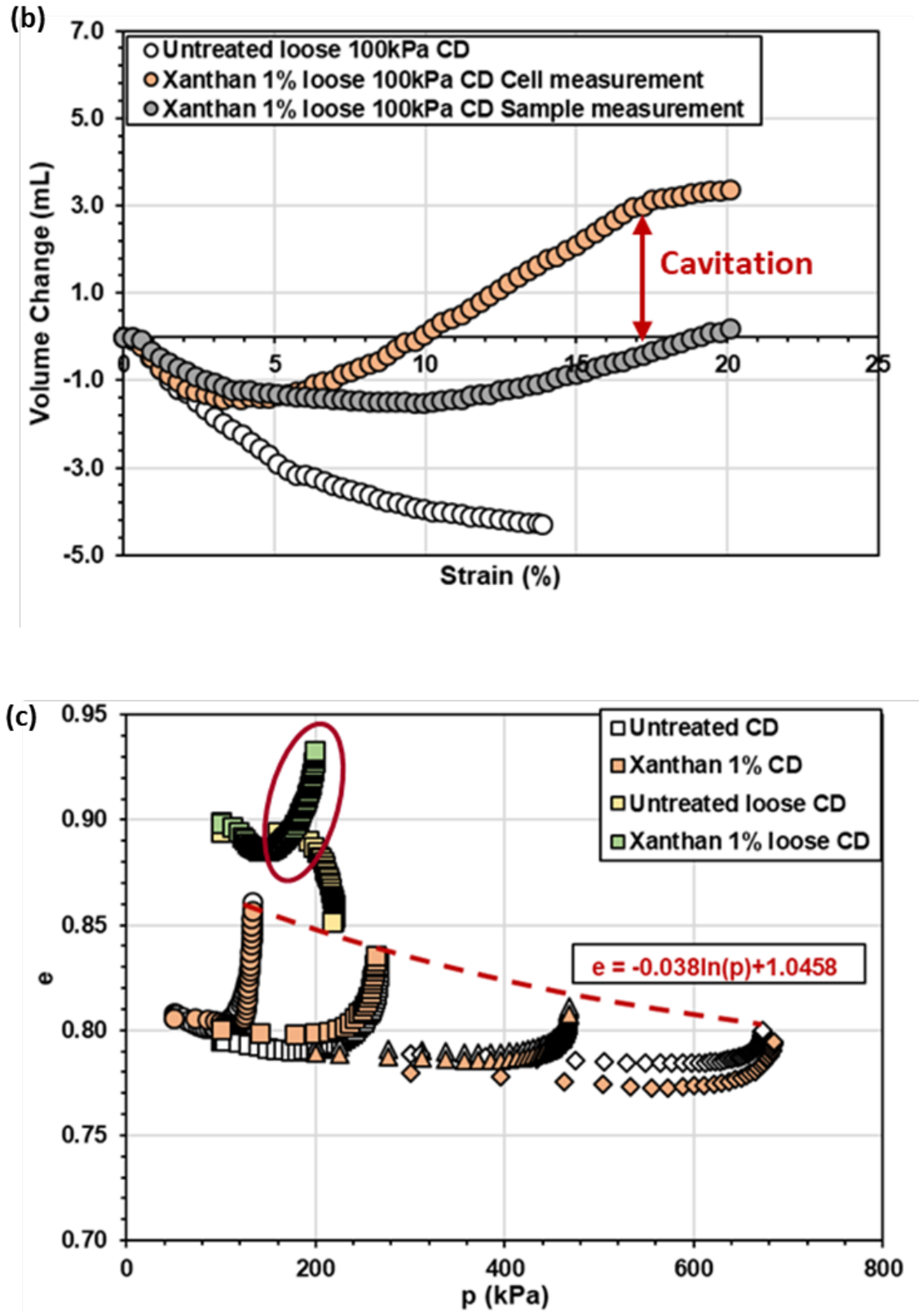

Fig. 4.10 (a) Stress strain curve, (b) volume change, and (c) stress path of loose xanthan gum treated and untreated sand at 100kPa effective confining pressure

Liquefaction (Loose CU) Tests

As both the loose and undrained conditions of xanthan gum treatment exhibited expansive behaviors, the effects of xanthan gum treatment on liquefaction conditions were observed. In the case of untreated sands, the pore pressure was observed to increase with loading until liquefaction of the sample was observed. However, with xanthan gum treatment, volume expansion was observed and there was no measured increase in the pore pressure. Moreover, with no increase in the pore pressure, there was no decrease in the effective stress and liquefaction of the sample was not observed.

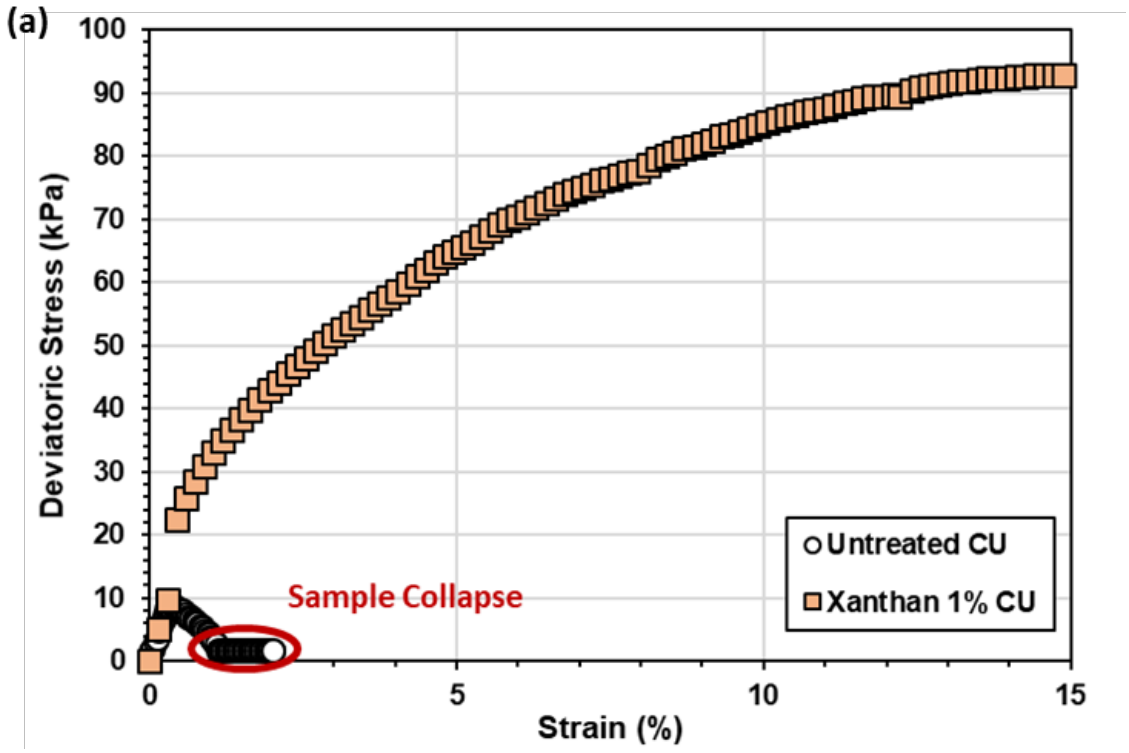

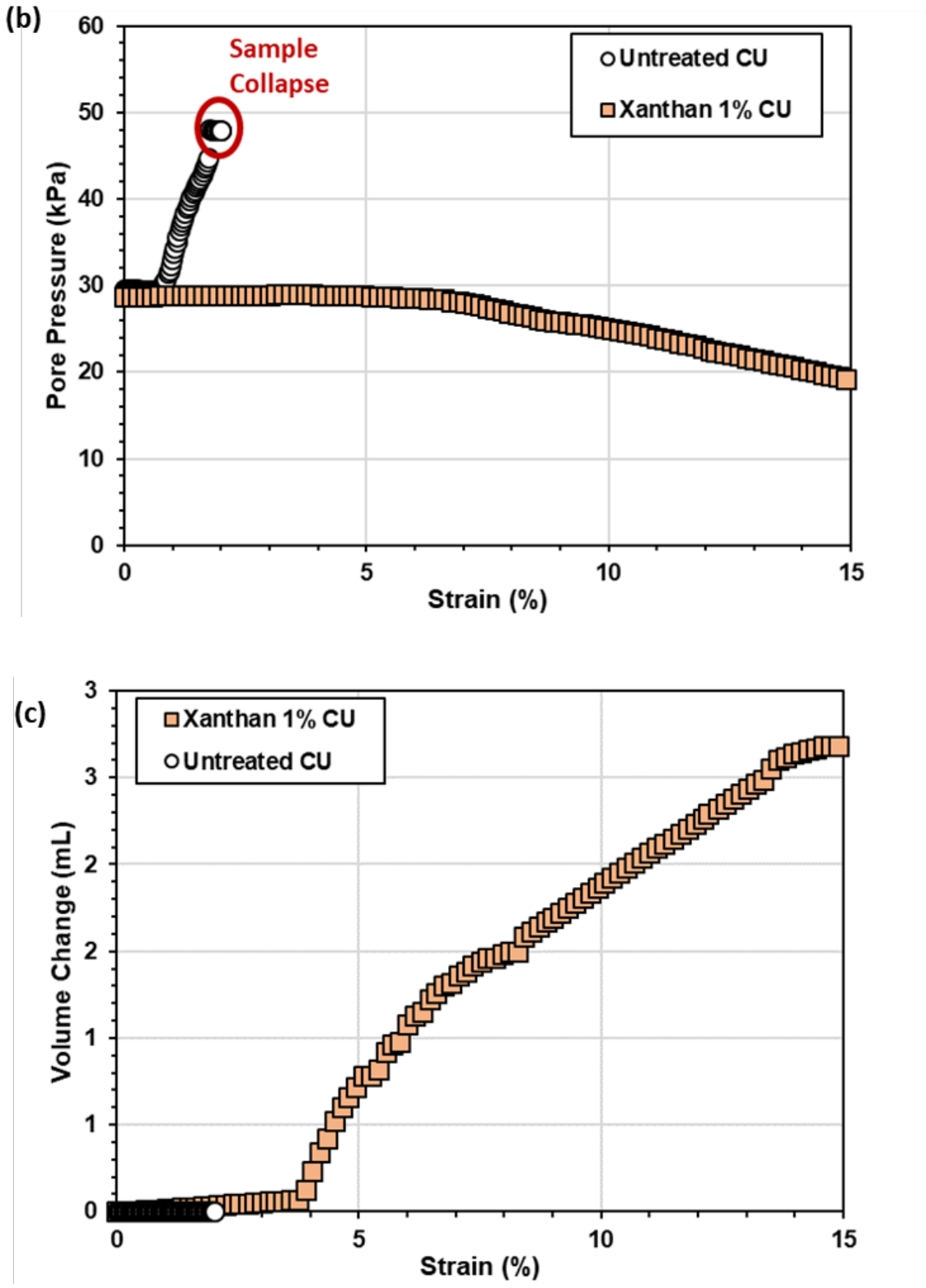

Fig. 4.11 (a) Stress strain curve, (b) pore pressure, and (c) volume change of 1% xanthan gum treated and untreated sand at liquefaction conditions (loose CU tests)

4.2.3 Gellan Gum Treated Sand

Dense Consolidated Drained (CD) Tests

The effects of gellan gum on the dense CD conditions of sand are shown in Fig. 4.12 and Fig.4.13. Results show that the use of gellan gum has a definitive strengthening effect on sand, particularly at low confining conditions.

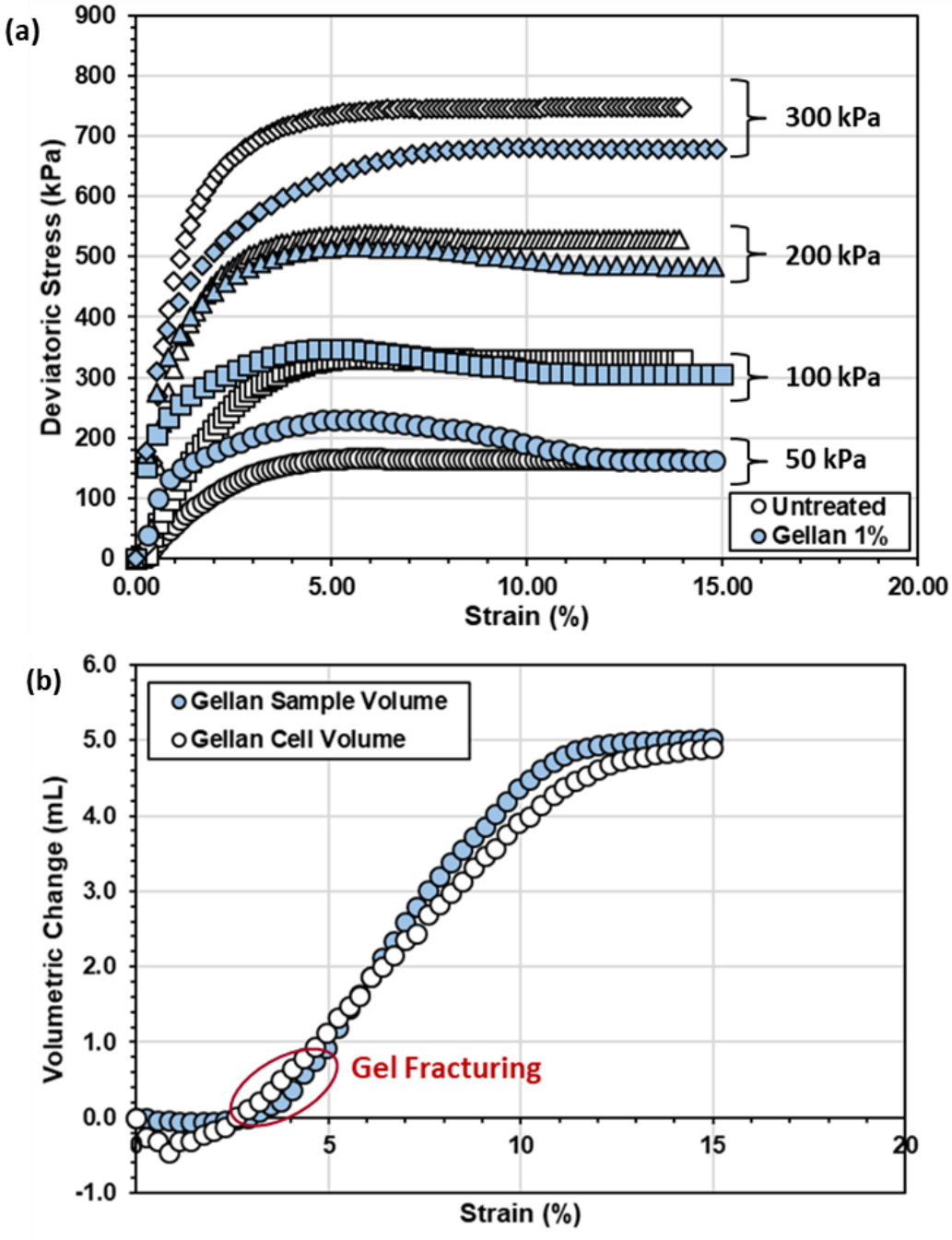

Fig. 4.12 (a) Stress strain curve and (b) typical volume change of 1% gellan gum treated sand

As gellan gum has a gelling effect which has been shown to increase the tensile strength of sands in Ch. 3, the strengthening mechanism can be said to be directly related to the tensile strength provided by the gellan gum hydrogel.

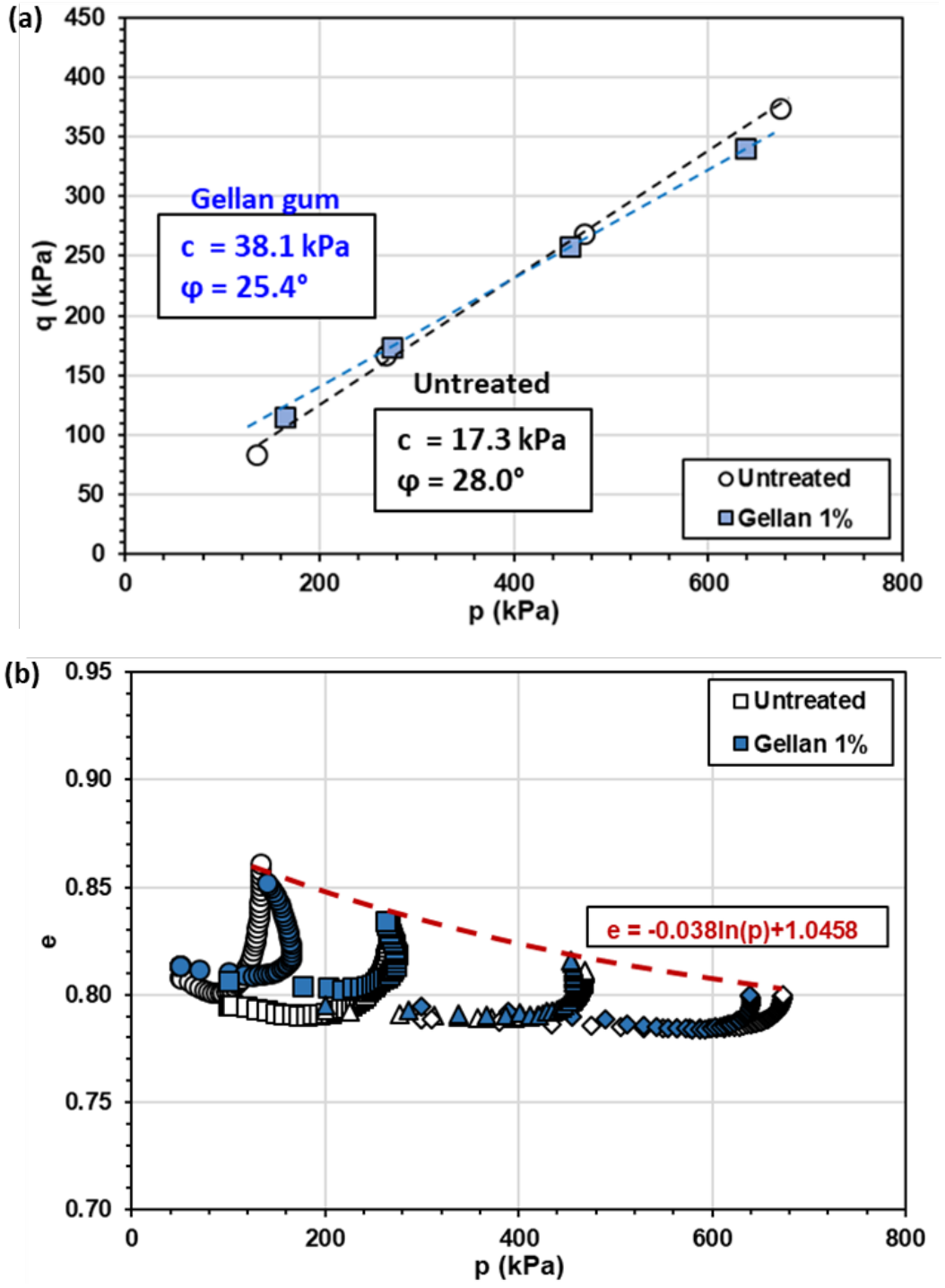

Fig. 4.13 (a) Mohr Coulomb failure curve and (b) critical state line of 1% gellan gum treated sand

When comparing the Mohr Coulomb failure curve, we see that gellan gum increases the cohesion of the sand while reducing the friction angle. One thing to note was that although gellan gum has a similarly low hydraulic conductivity as xanthan gum, there was no large disparity observed between the volume measurements from the cell pipette and the sample pipette, Fig. 4.12b. It is estimate that with loading the hydrogels fracture allowing for pathways to form for the easy movement of water. Additionally, with gellan treatment a clear failure plane was observed during failure, Fig. 4.14. This failure plane was especially prominent in the low confinement conditions.

Fig. 4.14 Typical failure plane of gellan treated sands

Biopolymer Concentration

As Fig. 2.7 shows, in the case of gellan gum the initial mixing biopolymer concentration results in different tensile strengths. The effects of higher gellan concentrations in sands are shown in Fig. 4.15 and Table 4.1. Results showed that with higher gellan concentrations, a more prominent peak behavior was shown. It was also seen that higher concentrations of gellan gum had an increase in cohesion and a decrease in the friction angle of sands.

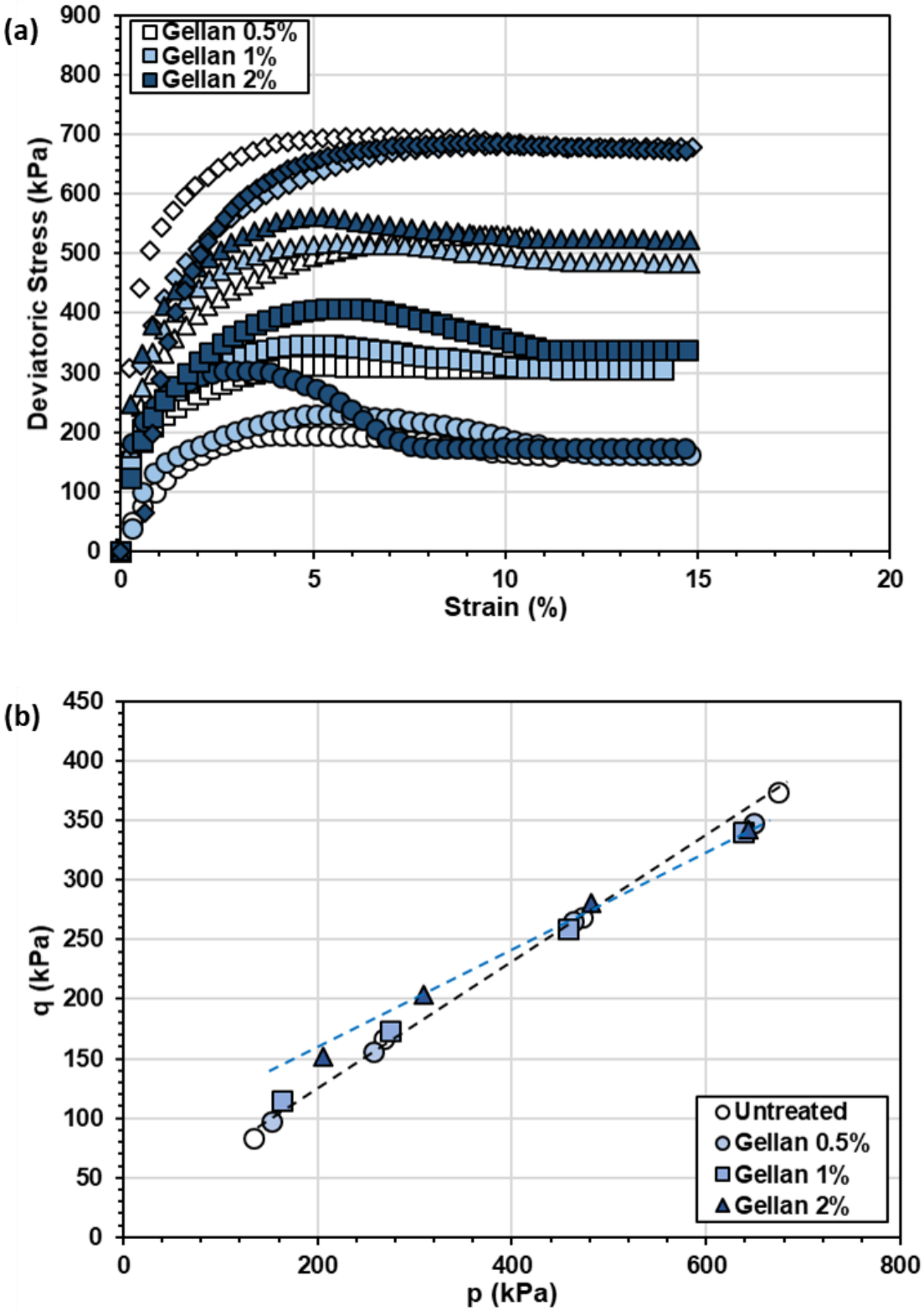

Fig. 4.15 (a) Stress strain curve and (b) Mohr Coulomb failure curve of gellan gum treated sand at various biopolymer concentrations

Table 4.1 Cohesion and friction angle of biopolymer treated sands

Treatment m_b/m_s (%)	Cohesion, c (kPa)	Friction angle φ (°)
Untreated	17.3	28.0
Xanthan 0.5%	14.2	28.2
Xanthan 1.0%	18.0	28.3
Xanthan 1.5%	17.6	28.2
Gellan 0.5%	23.9	26.9
Gellan 1.0%	38.1	25.4
Gellan 2.0%	67.0	23.4

Liquefaction (Loose CU) Tests

As gellan gum treated sands provided cohesion to sands, its behavior during liquefaction conditions were tested. Results are shown in Fig. 4.16. As shown, gellan treated sands did not exhibit liquefaction during the testing conditions. As gellan gum provided cohesion to the sand, a peak behavior was observed, and the gellan gum treated sands showed expansive behavior due to the formation of a failure plane.

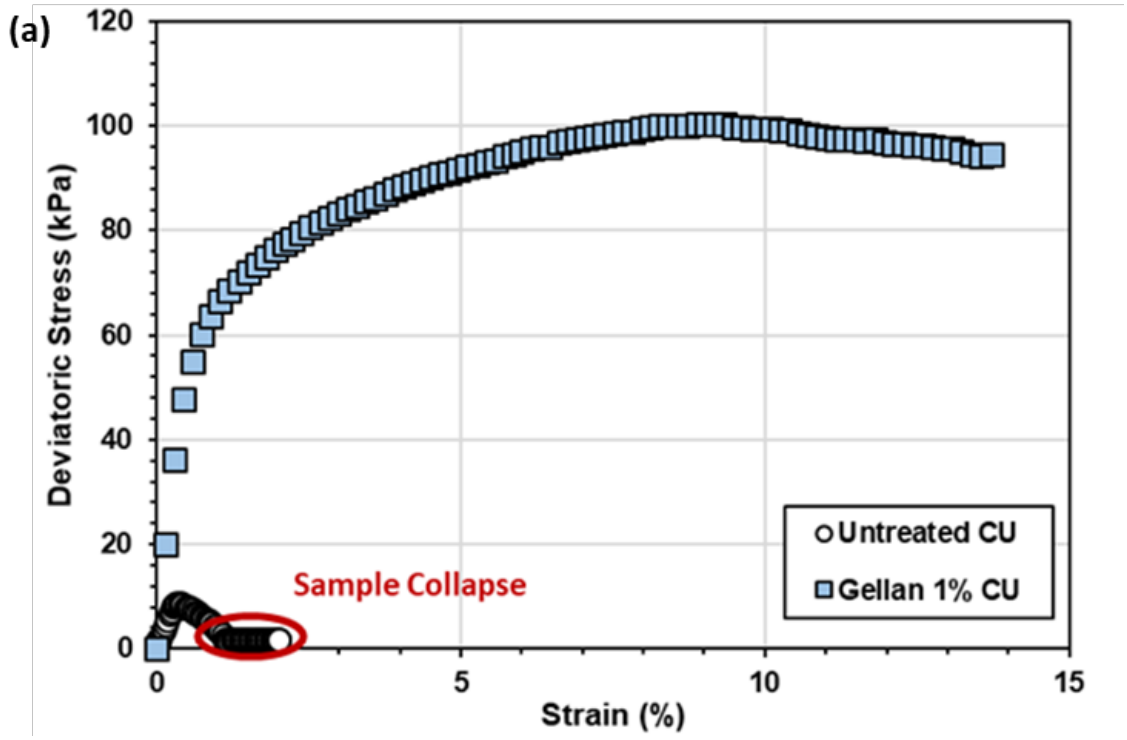

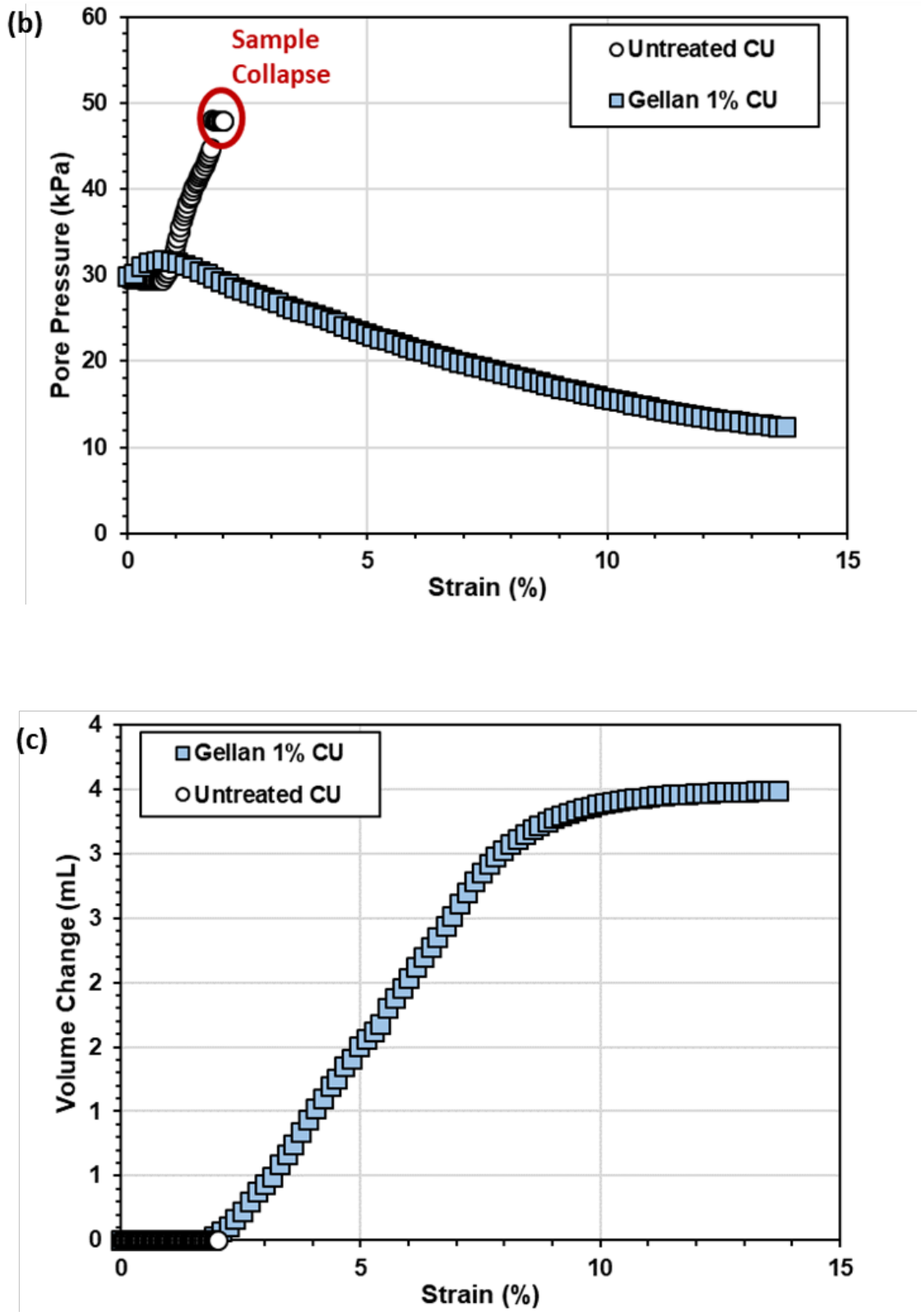

Fig. 4.16 (a) Stress strain curve, (b) pore pressure, and (c) volume change of 1% gellan gum treated and untreated sand at liquefaction conditions (loose CU tests)

4.3 Discussion

Xanthan Gum Treated Sands

As the triaxial tests were conducted in the fully saturated state (i.e. biopolymer concentrations were below the critical concentration) no strengthening effect was observed with xanthan gum treatment on sands. This reinforces the idea that the viscosity does not have a major effect on strengthening the sand, and only when the tensile strength of the biopolymer is enhanced through dehydration does the strengthening efficiency increase. However, one area in which xanthan gum showed a large effect on the sand was its expansive behavior.

The expansive behavior is believed to be a result of the mechanisms shown in Fig. 4.17 and Fig. 4.18. As viscosity is a measure of a fluid's resistance to deformation, when a viscous fluid is present in the pore spaces of a soil matrix, it can be expected that the viscous fluid helps prevent the motion of particles, Fig. 4.17. This effect is also shown in Table 4.2, where on average the xanthan gum treated sands reached the residual stress at higher strains than that of untreated sands, indicating that for xanthan treated sands a larger strain is necessary to achieve a similar failure criteria.

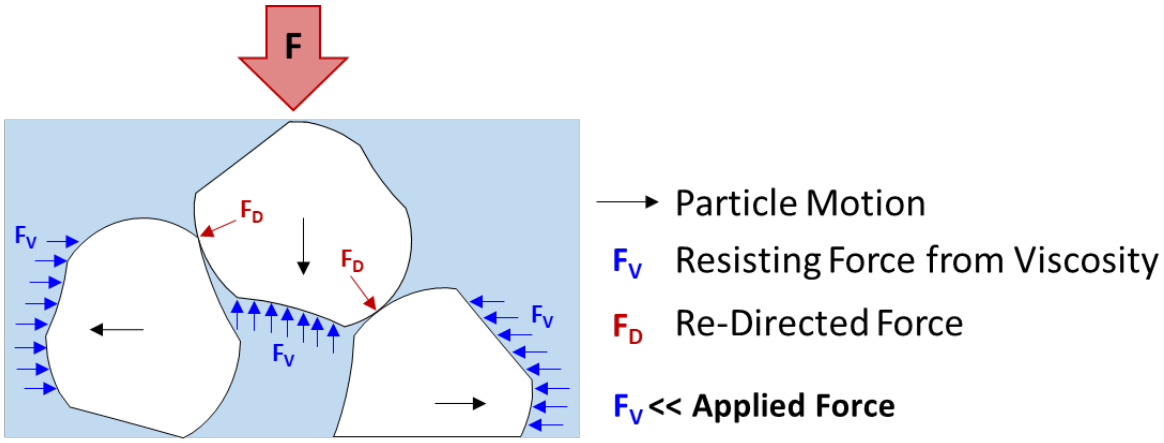

Fig. 4.17 Effects of viscosity on sand particles

Table 4.2 Average strains at maximum and residual stress for biopolymer treated sands

Treatment m_b/m_s (%)	Strain at Max σ_1 (%)	Strain at Residual σ_1 (%)
Untreated	-	6.27
Xanthan 0.5%	-	7.67
Xanthan 1.0%	-	8.84
Xanthan 1.5%	-	8.93
Gellan 0.5%	6.56	8.00
Gellan 1.0%	6.27	10.11
Gellan 2.0%	5.67	9.57

With particle motion restricted, it is expected that stronger particle contacts may develop especially in the loose conditions. Along with the restriction of particle motion, this increase in particle contact may allow for the aggregation of particles (Fig. 4.18) resulting in a larger dilatancy angle. However, this behavior has not been conclusively proven and additional tests will need to be conducted.

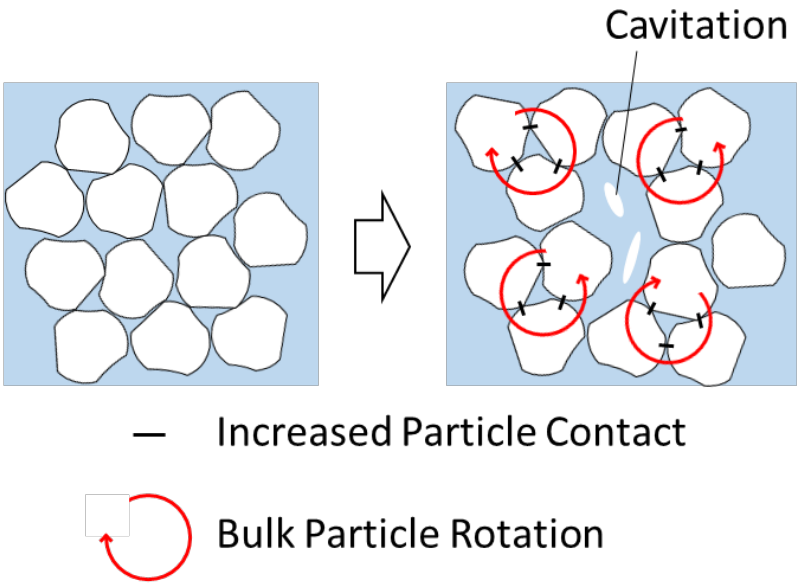

Fig. 4.18 Expansion mechanism of viscous biopolymers in sands

Gellan Gum Treated Sands

In the case of gellan gum, as tensile strength is provided by the gellan hydrogel, a strengthening behavior is observed, particularly in low confinements. It was also observed that with higher gellan gum concentrations there was an increase in the cohesion and a decrease in the friction angle of the sands. The decrease in friction angle can be attributed to the effects of a stiff gellan gum hydrogel limiting the consolidation behavior of the sands.

Chapter 5. Possible Enhancement Methodologies

Although the use of viscous and gelling polysaccharide biopolymers, in the form of xanthan gum and gellan gum respectively, has shown their varying benefits, performance enhancement is always an option sought after. In this chapter the possibilities of biopolymer enhancement, specifically the enhancement of the resubmerged strengths, are investigated through two avenues: 1) crosslinking and 2) hydrophobic biopolymers.

5.1 Crosslinking

Crosslinking is a method of connecting two or more molecules through the use of a covalent bond [80]. The method is used to alter certain characteristics in a molecule, and it is used in many industries [81-83]. It is thought that by chemically binding the hydroxyl groups found on the glucose molecule, the intermolecular binding strength can increase and its reactivity to water would decrease. One of the most commonly used materials for crosslinking is starch.

5.1.1 Starch – Malonic Acid Crosslinking

Due to its low price and availability, starch us widely used in many industries and is often crosslinked with other additives for better performance [84-86]. However, the crosslinking of starch is generally associated with the use of several toxic substances that would cause harm if released into groundwater systems [87-89]. In a study performed by Trina Ghosh Dastidar (2012), an organic acid called malonic acid was used to crosslink starch, shown in Fig. 5.1 [90]. As this acid is known to have non-toxic properties it was chosen as the target of this study.

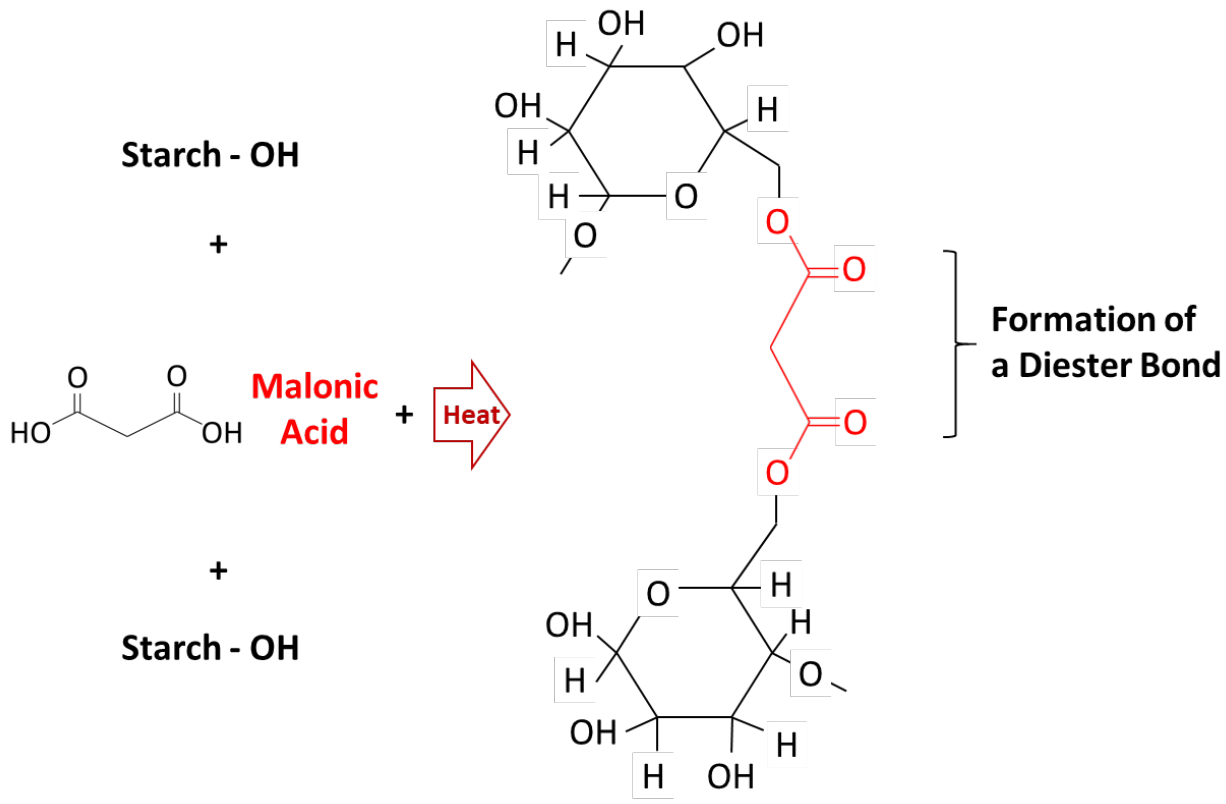

Fig. 5.1 Crosslinking mechanism of starch and malonic acid

Starch

Starch is mainly made of two polysaccharides: amylose and amylopectin. Amylose is a linear structured polysaccharide that has gelling properties when heated in water, while amylopectin has a branched structure and swells in water thereby increasing the viscosity [91]. Based on the source of the starch, the ratios of amylose to amylopectin along with its molecular length varies greatly, and different ratios of amylose and amylopectin have been shown to have large differences in properties especially when crosslinked [92]. In this study, corn starch and potato starch were used to crosslink with malonic acid. Corn starch is composed of approximately 25% amylose with the molecular sizes ranging between 5 and 20 microns, while potato starch is composed of 20% amylose with a molecular size ranging around 15 to 75 microns [93].

Malonic acid

Malonic acid (MA) is a dicarboxylic acid that is derived from a plant. It is a non-toxic acid that is capable of interacting with the hydroxyl groups found on the D-glucopyranose molecules [90]. In starch it has been shown to be capable of forming diester bonds.

5.1.2 Experimental Procedure

Testing procedure and parameters

Cubic samples of starch and malonic acid were prepared by first dissolving the starch in deionized water. Starch was prepared at a m_b/m_s concentration of 4% with an initial water content of 20%. The water was first heated to approximately 90°C before the starch was added. The starch was then continuously stirred and allowed to gel for 30 minutes. At this point the malonic acid was added into the solution at a concentration of 30% (to the mass of starch) along with sodium hypophosphite monohydrate ($NaPO_2H_2$), at a concentration of 15% (to the mass of starch), to act as a catalyst for the reaction. Once the solution was fully mixed, it was then directly mixed with sand and molded into cubic molds of 40 mm. The samples were then left to cool and dry at room temperature for 2 weeks. Dry and resubmerged UCS tests were performed on the samples. Resubmerged tests were performed after drying the samples then submerging the specimens in water for 24 hrs.

Starch Hydrolysis

One important parameter to note is the hydrolysis of starch, shown in Fig. 5.2. This process occurs as starch is exposed to either acidic solutions or heat and water for extended periods. It is a process in which the long polymer chains break down into shorter smaller chains, and generally results in a reduction of viscosity, shown in Fig. 5.3.

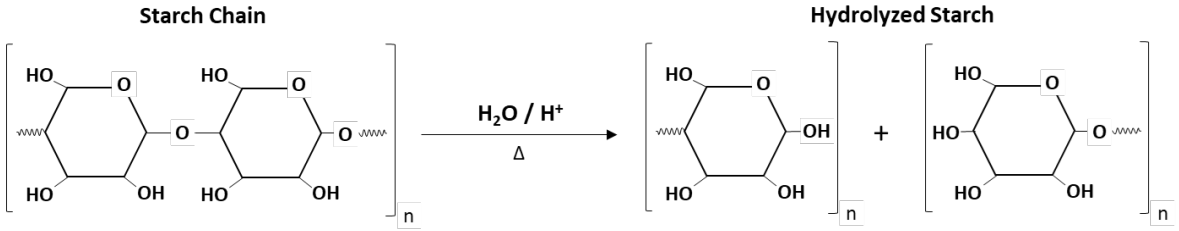

Fig. 5.2 Hydrolysis of Starch

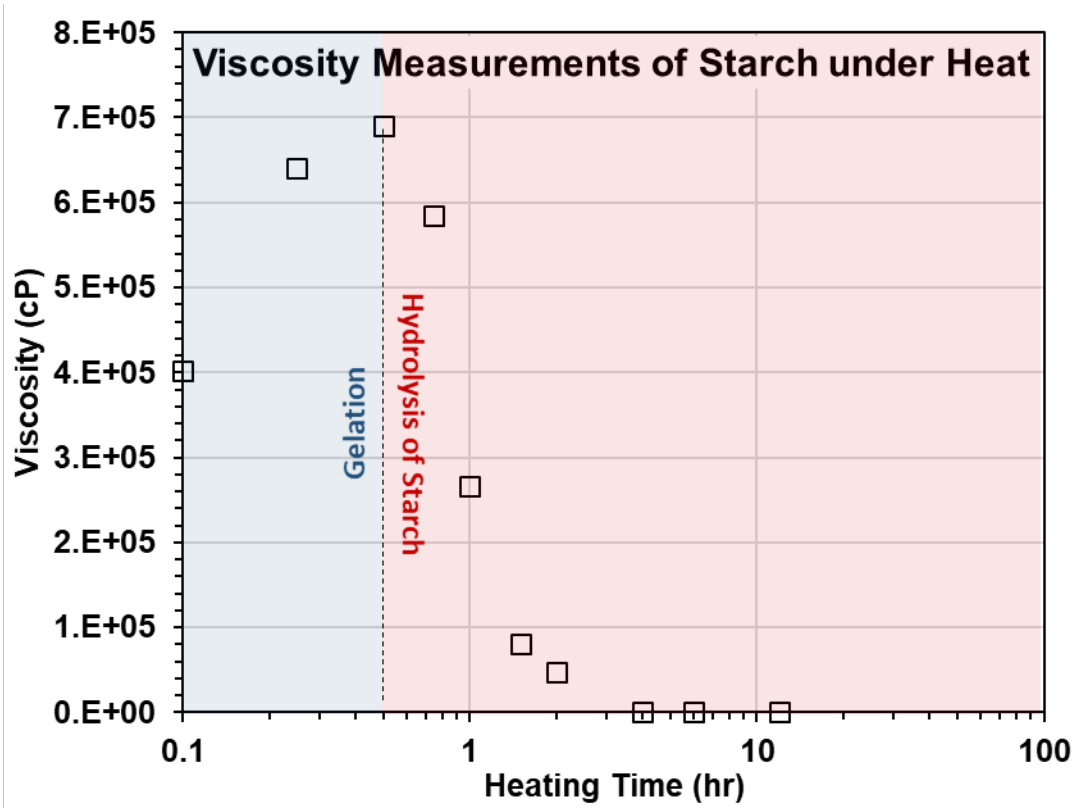

Fig. 5.3 Viscosity measurements with starch gelation and hydrolysis

In order to test the effects of hydrolysis on the crosslinking of starch and malonic acid, several additional tests were performed. Two conditions with hydrolysis were observed: 1) Hydrolysis before the crosslinking reaction and 2) hydrolysis after the crosslinking reaction. With hydrolysis before the crosslinking reaction, the starch solution was exposed to extended periods of heating at 90°C on a hot plate. At the target times (t) of 0, 0.5, and 1 hr, malonic acid and sodium hypophosphite were added into the mixture to initiate the crosslinking reaction. The mixture was then taken off the hot plate and directly mixed with sand and molded into cubic samples.

In the case of hydrolysis after the crosslinking reaction, a starch solution was first heated to 90°C at which point the malonic acid and sodium hypophosphite were added into the mixture. The mixture was maintained at 90°C on a hot plate for an extended period of time. At the target times of 0, 0.5, 1, 2, 6, and 12 hrs, the solution was taken off the hot plate and mixed directly with sand and molded into cubic samples. Both cases were tested in the dry and resubmerged conditions.

5.1.3 Starch – Malonic Acid Results

Effects of crosslinking

The effects of MA crosslinking on corn and potato starch are shown in Fig. 5.4. Although there does not seem to be a large strengthening effect on the dry strength, there is a definite increase in the resubmerged strength of the sands, up to 68 kPa and 182 kPa increase for corn and potato starch respectively. As corn starch has a higher amylose content, which is a gelling polysaccharide and should thereby contribute more to strength than amylopectin, it is expected that the corn starch would have a higher resubmerged strength than that of potato starch. However, it can be seen that with crosslinking potato starch has a higher resubmerged strength than that of corn starch. In a study conducted by J. L. Jane 1992, it was noted that amylopectin molecules, a viscous polysaccharide, with long branches actually had tendencies to gel, and that the gel strength increased as the branch length increased [94]. Therefore, it can be seen that although corn starch has a higher amylose ratio than potato starch, as potato starch has nearly 3 times larger molecules, the strengthening effects of potato starch are shown to be higher.

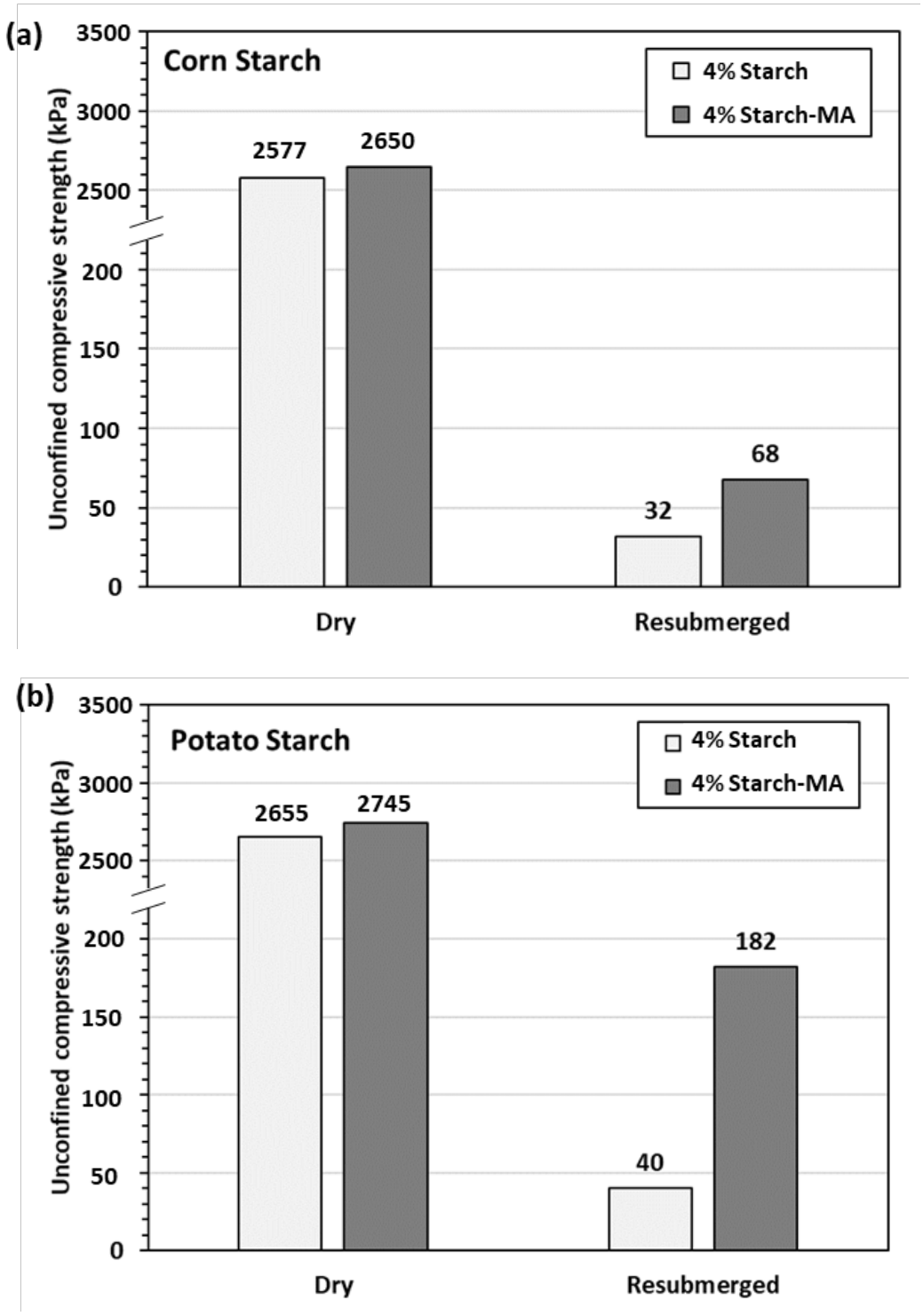

Fig. 5.4 Effects of crosslinking on (a) corn and (b) potato starch

Effects of hydrolysis

With hydrolysis, two conditions were tested: 1) hydrolysis before crosslinking and 2) hydrolysis after crosslinking. The results are shown in Fig. 5.5.

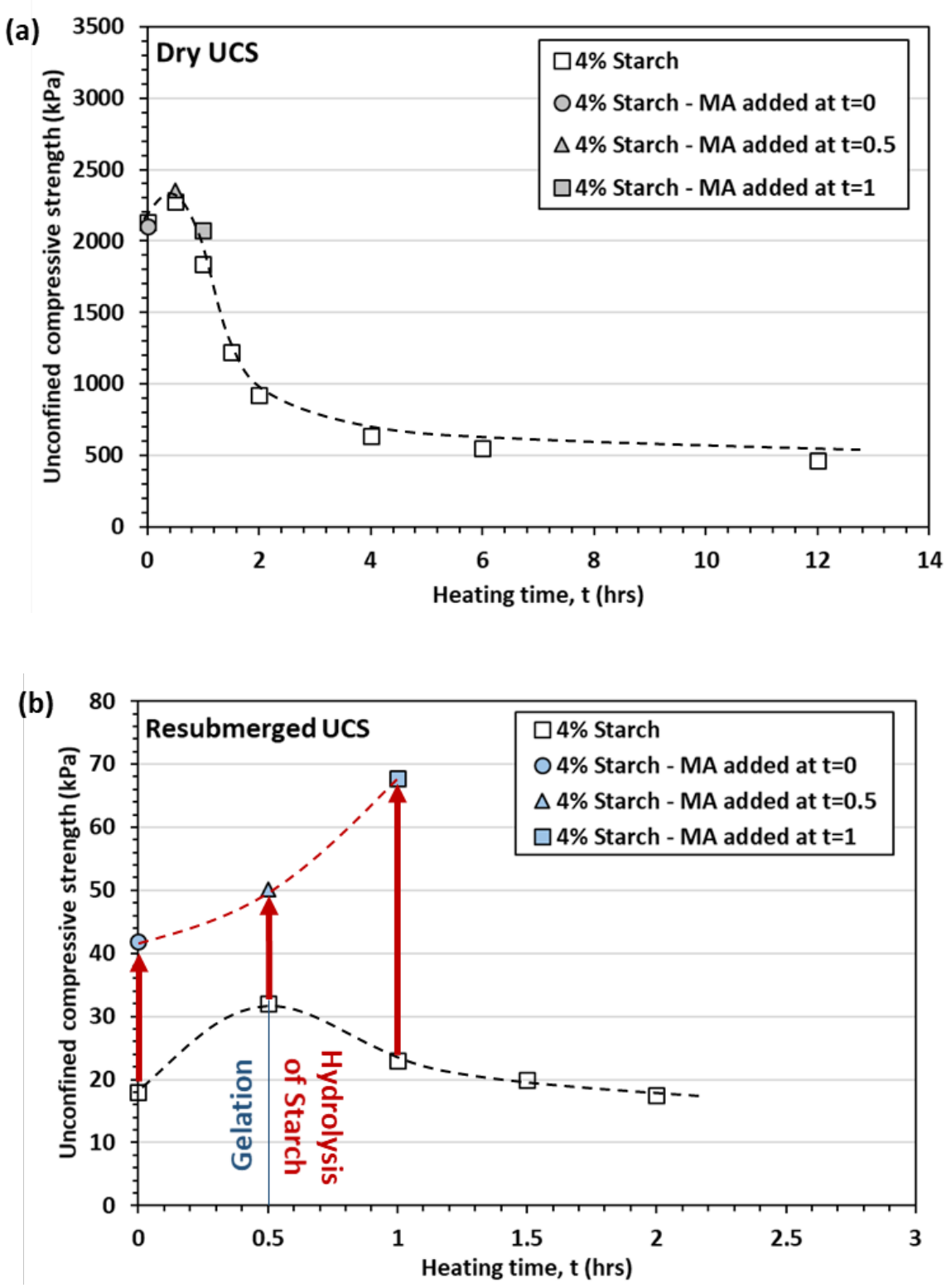

Fig. 5.5 Effects of hydrolysis before crosslinking (a) dry and (b) resubmerged strengths

Results show that the dry strength is very closely tied to the hydrolysis of the starch and the addition of MA does not seem to have a large effect on its strength. The resubmerged strength on the other hand shows that a slight increase in the hydrolysis of starch results in an overall higher resubmerged strength. This is most likely the result of an increased number of reaction points for the MA to react to with hydrolysis, however, without sufficient MA in the system it can be expected that additional hydrolysis may result in a reduction in overall strength.

In the case of hydrolysis after crosslinking, the results are shown in Fig. 5.6. In this case both the dry and resubmerged strengths had a large decrease in strength around the 1 hr mark. This indicates that continued heating after the crosslinking reaction is allowed to occur only damages the molecular strength.

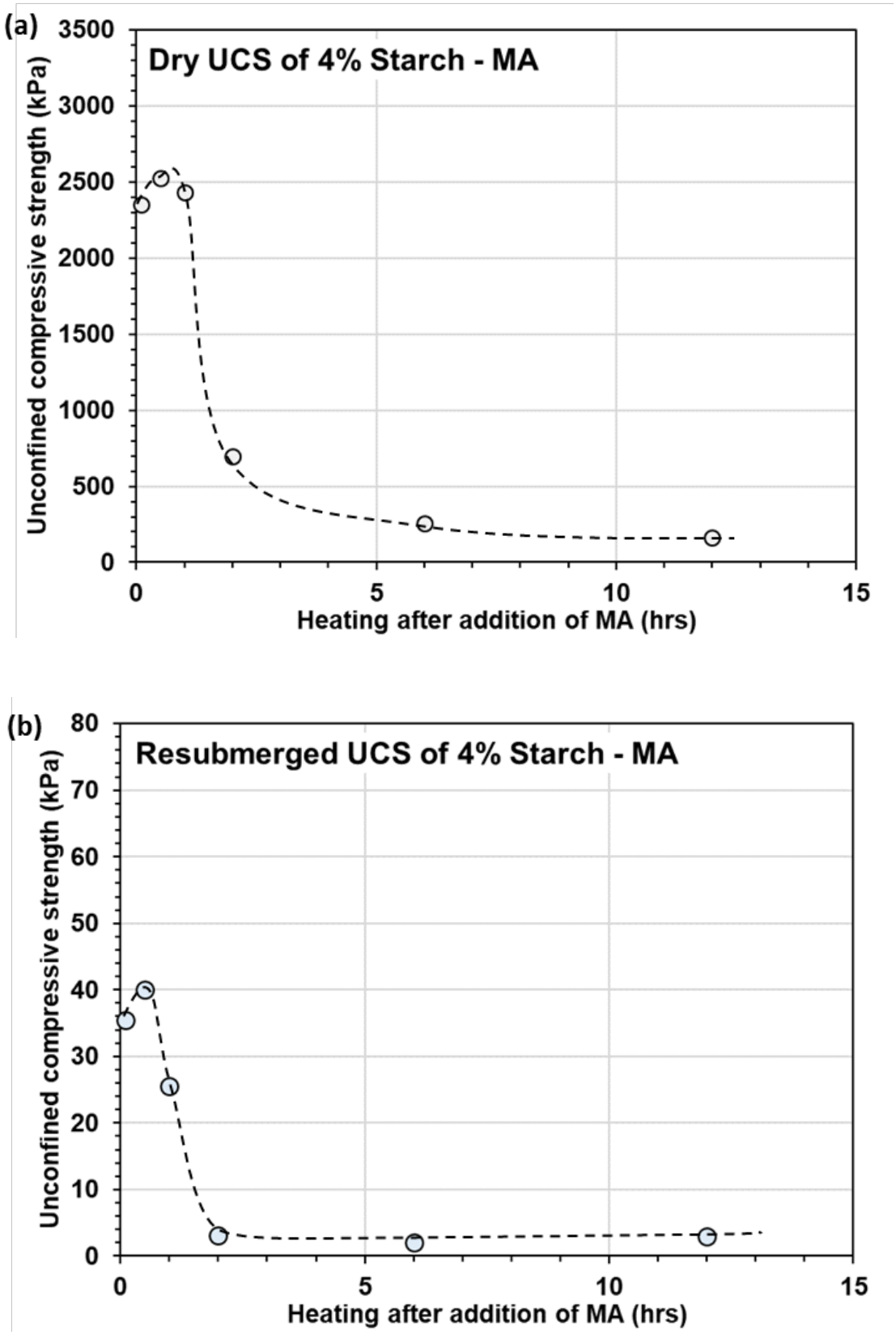

Fig. 5.6 Effects of hydrolysis after crosslinking (a) dry and (b) resubmerged strengths

5.2 Hydrophobic Biopolymers

The second method of biopolymer enhancement would be the use of more water resistant biopolymers. As most biopolymers used for soil enhancement are hydrophilic in nature, they are very reactive with water. However, if a hydrophobic biopolymer were to be used, it would result in a larger resubmerged strength. The biopolymer considered in this case is casein proteins.

Casein proteins

Casein is a family of phosphoproteins that are largely found in mammalian milk. Casein proteins are normally found in a suspension of particles known as casein micelles, shown in Fig. 5.7 [95]. These micelles are held together through a combination of hydrophobic interactions and calcium ions [96].

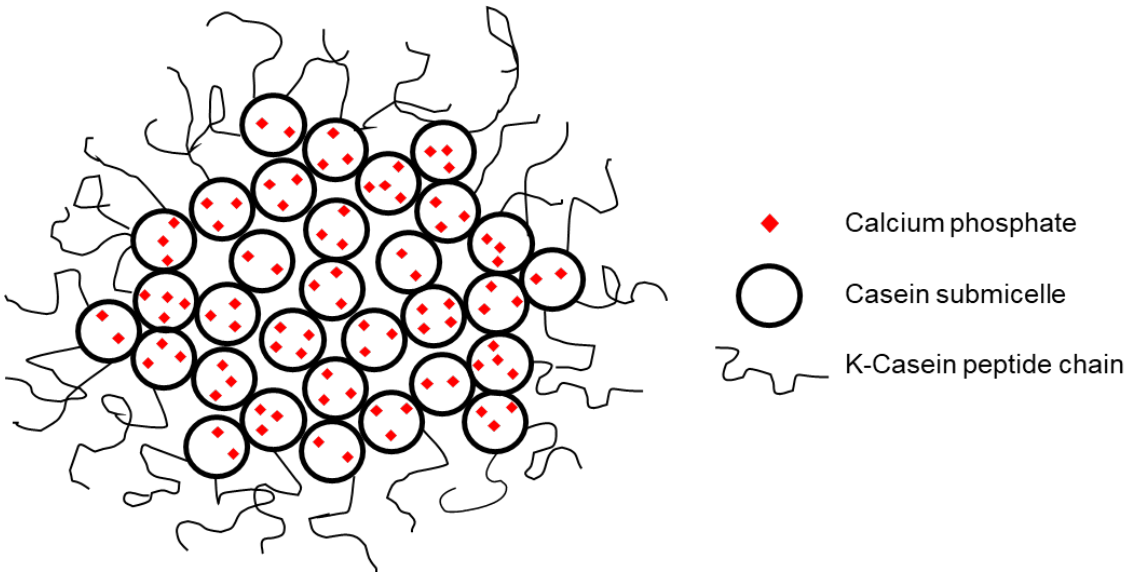

Fig. 5.7 Schematic diagram of casein micelle structure

5.2.1 Experimental Procedure

In order to use casein proteins as a binder in soils, they must first be dissolved in water, and a mixture of calcium hydroxide and sodium hydroxide were used with casein for the formation of a binder. Using calcium hydroxide and sodium hydroxide at a ratio of 2:1, powdered casein purchased from SigmaAldrich (CAS #: 9000-71-9) was dissolved and

heated at a pH between 10-12. The solution was heated at 90°C for 30 min before mixing directly into sand. The casein sand mixtures were then molded into 40 mm cubic molds and allowed to dehydrate at room temperature. Dry strengths were measured after 2 weeks of dehydration and resubmerged strengths were measured after saturating the dry samples in water for 24 hrs.

5.2.2 Experimental Results

The UCS of casein treated sands at varying concentrations are shown in Fig. 5.8.

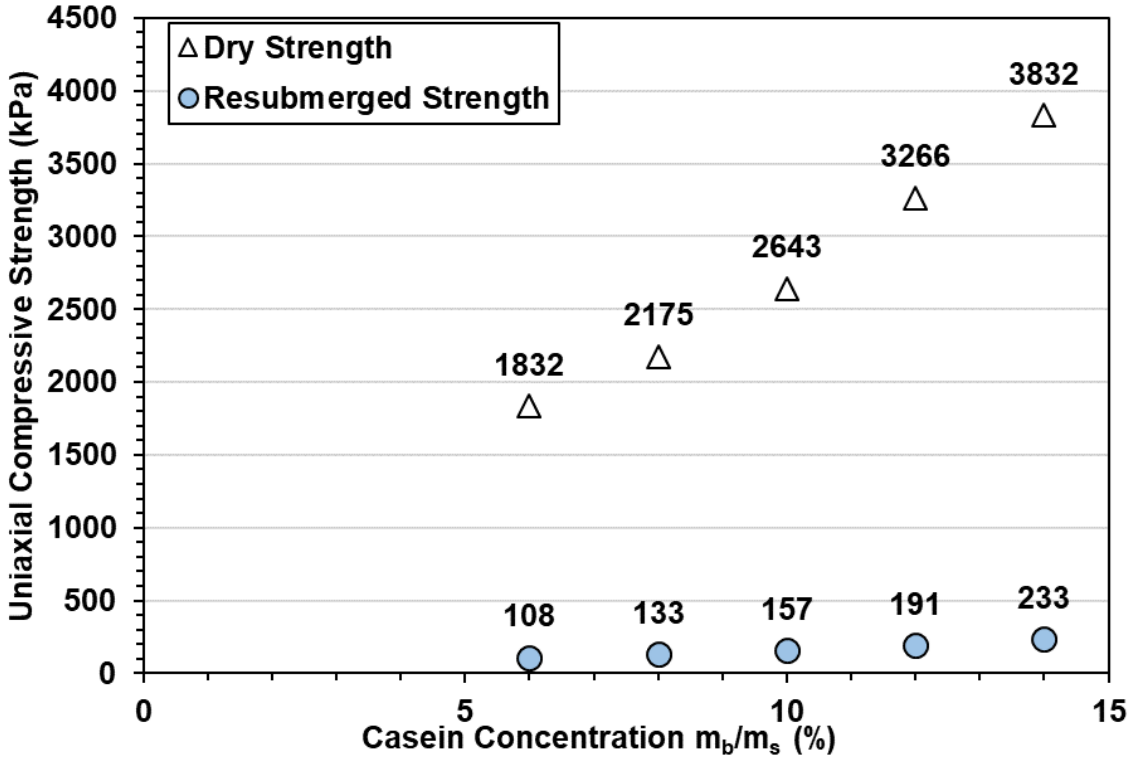

Fig. 5.8 Strengthening effects of casein proteins on sands

As shown, the strengthening efficiency increases in a linear fashion with an increase in biopolymer concentration. However, in comparison with polysaccharide biopolymers, casein requires a significantly larger concentration to be effective. In comparison to the resubmerged strengths of gellan and xanthan gum treated sands, it can be seen that casein has a higher overall resubmerged strength.

5.3 Discussion

Crosslinking was used to enhance the intermolecular bonding of the polysaccharides thereby enhancing its overall structure and reducing its reactivity to water by binding on the hydroxyl groups of the glucose chains. Results showed that crosslinking can be used to successfully enhance the resubmerged strength of polysaccharide biopolymers.

With casein proteins, the hydrophobic characteristics allowed for a higher resistance towards water, showing a higher resubmerged strength than unmodified biopolymers. However, a much larger concentration of casein was required to effectively use casein as a binder. The overall dry and resubmerged strengths of modified and unmodified polysaccharide biopolymers along with casein are shown in Fig. 5.9. Although an increase in strength was shown, further development will be necessary for biopolymers to be easily applicable in various fields.

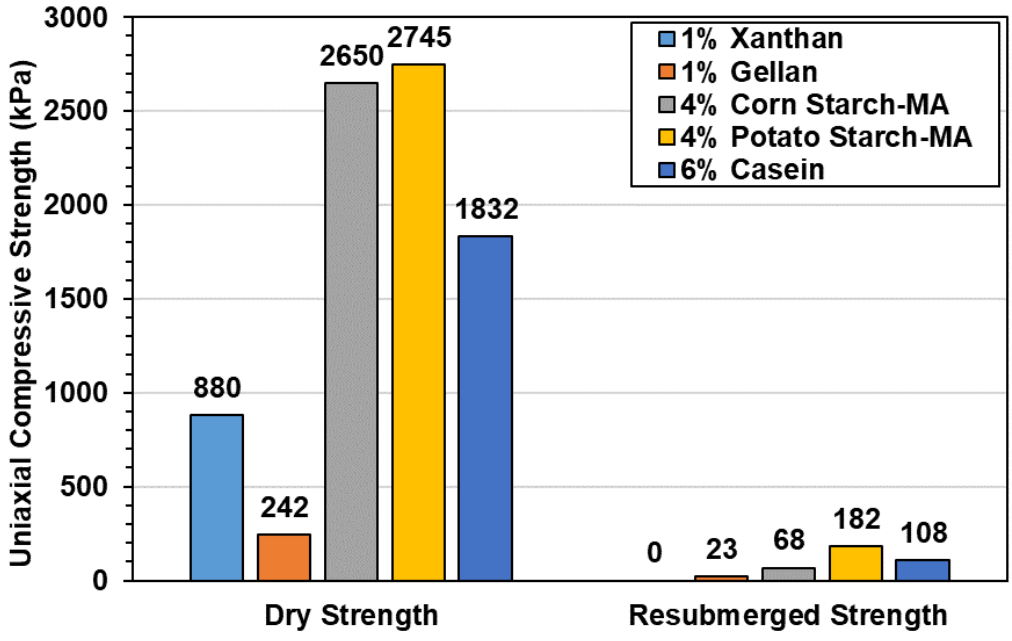

Fig. 5.9 Comparison between modified, unmodified polysaccharides and casein binders

Chapter 6. Possible Applications and Conclusion

6.1 Possible Applications

As current biopolymer treatment methods are still particularly weak when saturated, its use as a strengthening material is limited to areas with limited exposure to water. However, as the viscous biopolymers have shown properties in the prevention of particle movement, its applications in several fields such as surface erosion resistance and prevention of piping seems promising. Additionally, as both xanthan gum and gellan gum have shown particular promise in the resistance of liquefaction, its use in fields such as earthquake loading can be considered.

6.2 Conclusion

Polysaccharide properties

The two polysaccharide biopolymer properties considered in this study were viscous and gelling biopolymers. Gelling biopolymers are largely linear in nature, which allows for the formation of a double helix with heat, while viscous biopolymers have a branching structure that inhibits the formation of the double helix and results in the swelling of the biopolymer granules.

Results showed that as these biopolymers dehydrated, there was a phase shift at a critical concentration (approximately 20% m_b/m_w) in which the biopolymers went from a hydrogel to a biopolymer film. The critical concentration was the m_b/m_w concentration at which the final biopolymer saturation levels were achieved (i.e. no further volume changes with dehydration) and the point at which there was a drastic increase in the tensile strength. At concentrations below the critical concentration, the behavior was seen to be dictated by its viscous properties or its gelling properties.

Strengthening criteria

Strengthening results with UCS showed that the overall strengthening criteria of biopolymer treated sands was largely dictated by the tensile strength of the biopolymers, while the effects of viscosity showed little to no effect on the strengthening of sands. The

tensile strength of the biopolymers was shown to act as cohesion in the sands. At different biopolymer concentrations, the strengthening efficiency was shown to be a factor of the degree of biopolymer saturation.

Effects of gelling on loading

Gelling biopolymers were shown to provide small amounts of tensile strength through formation of a double helix structure. Gellan treatment of sands were shown to reduce hydraulic conductivity, but with loading this reduction was seen to become negligible with the formation of fractures in the gels. As concentrations of gellan gum increased, increased cohesion was observed with a slight decrease in the friction angle. Through the increase in cohesion and the formation of rigid gels in the pores of sands, it was shown that gellan gum treatment shows great promise in the prevention of soil liquefaction.

Effects of viscosity on loading

Although viscosity was shown to have no substantial increase in the strength of sands, it has shown other behaviors in sands. Unlike gellan gum, xanthan gum treated sands has shown a reduction in hydraulic conductivity regardless of the soil strain during loading. It has also shown expansive behaviors, particularly in loose sands. These behaviors have shown that xanthan gum may be beneficial for the prevention of liquefaction of soils.

Enhancement through crosslinking

Crosslinking was used on polysaccharide biopolymers to enhance the resubmerged strength of these biopolymers. This was done by the crosslinking reaction providing stronger bonds between the polymer chains, and by reducing the biopolymer's sensitivity to water by reacting with the hydroxyl groups in the polymer chains. Results showed that the use of crosslinking can be used to increase the resistance of these polysaccharides in water.

Enhancement through protein binders

Another method of enhancement shown was through the use of protein binders. Hydrophobic casein proteins were used to form a soil binder. Results showed that casein treated sands had a higher resubmerged strength in comparison with conventional polysaccharide biopolymers. However, it was also noted that higher concentrations of casein

were required for efficient binding of sand. This shows that alternative hydrophobic biopolymers may be used to enhance the resubmerged strength.

6.3 Further Studies

For further studies, a correlation between the biopolymer fluid viscosity and the magnitude at which it restricts soil movement will need to be studied. The exact mechanism in which viscous biopolymers show expansive behaviors in loose soils will also need to be investigated. Additionally, as previous studies have shown that biopolymers interact directly with the surface charges and ions present in fine soils, a microscale analysis on these biopolymer interactions with fine soils will be necessary.

References

[1] I. Chang, G.-C. Cho, Strengthening of Korean residual soil with β-1,3/1,6-glucan biopolymer, Construction and Building Materials 30(0) (2012) 30-35.

[2] R.K. Pachauri, M.R. Allen, V.R. Barros, J. Broome, W. Cramer, R. Christ, J.A. Church, L. Clarke, Q. Dahe, P. Dasgupta, Climate change 2014: synthesis report. Contribution of Working Groups I, II and III to the fifth assessment report of the Intergovernmental Panel on Climate Change, Intergovernmental Panel on Climate Change (IPCC), Geneva, Switzerland, 2014.

[3] E. Dlugokencky, P. Tans, National Oceanic & Atmospheric Administraion (NOAA) Earth System Research Laboratory (ESRL). https://www.esrl.noaa.gov/gmd/ccgg/trends/.

[4] C. Le Quéré, R.M. Andrew, P. Friedlingstein, S. Sitch, J. Pongratz, A.C. Manning, J.I. Korsbakken, G.P. Peters, J.G. Canadell, R.B. Jackson, Global carbon budget 2017, Earth System Science Data 10(1) (2018) 405.

[5] I. Chang, M. Lee, C. Gye-Chun, Global CO_2 Emission-Related Geotechnical Engineering Hazards and the Mission for Sustainable Geotechnical Engineering, Energies 12(13) (2019) 2567.

[6] K. Yasuhara, S. Murakami, N. Mimura, H. Komine, J. Recio, Influence of global warming on coastal infrastructural instability, Sustainability Science 2(1) (2007) 13-25.

[7] M. Huber, R. Knutti, Anthropogenic and natural warming inferred from changes in Earth's energy balance, Nature Geoscience 5 (2012) 31-36.

[8] K.E. Trenberth, Changes in precipitation with climate change, Climate Research 47(1/2) (2011) 123-138.

[9] K.E. Trenberth, Atmospheric moisture residence times and cycling: Implications for rainfall rates and climate change, Climatic change 39(4) (1998) 667-694.

[10] K.E. Trenberth, A. Dai, R.M. Rasmussen, D.B. Parsons, The changing character of precipitation, Bulletin of the American Meteorological Society 84(9) (2003) 1205-1217.

[11] D. Ren, Storm-Triggered Landslides in Warmer Climates, Springer, Switzerland, 2015.

[12] N. Mimura, Sea-level rise caused by climate change and its implications for society, Proceedings of the Japan Academy, Series B, Physical and Biological Sciences 89(7) (2013) 281-301.

[13] J.A. Church, N.J. White, L.F. Konikow, C.M. Domingues, J.G. Cogley, E. Rignot, J.M. Gregory, M.R. van den Broeke, A.J. Monaghan, I. Velicogna, Revisiting the Earth's sea-level and energy budgets from 1961 to 2008, Geophysical Research Letters 38(18) (2011).

[14] NESTA, Melting Arctic Sea Ice and Ocean Circulation, 2011. https://scied.ucar.edu/longcontent/melting-arctic-sea-ice-and-ocean-circulation.

[15] T.W.K. Armitage, G.E. Manucharyan, A.A. Petty, R. Kwok, A.F. Thompson, Enhanced eddy activity in the Beaufort Gyre in response to sea ice loss, Nature Communications 11 (2020).

[16] J. Pollard, T. Spencer, S. Brooks, The interactive relationship between coastal erosion and flood risk, Progress in Physical Geography: Earth and Environment, SAGE Publications, p. 12.

[17] A.J. Peacock, A. Calhoun, Polymer Chemistry: Properties and Applications, Hanser Gardner Publications2006.

[18] D.A. Laird, Bonding between polyacrylamide and clay mineral surfaces, Soil Science 162(11) (1997) 826-832.

[19] M. Malik, J. Letey, Adsorption of polyacrylamide and polysaccharide polymers on soil materials, Soil Science Society of America Journal 55(2) (1991) 380-383.

[20] D. Fox, R.B. Bryan, Influence of a polyacrylamide soil conditioner on runoff generation and soil erosion: Field tests in Baringo District, Kenya, Soil Technology 5(2) (1992) 101-119.

[21] B. Xiong, R.B. Loss, D. Shields, T. Pawlik, R. Hochreiter, A.L. Zydney, M. Kumar, Polyacrylamide degradation and its implications in environmental systems, npj Clean Water 1 (2018).

[22] R.H. Karol, Chemical Grouting and Soil Stabilization, Third Edition, Revised, and Expanded ed., Marcel Dekker, Inc., New York, 2003.

[23] C. Boutterin, J. Davidovits, Geopolymeric Cross-Linking (LTGS) and Building Materials, Geopolymer'88 Proceedings 1 (2003) 79-88.
[24] V.D. Glukhovsky, Soil Silicates, Gosstroyizdat, Kiev, 1959.
[25] J. Davidovits, Geopolymer Cement, Institut Geopolymere (2013).
[26] W. Hajjaji, S. Andrejkovičová, C. Zanelli, M. Alshaaer, M. Dondi, J.A. Labrincha, F. Rocha, Composition and technological properties of geopolymers based on metakaolin and red mud, Materials & Design 52(0) (2013) 648-654.
[27] L.L. Hench, Sol-Gel Silica. Properties, Processing and Technology Transfer, Noyes Publications1998.
[28] P. Duxson, A. Fernández-Jiménez, J.L. Provis, G.C. Lukey, A. Palomo, J.S.J. van Deventer, Geopolymer technology: the current state of the art, Journal of Materials Science 42(9) (2007) 2917-2933.
[29] J.E. Oh, P.J.M. Monteiro, S.S. Jun, S. Choi, S.M. Clark, The evolution of strength and crystalline phases for alkali-activated ground blast furnace slag and fly ash-based geopolymers, Cement and Concrete Research 40(2) (2010) 189-196.
[30] P. Rovnaník, Effect of curing temperature on the development of hard structure of metakaolin-based geopolymer, Construction and Building Materials 24(7) (2010) 1176-1183.
[31] J.G.S. van Jaarsveld, J.S.J. van Deventer, G.C. Lukey, The effect of composition and temperature on the properties of fly ash- and kaolinite-based geopolymers, Chemical Engineering Journal 89(1–3) (2002) 63-73.
[32] T. Bakharev, Resistance of geopolymer materials to acid attack, Cement and Concrete Research 35(4) (2005) 658-670.
[33] F.-B. Yu, X.-P. Luo, C.-F. Song, M.-X. Zhang, S.-D. Shan, Concentrated biogas slurry enhanced soil fertility and tomato quality, Acta Agriculturae Scandinavica 60(3) (2009) 262-268.
[34] J. Smith, A. Abegaz, R.B. Matthews, M. Subedi, E.R. Orskov, V. Tumwesige, P. Smith, What is the potential for biogas digesters to improve soil fertility and crop prodcution in Sub-Saharan Africa?, Biomass and Bioenergy 70 (2014) 58-72.
[35] A. Sigel, H. Sigel, R.K.O. Sigel, Biomineralization: From Nature to Application, Wiley2008.
[36] J. DeJong, M. Fritzges, K. Nüsslein, Microbially induced cementation to control sand response to undrained shear, Journal of Geotechnical and Geoenvironmental Engineering 132(11) (2006) 1381-1392.
[37] V.S. Whiffin, L.A. van Paassen, M.P. Harkes, Microbial carbonate precipitation as a soil improvement technique, Geomicrobiology Journal 24(5) (2007) 417-423.
[38] S. Stockes-Fischer, J.K. Galinat, S.S. Ban, Microbiological precipitation of CaCO3, Soil Biol. Biochem. 31(11) (1999) 1563-1571.
[39] Y. Fujita, F.G. Ferris, R.D. Lawson, F.S. Colwell, R.W. Smith, Calcium Carbonate Precipitation by Ureolytic Subsurface Bacteria, Geomicrobiology Journal 17 (2000) 305-318.
[40] B. Mortensen, J. DeJong, Strength and stiffness of MICP treated sand subjected to various stress paths, Geo-Frontiers 2011: Advances in Geotechnical Engineering2011, pp. 4012-4020.
[41] Y. Fujita, J.L. Taylor, T.L. Gresham, M.E. Delwiche, F.S. Colwell, T.L. Mcling, L.M. Mcling, L.M. Petzke, R.W. Smith, Stimulation of microbial urea hydrolysis in groundwater to enhance calcite precipitation, Environ Sci Technol. 42(8) (2008) 3025-32.
[42] R. Renforth, D.A.C. Manning, E. Lopez-Capel, Carbonate precipitation in artificial soils as a sink for atmospheric carbon dioxide, Applied Geochemistry 24(9) (2009) 1757-1764.
[43] S.K. Ramachandran, V. Ramakrishnan, S.B. Sookie, Remediation of concrete using microorganisms, Materials Journal 98(1) (2001) 3-9.
[44] V. Ramakrishnan, S.S. Bang, K.S. Deo, A novel technique for repairing cracks in high performance concrete using bacteria, Proc. Int. Conf. on High Performance High Strength Concrete, Curtin Univ. of Technology, Perth, Australia, 1998, pp. 597-618.
[45] S. Kalia, L. Averous, Biopolymers: Biomedical and Environmental Applications, Wiley2011.
[46] S. Kalia, A. Dufresne, B.M. Cherian, B.S. Kaith, L. Avérous, J. Njuguna, E. Nassiopoulos, Cellulose-Based Bio- and Nanocomposites: A Review, International Journal of Polymer Science 2011 (2011) 1-35.
[47] I. Chang, J. Im, A.K. Prasidhi, G.-C. Cho, Effects of Xanthan gum biopolymer on soil

strengthening, Construction and Building Materials 74(0) (2015) 65-72.
[48] H. Khatami, B. O'Kelly, Improving mechanical properties of sand using biopolymers, Journal of Geotechnical and Geoenvironmental Engineering 139(8) (2012) 1402-1406.
[49] I. Chang, A.K. Prasidhi, J. Im, H.-D. Shin, G.-C. Cho, Soil treatment using microbial biopolymers for anti-desertification purposes, Geoderma 253–254(0) (2015) 39-47.
[50] W.J. Orts, R.E. Sojka, G.M. Glenn, Biopolymer additives to reduce erosion-induced soil losses during irrigation, Industrial Crops and Products 11(1) (2000) 19-29.
[51] I. Chang, J. Im, G.-C. Cho, Soil-hydraulic conductivity control via a biopolymer treatment-induced bio-clogging effect, Geotechnical and Structural Engineering Congress 2016, ASCE2016, pp. 1006-1015.
[52] R. Khachatoorian, I.G. Petrisor, C.-C. Kwan, T.F. Yen, Biopolymer plugging effect: laboratory-pressurized pumping flow studies, Journal of Petroleum Science and Engineering 38(1–2) (2003) 13-21.
[53] A.T.P. Tran, I. Chang, G.-C. Cho, Soil water retention and vegetation survivabiity improvement using microbial biopolymers in drylands, Geomechanics and Engineering 17(5) (2019) 475-483.
[54] I. Chang, A.K. Prasidhi, J. Im, G.-C. Cho, Soil strengthening using thermo-gelation biopolymers, Construction and Building Materials 77(0) (2015) 430-438.
[55] I. Chang, J. Im, S.-W. Lee, G.-C. Cho, Strength durability of gellan gum biopolymer-treated Korean sand with cyclic wetting and drying, Construction and Building Materials 143 (2017) 210-221.
[56] Y.-M. Kwon, S.-M. Ham, T.-H. Kwon, G.-C. Cho, I. Chang, Surface-erosion behaviour of biopolymer-treated soils assessed by erosion function apparatus, Geotechnique Letters 10(2) (2020) 1-7.
[57] A. Shields, Anwendung der aehnlichkeitsmechanik und der turbulenzforschung auf die geschiebebewegung, Preußische Versuchsanstalt fur Wasserbau und Schiffbau, Germany, 1936.
[58] N. Benkeblia, Polysaccharides : natural fibers in food and nutrition, CRC Press, Taylor & Francis Group, Boca Raton, 2014.
[59] G. Lorenzo, N. Zaritzky, A. Califano, Rheological analysis of emulsion-filled gels based on high acyl gellan gum, Food Hydrocolloids 30 (2012) 672-680.
[60] D. Saha, S. Bhattacharya, Hydrocolloids as thickening and gelling agents in food: a critical review, Journal of Food Science Technology 47(6) (2010) 587-597.
[61] K. Van de Velde, P. Kiekens, Biopolymers: overview of several properties and consequences on their applications, Polymer Testing 21(4) (2002) 433-442.
[62] A. Varki, R. Cummings, J. Esko, H. Freeze, G. Hart, J. Marth, Essentials of Glycobiology, Cold Spring Harbor, New York, 1999.
[63] K. Adibkia, S.S. MR, A. Nokhodchi, A. Javadzedeh, M. Barzegar-Jalali, J. Barar, G. Mohammadi, Y. Omidi, Piroxicam nanoparticles for ocular delivery: Physicochemical characterization and implementation in endotoxin-induced uveitis, Journal of Drug Targeting 15(6) (2007) 407-416.
[64] G.C. Barrére, C.E. Barber, M.J. Daniels, Molecular cloning of genes involved in the production of the extracellular polysaccharide xanthan by Xanthomonas campestris pv. campestris, International Journal of Biological Macromolecules 8(6) (1986) 372-374.
[65] Y.J. Chang, S. Lee, M.A. Yoo, H.G. Lee, Structural and Biological Characterization of Sulfated-Derivatized Oat β-Glucan, Journal of Agricultural and Food Chemistry 54(11) (2006) 3815-3818.
[66] J. Daniel, R.L. Whistler, A.C.J. Voragen, W. Pilnik, Starch and other polysaccharides, Ullmann's Encyclopedia of Industrial Chemistry, VCH Verlagsgesellschaft mbH, Weinheim, 1994.
[67] T. Harada, A. Misaki, H. Saito, Curdlan: A bacterial gel-forming β-1, 3-glucan, Archives of Biochemistry and Biophysics 124 (1968) 292-298.
[68] H. Hassan, S. Al-Oraimi, R. Taha, Evaluation of open-graded friction course mixtures containing cellulose fibers and styrene butadiene rubber polymer, Journal of Materials in Civil Engineering 17(4) (2005) 416-422.
[69] I. Chang, J. Im, G.-C. Cho, Introduction of microbial biopolymers in soil treatment for future

environmentally-friendly and sustainable geotechnical engineering, Sustainability 8(3) (2016) 251.
[70] R. Smith, Biodegradable Polymers for Industrial Applications, Woodhead Publishing2005.
[71] S. Arnott, A. Fulmer, W.E. Scott, I.C.M. Dea, R. Moorhouse, D.A. Rees, The agarose double helix and its function in agarose gel structure, Journal of Molecular Biology 90(2) (1974) 269-284.
[72] C.-S. Wang, N. Virgilio, P.M. Wood-Adams, M.-C. Heuzey, A gelation mechanism for gelatin/polysaccharide aqueous mixtures, Food Hydrocolloids 79 (2018) 462-472.
[73] R. Nugent, G. Zhang, R. Gambrell, Effect of exopolymers on the liquid limit of clays and its engineering implications, Transportation Research Record: Journal of the Transportation Research Board 2101 (2009) 34-43.
[74] A. Bouazza, W. Gates, P. Ranjith, Hydraulic conductivity of biopolymer-treated silty sand, Géotechnique 59(1) (2009) 71-72.
[75] M. Huang, J.F. Kennedy, B. Li, X. Xu, B.J. Xie, Characters of rice starch gel modified by gellan, carrageenan, and glucomannan: A texture profile analysis study, Carbohydrate Polymers 69(3) (2007) 411-418.
[76] J. Tang, M.A. Tung, Y. Zeng, Gelling Properties of Gellan Solutions Containing Monovalent and Divalent Cations, Journal of Food Science 62(4) (1997) 688-692.
[77] I. Chang, G.-C. Cho, Shear strength behavior and parameters of microbial gellan gum-treated soils: from sand to clay, Acta Geotechnica (2018) 1-15.
[78] P. Van Musschenbroek, Physicae experimentales, et geometricae: de magnete, tuborum capillarium vitreorumque speculorum attractione, magnitudine terrae, cohaerentia corporum firmorum : dissertationes ut et ephemerides meteorologicae Ultrajectinae, S. Luchtmans1729.
[79] C.A. Coulomb, Essai sur une application des règles de maximis et minimis à quelques problèmes de statique, relatifs à l'architecture, 1773.
[80] Easy molecular bonding crosslinking technology, Thermo Scientific, 2012.
[81] N. Reddy, R. Reddy, Q. Jiang, Crosslinking biopolymers for biomedical applications, Trends in Biotechnology 33(6) (2015) 362-369.
[82] N. Shah, R. Mewada, T. Mehta, Crosslinking of starch and its effect on viscosity behaviour, 2016.
[83] K.S. Soppimath, A.R. Kulkarni, T.M. Aminabhavi, Chemically modified polyacrylamide-g-guar gum-based crosslinked anionic microgels as pH-sensitive drug delivery systems: preparation and characterization, Journal of Controlled Release 75(3) (2001) 331-345.
[84] C. Lan, L. Yu, P. Chen, L. Chen, W. Zou, G. Simon, X. Zhang, Design, Preparation and Characterization of Self-Reinforced Starch Films through Chemical Modification, Macromolecular Materials and Engineering 295(11) (2010) 1025-1030.
[85] I. Pashkuleva, H.S. Azevedo, R.L. Reis, Surface Structural Investigation of Starch-Based Biomaterials, Macromolecular Bioscience 8(2) (2008) 210-219.
[86] N. Reddy, Y. Yang, Preparation and properties of starch acetate fibers for potential tissue engineering applications, Biotechnology and Bioengineering 103(5) (2009) 1016-1022.
[87] N. Reddy, Y. Yang, Citric acid cross-linking of starch films, Food Chemistry 118(3) (2010) 702-711.
[88] K. Woo, P.A. Seib, Cross-linking of wheat starch and hydroxypropylated wheat starch in alkaline slurry with sodium trimetaphosphate, Carbohydrate Polymers 33(4) (1997) 263-271.
[89] G.P.D.D. G. Hamdi, Formulation of epichlorohydrin cross-linked starch microspheres, Journal of Microencapsulation 18(3) (2001) 373-383.
[90] T. Ghosh Dastidar, A.N. Netravali, 'Green' crosslinking of native starches with malonic acid and their properties, Carbohydrate Polymers 90(4) (2012) 1620-1628.
[91] H.O. Egharevba, Chemical Properties of Starch and Its Application in the Food Industry, In Tech Open (2019).
[92] S. Mishra, T. Rai, Morphology and functional properties of corn, potato and tapioca starches, Food Hydrocolloids 20(5) (2006) 557-566.
[93] S. Hegenbart, Understanding Starch Functionality, 1996.
[94] J.L. Jane, J.F. Chen, Effect of Amylose Molecular Size and Amylopectin Branch Chain Length on Paste Properties of Starch., Cereal Chem 69 (1992) 60-65.

[95] J. Ruhsing Pan, C. Huang, S. Chen, Y.-C. Chung, Evaluation of a modified chitosan biopolymer for coagulation of colloidal particles, Colloids and Surfaces A: Physicochemical and Engineering Aspects 147(3) (1999) 359-364.
[96] D.G. Dalgleish, Casein Micelles as Colloids: Surface Structures and Stabilities, Journal of Dairy Science 81(11) (1998) 3013-3018.

Appendix A. Tensile Strength Tests

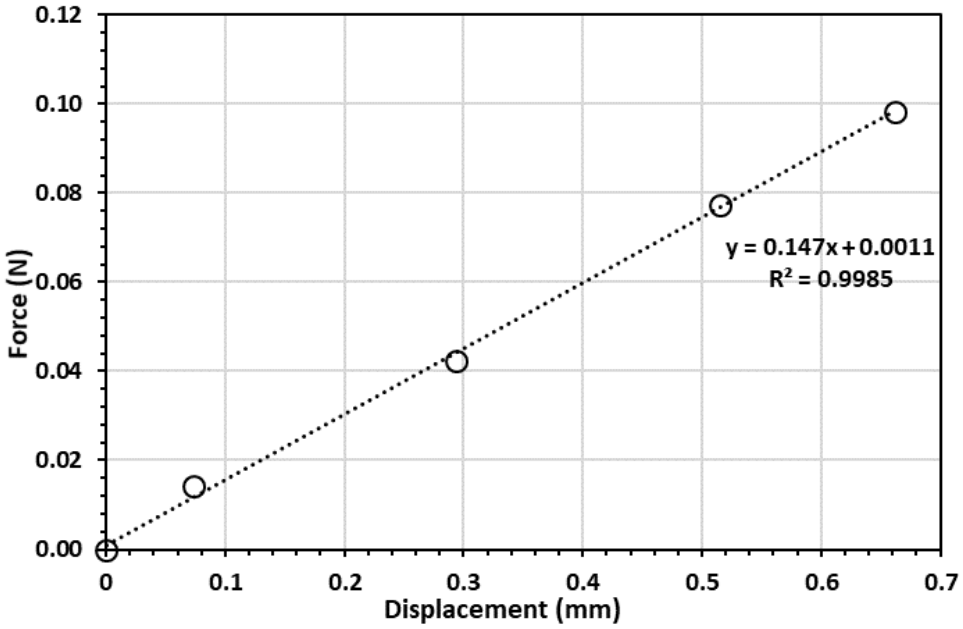

A.1 Stainless steel cantilever calibration

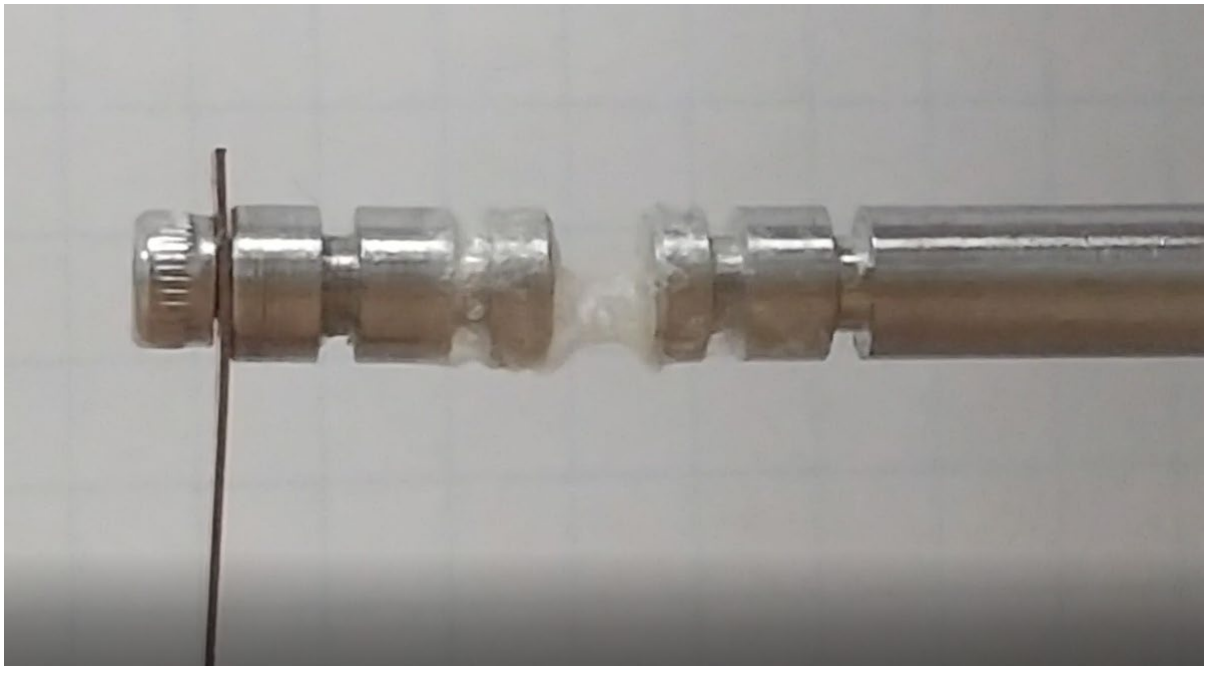

A.2 Dried biopolymer

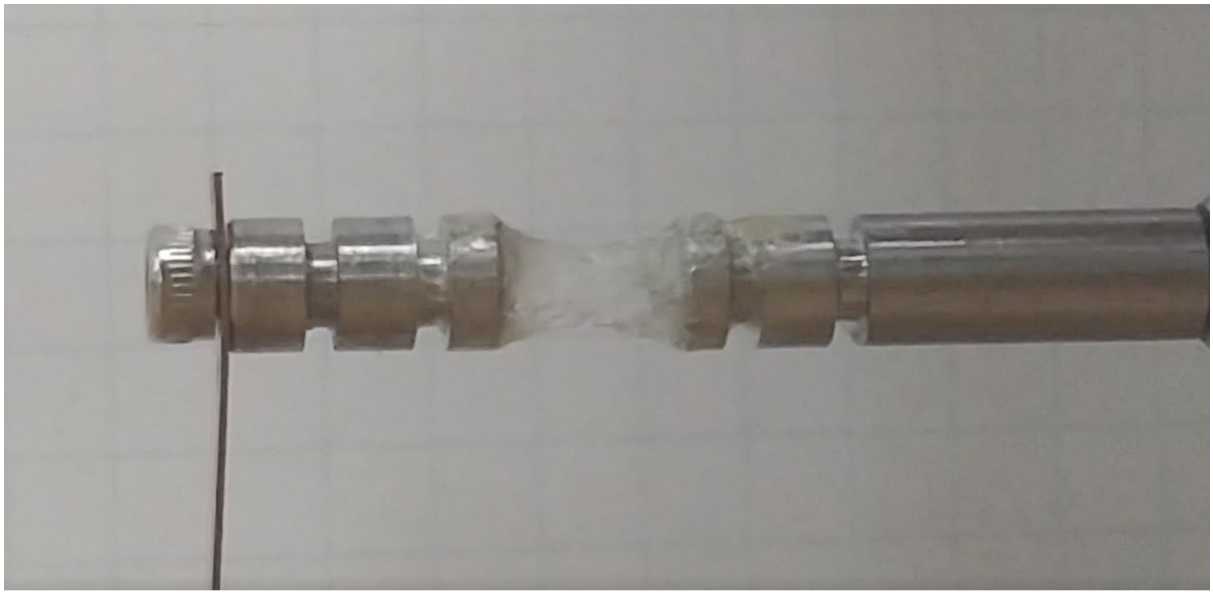

A.3 Tensile strength at failure

Appendix B. MicroFluid Chip Tests

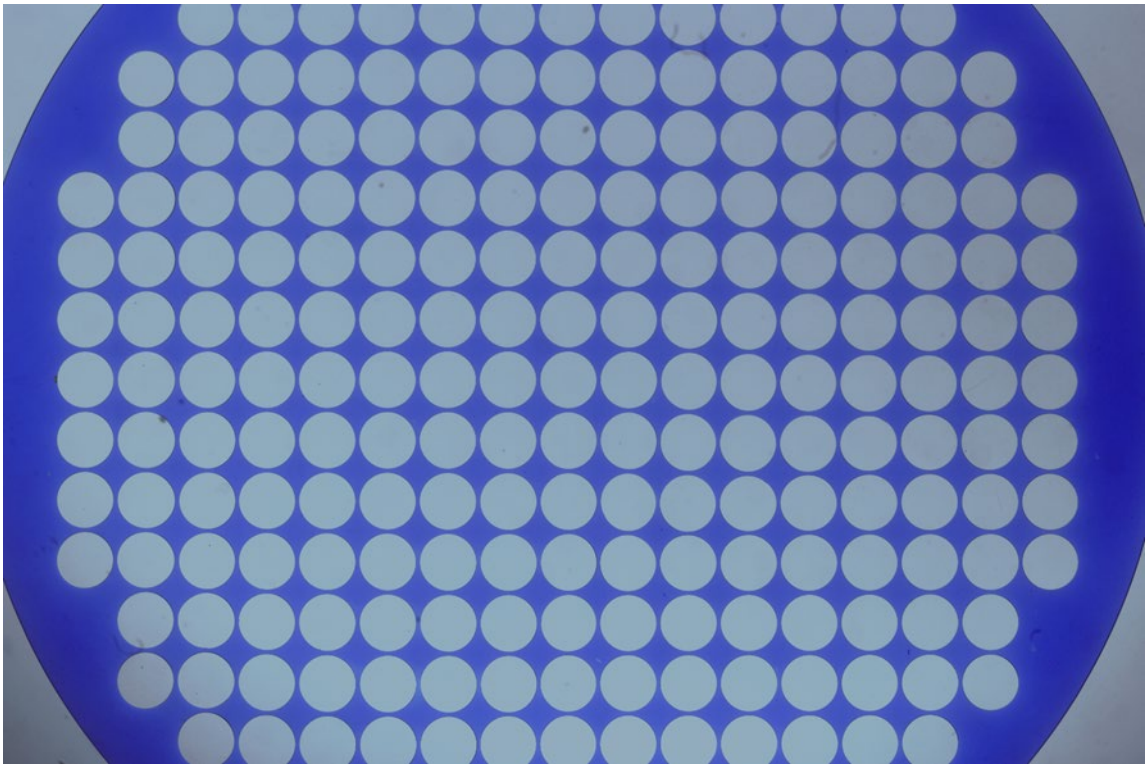

B.1 Porosity 0.3 dehydration time = 0 hrs

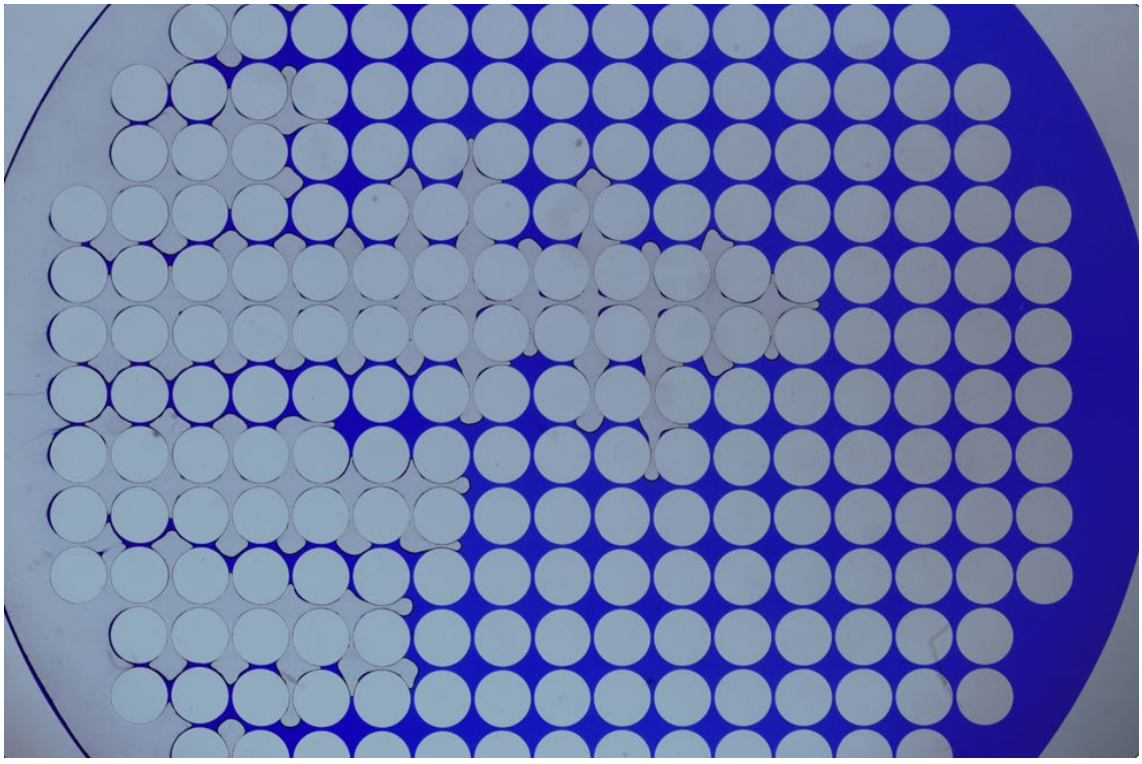

B.2 Porosity 0.3 dehydration time = 12 hrs

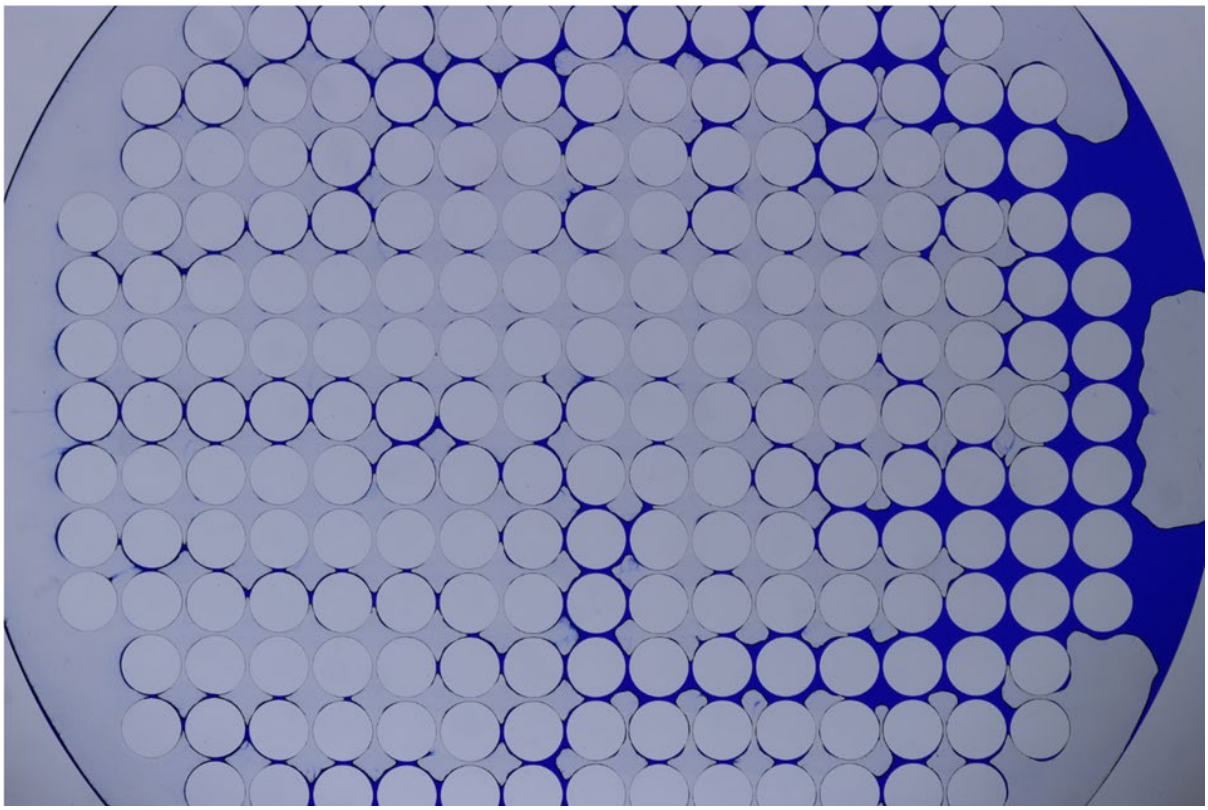

B.3 Porosity 0.3 dehydration time = 24 hrs

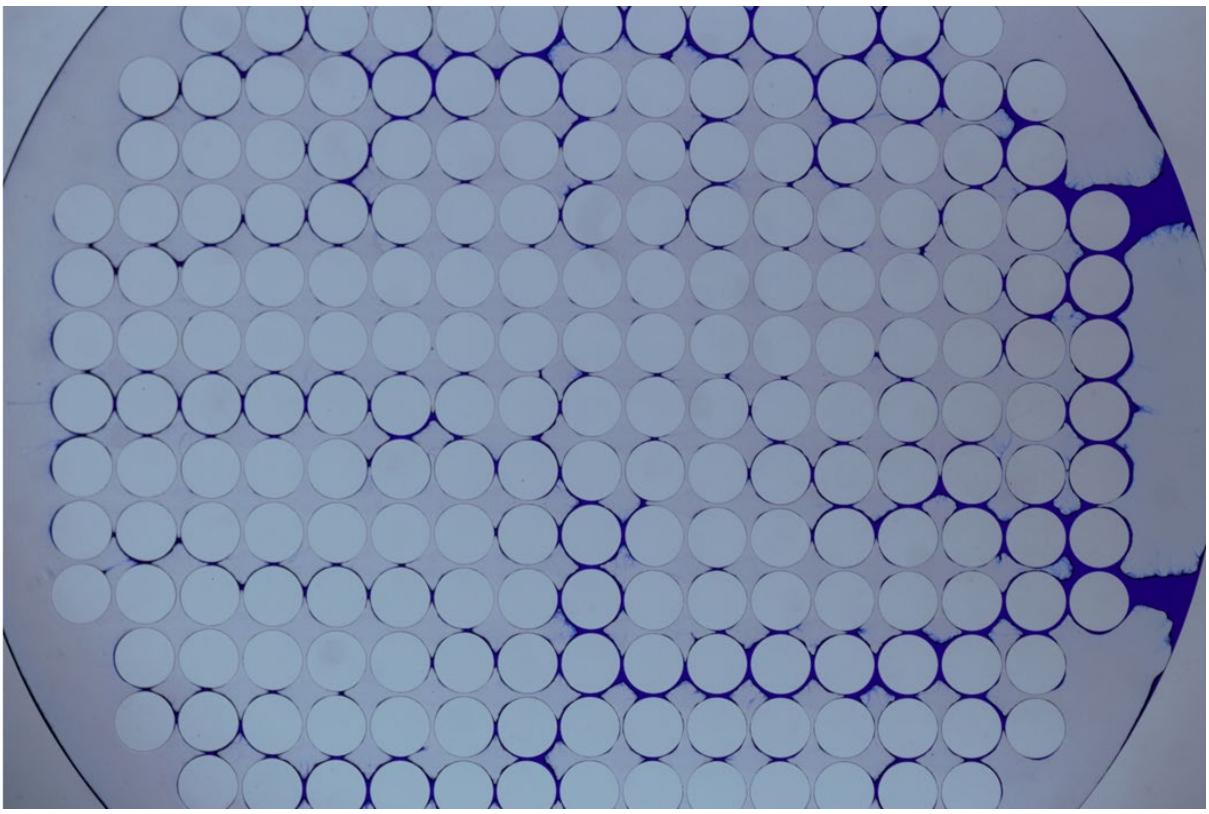

B.4 Porosity 0.3 dehydration time = 48 hrs

Appendix C. Triaxial Tests

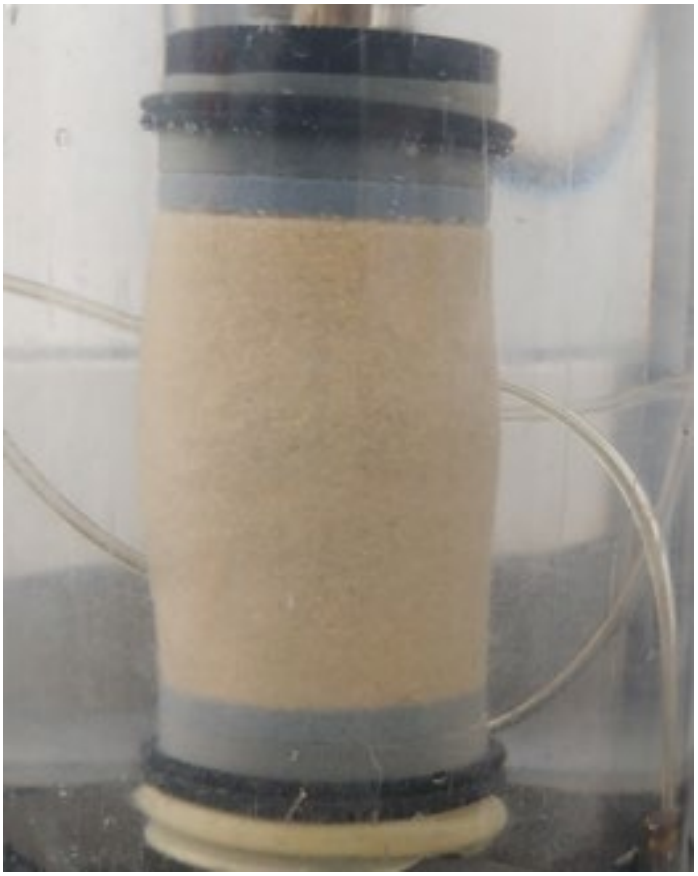

C.1 Typical bulk failure of untreated and xanthan gum treated sands

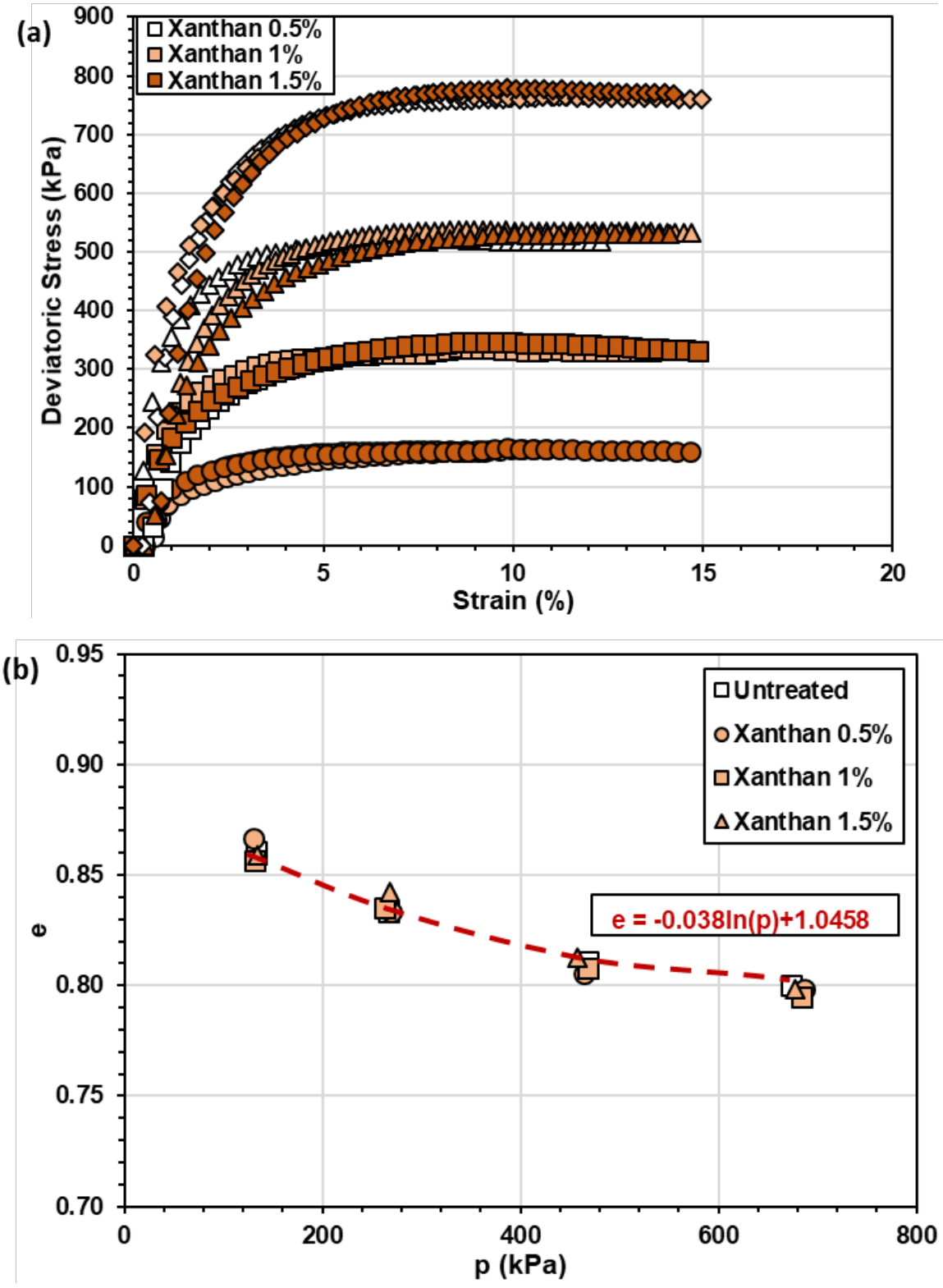

C.2 (a) stress strain and (b) critical state line of xanthan gum treated sands at various biopolymer concentrations

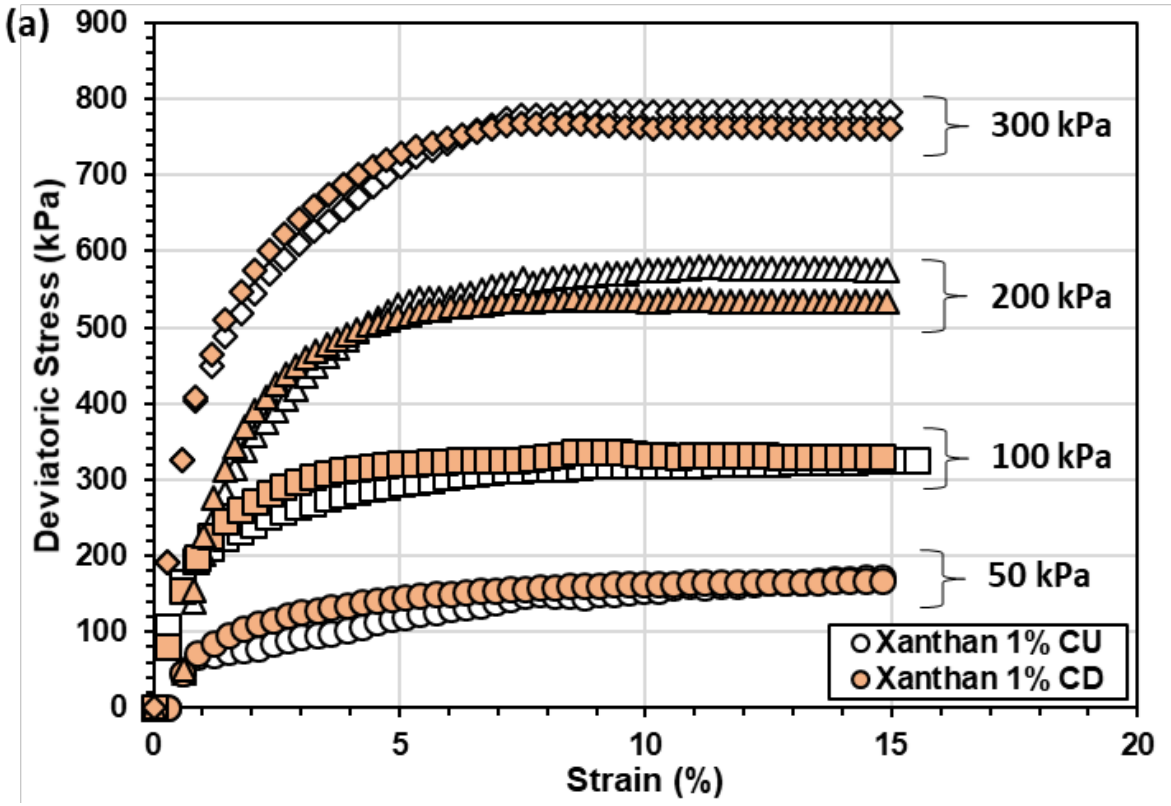

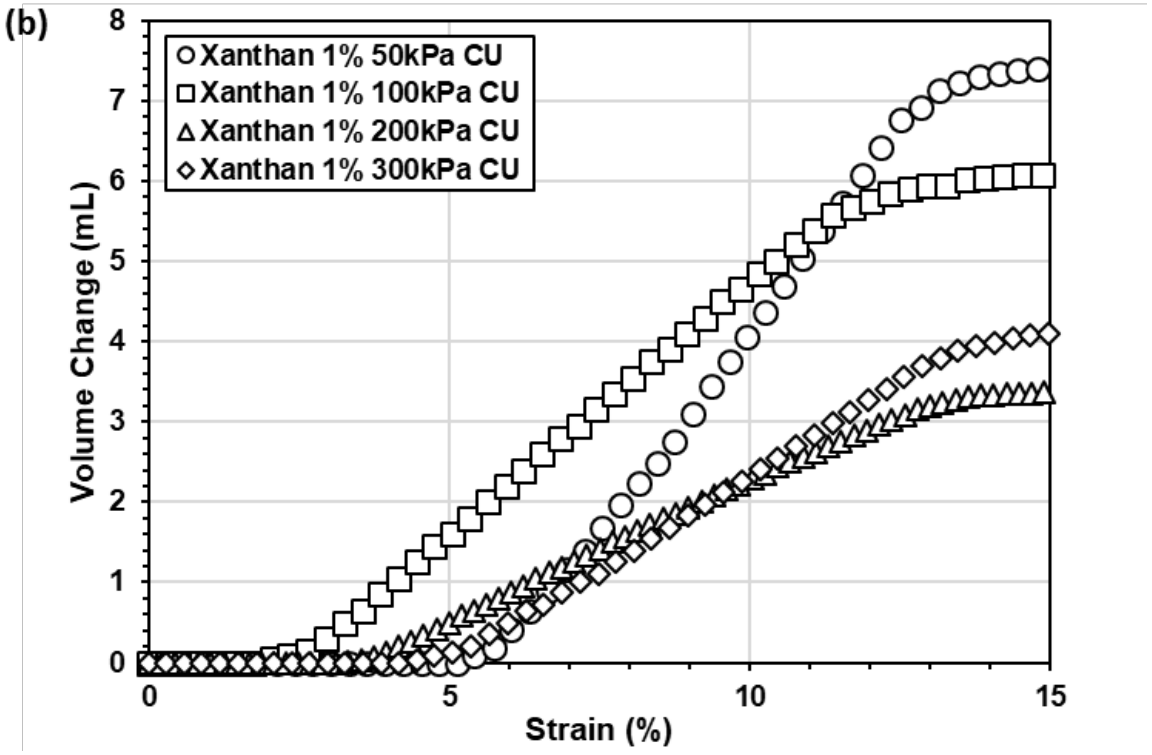

C.3 1% xanthan gum treated dense sand CU tests (a) stress strain (b) volume change

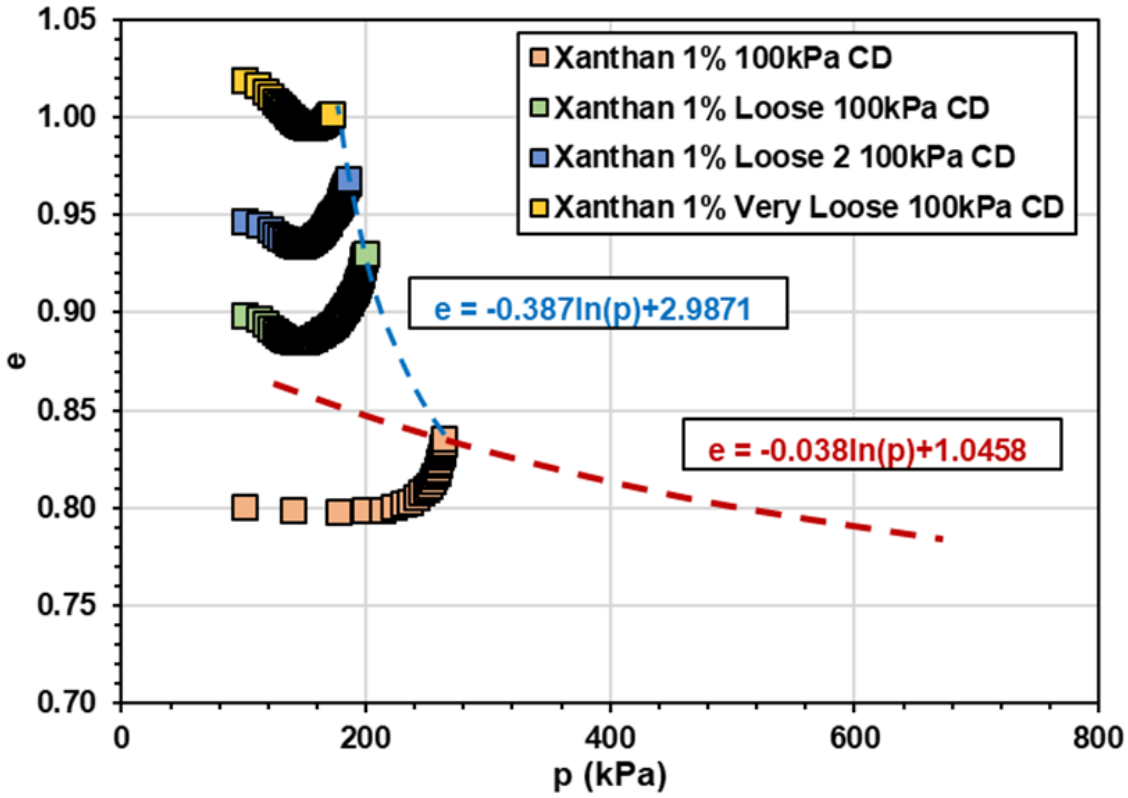

C.4 1% xanthan gum treated CD tests at 100kPa confinement and varying dry densities

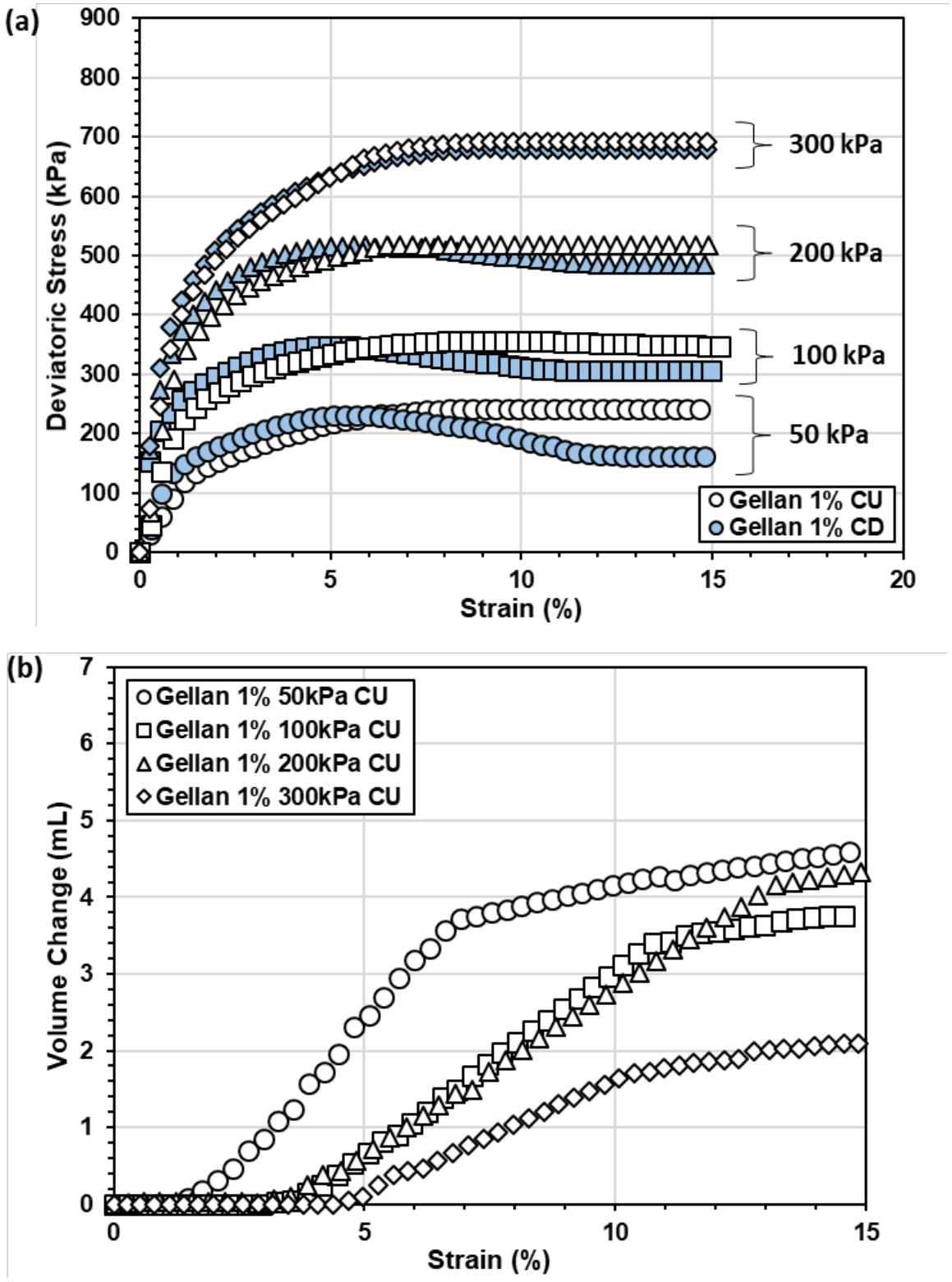

C.5 1% gellan gum treated dense sand CU tests (a) stress strain (b) volume change

Acknowledgement

The first and foremost, I want to thank my advisor Professor Gye-Chun Cho as he accepted me to work under his guidance in Geosystems laboratory and gave me a lot of constructive advices. I feel really indebted to him for his guidance, insight, advices throughout my study as a Ph.D. student at KAIST.

I would like to thank Prof. Seung-Rae Lee, Prof. Dong Soo Kim, and Prof. Tae-Hyuk Kwon for their helpful comments and insights regarding this research study. It helped me to make improvements for this study.

I am deeply indebted to Dr. Ilhan Chang for his advices, assistance, and patience, and for always making sure I make the best use of my limited time.

Last but not least, I am extremely thankful to my Geosystems Laboratory members for all the advice and help that they have provided me.

Curriculum Vitae

Name: Jooyoung Im

Date of Birth: November 1st, 1990

Education

Ph.D	2016.02 – 2020.08	Geosystems Laboratory (Advisor: Professor Gye-Chun Cho), Department of Civil and Environmental Engineering, Korea Advanced Institute of Technology (KAIST),
M.S	2014.02 – 2015.12	Geosystems Laboratory (Advisor: Professor Gye-Chun Cho), Department of Civil and Environmental Engineering, Korea Advanced Institute of Technology (KAIST),
B.S.	2009.08 – 2013.08	Department of Civil Engineering, Korea Advanced Institute of Technology (KAIST)

List of Publications

Dissertation

1. Jooyoung Im (2015), "Structural and Behavioral Analysis of Gellan Treated Soils", *M.Sc. Thesis*, Korea Advanced Institute of Science and Technology, Daejeon, South Korea
2. Jooyoung Im (2020), "Polysaccharide Biopolymers in Sands: Properties and Behaviors", Ph.*D. Thesis*, Korea Advanced Institute of Science and Technology, Daejeon, South Korea

International Conference papers

1. Im, J., Chang, I., and Cho, G.C., 2013, "Dynamic properties of Gellan treated Jumunjin sand", *Proceedings of the 26th KKHTCNN Symposium on Civil Engineering*, November 18-20, Furuma Hotel, Singapore, 4 pages (Electric Proceedings Paper No. G6-6).
2. Im, J., Chang, I., and Cho, G.C., 2014, "Soil strengthening behavior of 1% gellan treated jumunjin sand", *Proceedings of the 27th KKHTCNN Symposium on Civil Engineering*, November 18-20, Tongji University, Shanghai, China, 4 pages (Electric Proceedings Paper No. G6-6).
3. Im, J., Chang, I., Cho, G.C., and Lee, J.H., 2015, "Development of a water resistant biopolymer compound for soil strengthening", *Proceedings of the 28th KKHTCNN Symposium on Civil Engineering*, November 16-18, Bangkok, Thailand, 4 pages.
4. Im, J., Chang, I., and Cho, G.C., 2016, "Soil hydraulic conductivity control via biopolymer treatment induced bio-clogging effect", *Proceedings of the Geotechnical and Structural Engineering Congress 2016*, ASCE, February 14-17, Phoenix Convention Center (PCC), Phoenix, Arizona, USA, pp. 1006-1015.
5. Im, J., Cho, G.C., and Chang, I., 2016, "A new soil treatment method using casein from bovine milk", *Proceedings of the Geo-Chicago 2016: Sustainability, Energy, and the Geoenvironment*, ASCE Geotechnical Special Publication (GSP) 269, August 14-18, Chicago, Illinois, USA, pp. 1-6.
6. Im, J., Tran, An T.P., Chang, I., and Cho, G.C. 2017, "The effects of biopolymer use on erosion resistance of soils", *Proceedings of the 30th KKHTCNN Symposium on Civil Engineering*, November 2-

4, Taipei, Taiwan, 4 pages.

7. Im, J., Kwon, Y.M., Chang, I., and Cho, G.C., 2018, "Slope surface treatment using a bio-soil approach", *11th International Conference on Geosynthetics (ICG)*, Sept. 19, Seoul, Korea.
8. Im. J., Chang, I., and Cho, G.C., 2019, "Injection capabilities of xanthan gum for soil grouting", *The 2019 World Congress on Advances in Structural Engineering and Mechanics*, Sept. 19, Jeju, Korea.
9. Im, J., Lee, S., Cho, G.C., and Chang, I., 2019, "Effects of biopolymer on the consolidated-drained static triaxial test behavior of sand", *Asian Regional Conference on Soil Mechanics and Geotechnical Engineering*, Oct. 17, Taipei, Taiwan.

International Journal papers

1. Chang, I. Im, J., Prasidhi, A.K., and Cho, G.C., 2015, "Effects of Xanthan gum biopolymer on soil strengthening", *Construction and Building Materials*, Elsevier, Vol. 74, pp. 65-72. (doi:10.1016/j.conbuildmat.2014.10.026)
2. Chang, I., Prasidhi, A.K., Im, J., and Cho, G.C., 2015, "Soil strengthening using thermo-gelation biopolymers", *Construction and Building Materials*, Elsevier, Vol. 77, pp. 430-438. (doi:10.1016/j.conbuildmat.2014.12.116)
3. Chang, I., Kharis, P.A., Im, J., Shin, H.D., and Cho, G.C., 2015, "Soil treatment using microbial biopolymers for anti-desertification purposes", *Geoderma*, Elsevier, Vol. 253-254, pp. 39-47. (doi:10.1016/j.geoderma.2015.04.006; 15-Apr-2015).
4. Chang, I., Im, J., and Cho, G.C., 2016, "Introduction of microbial biopolymers in soil treatment for future environmentally-friendly and sustainable geotechnical engineering", *Sustainability*, MDPI, Vol. 8, No. 3, Article No. 251, pp. 23 pages. (doi: 10.3390/su8030251).
5. Chang, I., Im, J., and Cho, G.C., 2016, "Geotechnical engineering behaviors of a microbial gellan gum biopolymer treated sand", *Canadian Geotechnical Journal*, NRC Research Press, Vol. 53, No. 10, pp. 1658-1670. (doi:10.1139/cgj-2015-0475)
6. Chang, I., Im, J., Lee, S.W., and Cho, G.C., 2017, "Strength durability of Gellan gum biopolymer-treated sand with cyclic wetting and drying", *Construction and Building Materials*, Elsevier, Vol. 143, pp. 210-221.
7. Kwon, Y.M., Im, J., Chang, I., Cho, G.C., 2017, " ε -polylysine biopolymer for coagulation of clay suspensions", Geomechanics and Engineering, Techno Press, Vol. 12, No. 5, pp. 753-770.
8. Im, J., Tran, An T.P., Chang, I., Cho, G.C., 2017, "Dynamic properties of gel-type biopolymer-treated sands evaluated by Resonant Column (RC) Tests", *Geomechanics and Engineering*, Techno Press, Vol. 12, No. 5, pp. 815-830.
9. Chang, I., Im, J., Chung, M.C., and Cho, G.C., 2018, "Bovine casein as a new soil strengthening binder from diary wastes", *Construction and Building Materials*, Elsevier, Vol. 160, pp. 1-9.
10. Lee, S., Im, J., Chang, I., Cho, G.C., 2019, "Laboratory triaxial test behavior of xanthan gum biopolymer-treated sands", *Geomechanics and Engineering*, Techno Press, Vol. 17, No. 5, pp. 445-452.
11. Chang, I., Kwon, Y.M., Im, J., and Cho, G.C., 2019, "Soil Consistency and Interparticle Characteristics of Xanthan Gum biopolymer-Containing Soils with Pore-Fluid Variation", *Canadian Geotechnical Journal*, NRC Research Press, Vol. 56, No. 8, pp. 1206-1213.

Fellowships

1. NRF grant funded by the Korean Government (NRF-2016-Fostering Core Leaders of the Future Basic Science Program/**Global Ph.D. Fellowship Program**)